cGMP/PKG-REGULATED MECHANISMS OF PROTECTION FROM LOW OXYGEN AND OXIDATIVE STRESS

by

Olena Mahneva

A Dissertation Submitted to the Faculty of

The Charles E. Schmidt College of Science

In Fulfillment of the Requirements for the Degree of

Doctor of Philosophy

Florida Atlantic University

Boca Raton, FL

May 2018

cGMP/PKG-REGULATED MECHANISMS OF PROTECTION FROM LOW OXYGEN AND OXIDATIVE STRESS

by

Olena Mahneva

This dissertation was prepared under the direction of the candidate's dissertation co-advisors, Dr. Sarah L. Milton and Dr. Ken Dawson-Scully, Department of Biological Sciences, and has been approved by the members of her supervisory committee. It was submitted to the faculty of the Charles E. Schmidt College of Science and was accepted in partial fulfillment of the requirements for the degree of Doctor of Philosophy.

SUPERVISORY COMMITTEE:

Sarah L. Milton, Ph.D.
Thesis Co-Advisor

Ken Dawson-Scully, Ph.D.
Thesis Co-Advisor

Howard Prentice, Ph.D.

Kailiang Jia, Ph.D.

Rod Murphey, Ph.D.
Chair, Department of Biological Sciences

Ata Sarajedini, Ph.D.
Dean, Charles E. Schmidt College of Science

Diane E. Alperin, Ph.D.
Interim Dean, Graduate College

April 16, 2018
Date

ACKNOWLEDGMENTS

I would like to thank my Ph.D. advisors Dr. Sarah L. Milton and Dr. Ken Dawson-Scully for their tremendous support throughout my Ph.D. studies. Their guidance and cheerful attitude helped me to get through it. Their confidence in my ideas and my independence was essential for my growth as a scientist. Moreover, I am very thankful to my Ph.D. committee members Dr. Howard Prentice and Dr. Kailiang Jia for their advice, stimulating discussions, and mentorship.

I am also very thankful to Dr. William Ja for allowing me to take part in his research developing unique research collaborations. Dr. Ja's passion for science, natural curiosity, and energy has been contagious, while working with him and being his friend has been inspiring.

My colleagues and friends from Milton and Dawson-Scully labs made my Graduate college experience unique. Thanks to Melissa Reiterer, Dr. Itzel Sifuentes, Julieta DiMase, Ciny John, and Wes Bollinger for their support, help, encouragement, and great times that we had throughout the years.

And last, but not least, I would like to thank my dear parents for their love, patience, for believing in me and supporting me in so many ways throughout all those years.

ABSTRACT

Author: Olena Mahneva

Title: cGMP/PKG-regulated mechanisms of protection from low oxygen and oxidative stress

Institution: Florida Atlantic University

Dissertation Co-Advisors: Dr. Sarah L. Milton and Dr. Ken Dawson-Scully

Degree: Doctor of Philosophy

Year: 2018

Stroke is one of the leading causes of human death in the United States. The debilitating effects of an ischemic stroke are due to the fact that mammalian neurons are highly susceptible to hypoxia and subsequent oxygen reperfusion. From studies in *Drosophila melanogaster*, cGMP-dependent Protein Kinase (PKG) enzyme is thought to affect anoxia tolerance by modifying the electrical current through potassium ion channels.

In this research, two animal models were employed: *Drosophila melanogaster* and mammalian neurons exposed to stroke-like conditions. First, *in vivo* studies using *Drosophila* were performed to further our knowledge about the differences between the naturally occurring variants of the *Drosophila foraging* gene, which shows different protein levels of PKG. Mitochondrial density and metabolic activity between two fly genotypes exposed to anoxia and reoxygenation were compared. It was found that flies with less enzyme potentially showed mitochondrial biogenesis and higher metabolic rates upon reoxygenation. Next, *in vivo* studies where PKG enzyme was activated pharmacologically were performed; it was found that the activation of the cGMP/PKG

pathway led to neuroprotection upon anoxia and reoxygenation. Furthermore, this model was translated into the *in vitro* model using *Drosophila* cells. Instead of anoxia and reoxygenation, hypoxia mimetics and hydrogen peroxide were used to induce cellular injury. After showing the cGMP/PKG pathway activation-induced cell protection, the potential downstream targets of the molecular signaling as well as underlying biochemical changes were assessed. It was found that mitochondrial potassium ion channels were involved in the protective signaling and the signaling modulated metabolic function. Furthermore, it was found that acidosis protected *Drosophila* cells from cell death, metabolic disruption, and oxidative stress. Finally, this research was translated to a mammalian *in vitro* model of neuronal damage upon stroke-like conditions; there, it was demonstrated that the cGMP/PKG pathway activation in rat primary cortical neurons and human cortical neurons was protective from low oxygen and acute oxidative stress.

The results of this study lead to a better understanding of molecular mechanisms taking place during low oxygen and oxidative stresses. Consequently, this knowledge may be used to identify potential therapeutic targets and treatments that may prevent detrimental neurological effects of an ischemic stroke in humans.

cGMP/PKG-REGULATED MECHANISMS OF PROTECTION FROM LOW OXYGEN AND OXIDATIVE STRESS

LIST OF FIGURES

BACKGROUND AND SIGNIFICANCE

Stroke epidemiology

According to the Centers for Disease Control and Prevention, stroke is the number 5 cause of human death in the United States with about 130,000 mortalities occurring each year (National Center for Health Statistics, 2016). This cerebrovascular pathology strikes nearly 800,000 people annually (Benjamin et al. 2017). Importantly, there are two types of stroke. From the American Heart Association statistical update, 13% of all strokes are hemorrhagic which occur when a blood vessel bursts and bleeds into the brain tissues, producing inflammation and swelling. The remaining 87% of all strokes are ischemic. An ischemic stroke happens when blood flow that carries nutrients and oxygen to the brain tissues becomes obstructed due to a clot in a blood vessel. This creates a low oxygen environment in the affected brain tissues leading to irreversible and often fatal neuronal damage. Due to its high mortality rates and high economic impact (costs related to hospital care, rehabilitation, loss of productivity, etc.), stroke is an important area for clinical and biological research.

Current stroke therapy

Currently, the only Food and Drug Administration-approved pharmacological therapy for brain ischemia and stroke is an intravenous administration of recombinant tissue plasminogen activator (tPA), which has thrombolytic action on the clot (Emberson et al

2014). Its use is constrained due to the possibility of cerebral hemorrhage and a small window of treatment since it has to be administered within 3-4.5 hours from the onset of symptoms (Male et al. 2016; Kumar et al. 2016). Moreover, this type of medication does not offer any benefits to the brain tissues damaged by oxygen reperfusion following the breakdown of the clot. Furthermore, many pharmacological compounds that are found to be protective in *in vitro* models of ischemia and reperfusion, are not able to cross the blood-brain barrier (BBB) or are protective *in vivo* only if the animal model is young and otherwise healthy. Conversely, in clinical trials, patients with brain ischemia show numerous co-morbidities including obesity, arthritis, diabetes, metabolic disorder. In addition, advanced age also exacerbates the onset of stroke-induced tissue damage (DiNapoli et al. 2010; Pradillo et al. 2012; Smith et al. 2013; Kumar et al. 2016; Haley and Lawrence 2016). Based on this knowledge, it is important to develop new cost-effective *in vitro* and *in vivo* models of ischemia and reperfusion injury that will allow for the investigation of complex molecular mechanisms to be modulated by pharmacology and genetic techniques.

Physiological effects of an ischemic stroke in mammalian brains

On the cellular level, low oxygen causes a decline in mitochondrial ATP synthesis, which results in the failure of ATP-dependent pumps such as the sodium-potassium pumps (Hochachka 1986). This process produces a massive efflux of potassium and an influx of sodium and calcium, creating a disrupted ion gradient across the cellular plasma membrane. This process eventually results in membrane depolarization, which in turn leads to an uncontrolled release of excitatory toxins such as glutamate and dopamine; these chemicals cause increased membrane excitability and activation of postsynaptic receptors

that regulate calcium influx (Hansen 1985; Sun and Reis 1994; Ottersen et al. 1996). High calcium concentrations inside the cells activate various cell-damaging enzymes such as proteases, lipases, and endonucleases (Kanje et al. 1985; Greenamyre 1986; Choi 1987; Arai et al. 1990; Lutz 1992; Rami and Krieglstein 1993; Liptin 1999). Another wave of neuronal damage occurs after the clot impeding the blood flow dissolves and normal blood circulation is restored. The resumption of blood flow leads to oxygen reperfusion of the ischemia-affected brain tissues where mitochondrial function has been disrupted. Excess oxygen results in mitochondrial overproduction of reactive oxygen species (ROS), which results in greater damage than an ischemic event (Halliwell and Gutteridge 1984). Examples of ROS include hydrogen peroxide, hydroxyl radical and superoxide anion. These highly reactive molecules produce irreversible cell damage by oxidizing lipids, proteins, and DNA, leading to neuronal death (Chance et al. 1979; Halliwell and Gutteridge 1984; Halliwell and Cross 1994; Richter 1995; Sohal et al. 1995; Simonian and Coyle 1996).

Physiological effects of low oxygen on different types of mammalian cells

Even though the human brain composes only about 2% of a person's whole body weight, its constituent cells, the neurons, use up to 20% of the body's energy (Nilsson et al. 1975). Consequently, these cells are very sensitive to fluctuations in nutrient and oxygen concentrations. Besides neurons, every cell of the body requires oxygen to function efficiently; nevertheless, different cell types from different tissues have a unique response to a lack of oxygen and nutrient scarcity, which eventually causes cell death. Some cell types such as epithelial cells, fibroblasts, and muscle cells are extremely resistant to oxygen lack as well as reperfusion whereas cardiac myocytes, hepatocytes, renal tubular cells and

gastrointestinal epithelial cells are only slightly more resistant to hypoxia than neurons (Manresa and Taylor 2017).

Some mammalian cells, though they are of the same type but from different organs, can have different levels of susceptibility to low oxygen. For example, it takes up to 18 hours of complete anoxia for 60% of the kidney cells result in death whereas lung cell cultures exposed to the same exact conditions, result in 0% cell death (Tretyakov and Farber 1995).

Role of increased potassium current in anoxia-affected mammalian brains: plasma membrane K^+ channels

During the initial phase of total cerebral ischemia (about 30-60 seconds), an increase of potassium ion current in the neurons is observed, as shown in Fig.1. This precedes the massive membrane depolarization that takes place when ATP-dependent pumps fail which leads to the loss of ionic gradient (Hansen 1985). The corresponding small elevation in potassium concentration outside the cell leads to a complete stop of the electroencephalography (EEG) activity of a rat brain cortex, as indicated in Fig. 1.

According to various studies, similar initial hyperpolarizations in hippocampal and dorsal vagal neurons result from activation of ATP-sensitive potassium ion channels that become activated by low ATP concentrations (as during brain ischemia) (Trapp and Ballanyi 1995; Fujimura et al. 1997; Huang et al. 2006). This leads to increased potassium currents and can eventually cause a short hyperpolarization (Trapp and Ballanyi 1995; Fujimura et al. 1997; Huang et al. 2006). Other reports show that in hippocampal neurons this hyperpolarization is due to an activation of calcium-dependent potassium ion channels since there is a small increase in calcium influx preceding the short-termed initial

hyperpolarizing potassium current (Kass and Lipton 1986; Yamamoto et al. 1997; Nowicky and Duchen 1998; Rundén-Pran et al. 2002). It has been hypothesized that this hyperpolarization is protective to a cell by initiating a functional downregulation before the neuronal membrane is irreversibly depolarized during hypoxia (Shimoda and Polak 2011). As a consequence, this short-term initial increase in potassium current could be a mechanism to save energy, and results in synaptic function shutdown (Nieber 1999; Krnjević 2008). With this being the case, the initiation of irreversible events, such as the release of excitatory toxins and massive Ca^{2+} influx could be delayed or even prevented through an early increased potassium efflux (Tanaka et al. 1995; Shimoda and Polak 2011).

Even though the natural "protective" hyperpolarization is brief and is soon taken over by membrane depolarization, it is possible that pharmacological stimulation of the molecular pathways stimulating the potassium current may be beneficial for the anoxia-affected neurons.

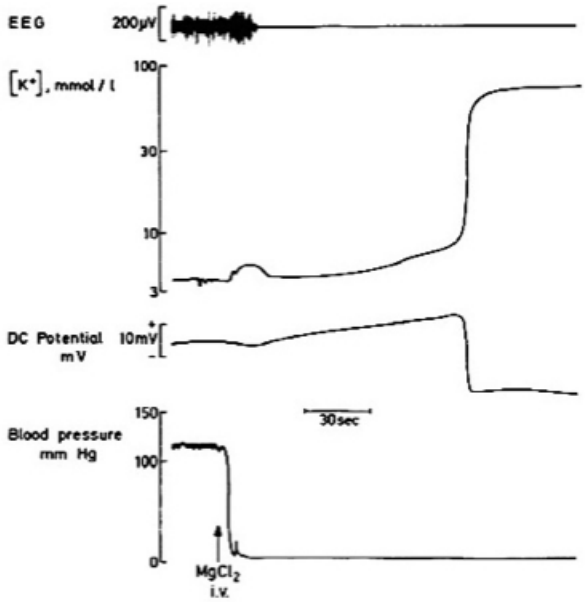

Figure 1. Interstitial potassium [K^+], EEG activity, interstitial electrical potential (DC potential) in rat brain cortex, and measurements of arterial blood pressure. Brain ischemia was produced through cardiac arrest induced by intravenous injection of magnesium chloride (Hansen 1985).

Role of increased potassium current in anoxia-affected brains: mitochondrial K^+ channels

Notwithstanding the possibility that plasma membrane K^+ channels may play a role in cytoprotection during anoxia and reoxygenation, growing evidence suggests that increased electric currents through mitochondrial K^+ channels (mitoK^+) play a critical role in protecting mammalian neurons as well as other types of cells from ischemia and oxidative stresses. The mitoK^+ channels spanning the mitochondrial inner membrane, such as ATP-regulated K^+ ion (mitoK_{ATP}) channels, large-conductance Ca^{2+}-activated potassium ion (mitoBK_{Ca}) channels, and voltage-dependent potassium (mitoKv1.3) channels are integrated in the inner membrane of mitochondria, and, when active, increase or decrease

K^+ concentration in the mitochondrial matrix (Gu et al. 2007; Szewczyk et al. 2009). Functionally, these types of ion channels are known to regulate mitochondrial matrix volume, influx of calcium, and rates of mitochondrial respiration (Busija et al. 2004).

Various research studies demonstrated that the activation of mitochondrial potassium ion channels leads to cellular protection from metabolic and oxidative damage. For example, it was shown that upon reperfusion, the ATP-sensitive mitochondrial K^+ channels inhibit apoptosis through prevention of Permeable Transition Pore (PTP) formation, inhibition of mitochondrial cytochrome c release, suppression of pro-apoptotic protein Bax translocation to mitochondria, and upregulated expression of anti-apoptotic protein Bcl-2 (Takuma et al. 2001; Liu et al. 2002; Hausenloy et al. 2006). Likewise, it was found that opening of mitoK_{ATP} or mitoK_{Ca} decreases mitochondrial membrane potential, reduces mitochondrial ROS levels, and leads to cellular protection resulting in increased survival of cardiac and neuronal cells subjected to oxidative and metabolic stresses (Ishida et al. 2001; Liu et al. 2002; Sato et al. 2005; Ljubkovic et al. 2006; Wang et al. 2008; Gáspár et al. 2008; Kulawiak et al. 2008). From these and similar studies, it has been hypothesized that besides reducing ROS formation, the increased mitoK^+ current may also lead to decreased Ca^{2+} overload in mitochondrial matrix by reducing the driving force for the entrance of Ca^{2+}, a recognized activator of apoptosis-promoting PTP (Debska et al. 2001; Busija et al. 2004; Ljubkovic et al. 2006; Annunziato 2009). Contrarily, when the effects of neuronal preconditioning with the mitoK_{ATP} channel activator diazoxide were examined, increased levels of ROS generation by mitochondria were detected (Andrukhiv et al. 2006). It is possible that this slight increase in ROS generation may be a stimulator for upregulated expression of antioxidant and other protective genes (Andrukhiv et al. 2006). Notably, there

is a report of cGMP/PKG stimulating the mitochondrial production of ROS, possibly through activation of the mitoK_{ATP}; this results in the subsequent activation of the plasma membrane K_{ATP} channels, yet the exact mechanism of the molecular signaling is unknown (Chai and Lin 2010).

Accordingly, the activation of mitochondrial potassium ion channels may play a protective role during low oxygen and oxidative stress injury; however, the exact mechanism of such protection has not yet been developed into an integrated scheme of molecular signaling events.

cGMP-dependent Protein Kinase and its molecular pathway in mammals

One molecular signaling pathway that regulates potassium ion current in plasma membrane and/or mitochondrial inner membrane is the cyclic guanosine monophosphate-dependent protein kinase (PKG) cascade. PKG is an enzyme that phosphorylates its substrate proteins at serine-threonine residues. As the name implies, it is activated by cGMPs. There are two isoforms of the enzyme: PKG I (types Iα and Iβ), and PKG II (Uhler 1993; el-Husseini et al. 1995). PKG I, a cytosol-soluble PKG isoform, is localized in a wide variety of tissues and cell types, and is important in physiological mechanisms such as smooth muscle relaxation and contraction, cardiac function, and neuronal function (brain development, memory and learning) (Han et al. 2001; Wang and Robinson 2002; Michelakis et al. 2003; Demyanenko et al. 2005). Pharmacological activation of the PKG I enzyme is currently being developed for vasodilation of blood vessels to treat arterial hypertension since activation of this kinase leads to arterial smooth muscle relaxation (Michelakis et al. 2003; Schlossmann and Schinner 2012). PKG II, a plasma membrane-bound PKG isoform, plays an important role in very distinct physiological processes such

as intestinal secretion, renin release, and bone growth (Hofmann et al. 2006). Since PKG I affects physiological processes of excitable cells such as neurons, the rest of the written proposal focuses on the PKG I – mediated molecular signaling.

In a study performed on bovine tracheal smooth muscle cells and Chinese hamster ovary cells transfected with the PKG Iβ, researchers investigated molecular targets upstream and downstream of PKG using pharmacological inhibitors and stimulators of various tentative targets of the pathway as well as through electrophysiological studies (Zhou et al. 1996). The possible cGMP/PKG pathway is shown in Fig. 2.

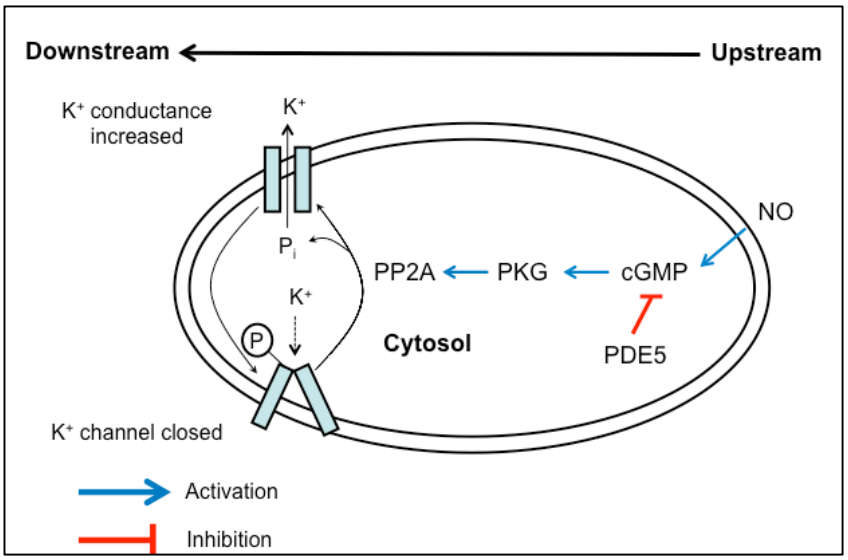

Figure 2. Diagram of the hypothesized cGMP/PKG pathway, adapted from Zhou et al. (1996). "+" sign means stimulation and "–" sign means inhibition of the pathway. AD means adenosine, NO is nitric oxide, PDE is phosphodiesterase, cGMP is cyclic guanosine monophosphate, PKG is a cGMP-dependent protein kinase, PP2A is protein phosphatase 2A, K^+ is a potassium ion channel, and K^+ with an attached "P" is a phosphorylated version of the potassium channel.

The pathway starts with adenosine-dependent stimulation of nitric oxide production by nitric oxide synthases (iNOS, nNOS) (Zhou et al. 1996). Increased levels of nitric oxide stimulate guanylyl cyclases to produce more cyclic guanosine 3′,5′-monophosphates (cGMPs), which in turn activate PKG. On the other hand, cGMPs can be hydrolyzed by phosphodiesterases (PDEs), which leads to the inhibition of PKG due to reduced levels of the cGMPs available for binding. From this study, activated PKG phosphorylates protein phosphatase 2A (PP2A) and consequently, the PP2A becomes activated and dephosphorylates the potassium ion channels located in the plasma membrane. This event activates the potassium ion channel and increases potassium ion current. Notably, Furukawa et al. (1996) developed a similar molecular pathway in hippocampal cells through pharmacological and electrophysiological interventions. They showed that potassium current activation is caused by NO/cGMP/PKG activation and leads to suppression of neuronal activity. However, they were unable to identify the phosphatase that directly activates the potassium channels.

Another research group investigated cGMP/PKG signaling and its effect on activation of plasma membrane K_{ATP} in HEK293 and human neuroblastoma cells (Chai and Lin 2010). Through electrophysiological studies in intact and transfected cells, they found that activation of PKG enzyme stimulates electrical current through the plasma membrane K_{ATP} channel. This effect was blocked through the application of 5-hydroxydecanoate (5-HD), which is a specific inhibitor of mitoK_{ATP}. Furthermore, the addition of NO donors or 8-Br-cGMP to murine respiratory neuronal slices revealed the activation of K_{ATP} as well as the inhibition of L-type Ca^{2+} channels (Mironov and Langohr 2007). This suggests the possibility of the plasma membrane K_{ATP} functioning downstream

of the cGMP/PKG-activated mitoK$_{ATP}$. Interestingly, a similar mechanism was proposed to function in myocytes subjected to *in vitro* and *in vitro* ischemia and reperfusion stresses (Ockaili et al. 2002; Cuong et al. 2006; Costa et al. 2006). It was found that stimulation of the cGMP/PKG pathway activates the K^+ currents in mitoK$_{ATP}$ and reduces cellular/tissue damage by attenuating lipid peroxidation, PTP formation, lactate dehydrogenase release (a marker of cellular death), DNA damage from apoptosis, and substantially reduces infarct size in whole hearts.

Evidence of PKG-mediated neuroprotection in mammals

There is an evidence of cellular protection mediated by the stimulation of PKG in mammalian neuron-like and neuronal cells. In PC12 cells, application of sodium nitroprusside (SNP), a nitric oxide donor, stimulated synthesis of cGMPs and decreased apoptotic DNA fragmentation in serum-deprived cells (Fiscus 2002). In another study that investigated the role of NO/cGMP/PKG as an anti-apoptotic mechanism, undifferentiated PC12 pheochromocytoma cells survived under serum-deprivation conditions when NO donors and cGMP analogs were applied (Kim et al. 1999). Moreover, application of 8-Br-cGMPs, pharmacological membrane permeable analogs of cGMPs, caused cellular protection from glutamate-induced toxicity in non-motor neurons (Urushitani et al. 1998).

Notably, there is a large quantity of data that suggests that guanosine, a purine nucleoside, also contributes to synthesis of cGMP and plays a protective role during ischemia- and reperfusion-like conditions in mammalian hippocampal neurons and brain cortical slices potentially through activation on K^+ ion channels (Oleskovicz et al. 2008; Lanznaster et al. 2016). Increased guanosine concentration could possibly lead to an upregulated synthesis of cGMP and subsequent activation of PKG enzyme.

Anoxia-tolerant organisms and their use as model of protection

As described above, mammalian brains are highly susceptible to hypoxia. Nevertheless, there are organisms that are able to withstand low oxygen stress on a chronic basis. Examples of such animals are fruit fly *Drosophila melanogaster*, crucian carp *Carassius carassius*, naked mole rat *Heterocephalus glaber*, and species of freshwater turtles such as *Trachemys scripta elegans* (Bickler 1992; Lutz et al. 1994; Wingrow and O'Farrell 1999; Haddad 2006; Gorr et al. 2010; Park et al. 2017). These organisms exhibit different mechanisms that make them anoxia-tolerant through evolution and changes in their physical environments. For instance, a freshwater turtle *T. scripta*, is an anoxia-tolerant vertebrate, which is able to survive without any oxygen under ice for months during winter time (Fernandes et al. 1997; Lutz et al. 2003). It does this by hibernating into a state of metabolic downregulation that prevents ionic pump failure, subsequent ionic imbalance, membrane depolarization, and the release of excitatory neurotransmitters (Milton et al. 2002; Milton and Lutz 2005). There are also additional neuroprotective mechanisms that impede cellular damage during anoxia and reperfusion such the upregulated expression of heat shock proteins and antioxidants (Lutz and Milton 2004).

It is important to emphasize that in anoxia-tolerant animal species, a response to physiological stress is "constitutively preconditioned", thus, neurons and other cell types affected by detrimental effects of anoxia and oxidative stress are in a constant state of preparedness (Lutz and Milton 2004). In such a manner, it is possible to study natural mechanisms of stress tolerance to further be able to mimic them in mammalian model organisms as well as potentially in humans to attain protection from a pathology incurred by an ischemic stroke.

Mechanisms of anoxia-tolerance in Drosophila from the metabolism point of view

D. melanogaster, commonly named a fruit fly, is another example of an anoxia-tolerant organism (Wingrove and O'Farrell 1999; Haddad 2006). The ability of *Drosophila* to survive the long-term lack of oxygen is remarkable. One of the well-studied mechanisms is the fruit fly's ability to fall into a state of hypometabolism and anoxic coma (Haddad et al. 1997; Haddad 2006; Dawson-Scully et al. 2010; Benasayag-Meszaros et al. 2015). It was previously shown that upon induction of anoxia, a wild type fruit fly's oxygen consumption decreases 10-fold as compared to the control levels; these decreased metabolic rates are thought to be due to metabolic modification and not due to the changes in gas exchange between environment and *Drosophila* respiratory system (Van Voorhies 2009). Possible reasons for this phenomenon include the tight regulation of mitochondrial function to oxygen concentrations in the environment as well as the complex oxygen sensing mechanisms that are unique to *Drosophila* (Van Voorhies 2009). For instance, during hypoxia, *Drosophila* shows a slowed down electron transport through electron transport chain (ETC), decreased activity of ETC Complex IV, opening of mitochondrial ion channels along with the upregulation of metabolism-stalling proteins (Lahiri et al. 2006; Teleman et al. 2005; Van Voorhies 2009). The low resting metabolic rates in conjunction with the efficient gas exchange systems further contribute to the above adaptations to hypoxia (Greenlee and Harrison 1998). Besides, chronic low-grade hypoxia leads to HIF-1 activation, which results in the activation of pro-survival genes (Teodoro and O'Farrell 2003). Mechanisms of protection from reoxygenation/oxidative stress include the activation of antioxidant molecular machinery, including methionine sulfoxide reductases, catalases, various selenoproteins, and disaccharides, such as trehalose (Chen et

al. 2002; Morozova et al. 2003; Roesijadi et al. 2007; Chung et al. 2010; Reyes-DelaTorre et al. 2012; Guan et al. 2017).

Evidence of PKG-mediated neuroprotection in anoxia-tolerant organisms

In mammals, decreased oxygen concentrations lead to cell injury and eventually death, whereas *Drosophila* can survive lack of oxygen without showing any obvious pathology (Haddad et al. 1997). Consequently, it is possible to study mechanisms of anoxia tolerance using *Drosophila* as a model organism (Liu et al. 2013; Zhao et al. 2012; Zhou and Haddad 2013). In flies, a PKG enzyme related to the PKG I mammalian isoform is encoded by the *Foraging* (*for*) gene, which shows a natural genetic variation: rover allele (for^R) and sitter allele (for^s). The *for* gene has been found to relate to a variety of phenotypes in the fruit fly such as food searching, learning and memory in addition to thermotolerance (Osborne 1997b; Ben-Shahar et al. 2002; Scheiner et al. 2004; Raizen et al. 2006; Mery et al. 2007; Dawson-Scully et al. 2007). Furthermore, it was demonstrated that PKG enzyme plays an important role in the organism's ability to tolerate low-oxygen levels (Dawson-Scully et al. 2010). In this study, the fruit flies carrying the rover allele expressed a PKG enzyme with high enzymatic activity, whereas the fruit flies with the sitter allele expressed a low-enzymatic activity PKG enzyme; the fruit flies with an s2 allele (for^{s2}) are mutants that have rover genetic background but show sitter phenotype expressing low-enzymatic activity PKG (Fig. 3A). It was further shown, that the for^R flies fall into the anoxic coma faster than the for^s flies (Fig. 3B); on the other hand, the for^R flies exposed to acute anoxia survive better than the for^s after 24 hours of reoxygenation (Fig. 3C). This evidence suggests that the high activity of the PKG is related to a faster downregulation of neurophysiological function and better survival rates after the onset of anoxia (Dawson-

Scully et al. 2010). The faster downregulation of the neuronal function could be a result of the "protective" plasma membrane hyperpolarization that was previously discussed. Correspondingly, the better post-anoxic survival of the rover fruit flies may indicate a potential involvement of mitochondria and a PKG-mediated attenuation of the oxidative stress.

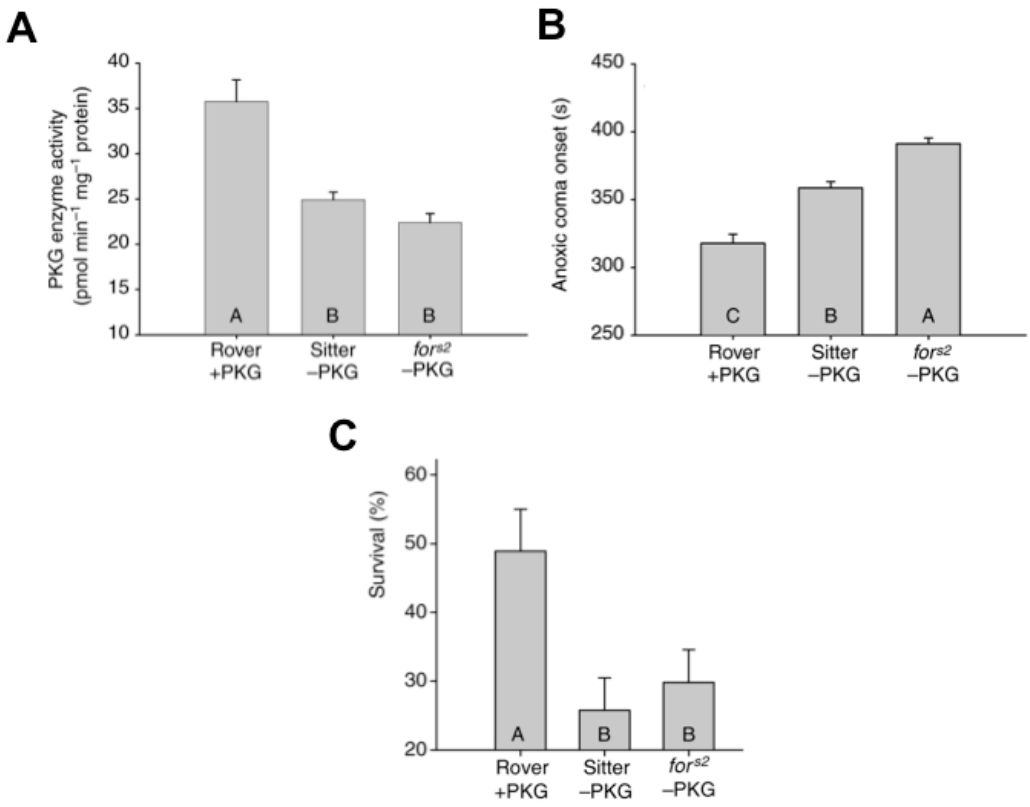

Figure 3. Characterization of the PKG enzyme in *D. melanogaster* subjected to anoxic stress (Dawson-Scully et al. 2010). A) PKG enzymatic activity versus allele of the *for* gene; B) anoxic coma onset versus alleles of the *for* gene; C) percent survival of the fruit flies returned to normal oxygen versus allele of the *for* gene.

Besides, it was established that in *Drosophila* S2 cells, NO or cGMP production or exogenous 8-Br-cGMP induce Rel/nuclear factor κB (NF - κB) - type transcription factor

translocation from cytosol into nucleus (Dijkers and Farrell 2009). This nuclear translocation is accompanied by the opening of non-specific cGMP-gated ion channels in the plasma membranes leading to calcium influx. Interestingly, NF – κB activation/nuclear translocation through upstream NO signaling by itself could be protective due to activation of several anti-apoptotic genes (Denk et al. 2000; Beere 2005).

Protective effects of the cGMP/PKG signaling appear to be evolutionarily conserved in vertebrates since a freshwater turtle *Trachemis scripta* also demonstrated protection against neuronal death with increased cGMP/PKG signaling as described further. In a study, in which *T. scripta* turtle primary neuronal cultures subjected to anoxia and reoxygenation were treated with pharmacological stimulators and inhibitors of PKG, an activation of PKG resulted in decreased neuronal death compared to the control treatment, whereas the inhibition of PKG stimulated cell death (Fig. 4, Nayak et al., unpublished). As a result of this study, it is possible that PKG enzyme is also involved in the anoxia-tolerance in *T. scripta.*

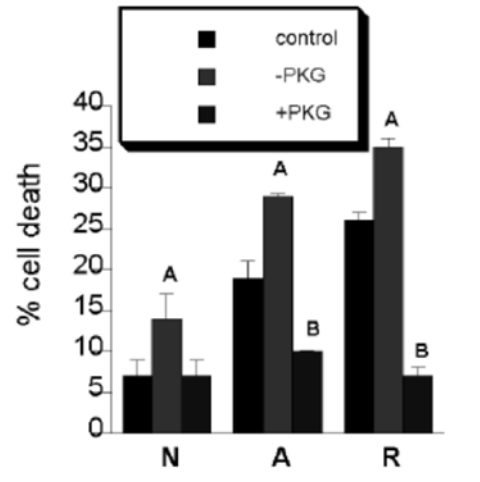

Figure 4. Cell death rates in the primary neuronal cell cultures of *T. scripta* subjected to cGMP/PKG pharmacological manipulation and various oxygen conditions. Oxygen conditions were the following: 1hr normoxia (N), 4hrs anoxia (A), 4hrs reoxygenation (R). Different letters above the bars refer to significant differences between subgroups in each of the oxygen conditions. The "–PKG" refers to the neuronal cultures treated with a PKG inhibitor; the "+PKG" refers to the neuronal cultures treated with a PKG activator (Nayak et al. unpublished).

Role of anoxia and cGMP/PKG signaling in mitochondrial biogenesis

Besides the above mechanisms of protection from low oxygen and oxidative stress, an increase in mitochondrial mass or mitochondrial biogenesis might be protective to an organism upon the aforementioned physiological stresses. Mitochondrial biogenesis is an intracellular process, by which new mitochondria are derived from pre-existing mitochondria. In mammalian cells, mitochondrial biogenesis is regulated by the transcriptional co-activator peroxisome proliferator-activated receptor γ co-activator 1α (PGC-1α), which in turn activates the transcription factors responsible for downstream transcription of mitochondrial DNA (mtDNA) and activation of antioxidant genes (Liang and Ward 2006). It was previously shown that in pathological conditions such as Alzheimer's disease, cardiac and muscle pathologies, renal failure, and aging, there is a decrease in mitochondrial density in cells such as neurons, hepatocytes, myocytes, and renal tubules (Santos et al. 2010; Weinberg 2011; Zhu et al. 2013; Pisano et al. 2016). In treatments that protect those tissues from toxic stimuli as well as in cancer, there is an increased rate of mitochondrial biogenesis detected (Liu et al. 2017; Nisoli et al. 2003; Zhang and Han 2017; Prakasam et al. 2017). Thus it is possible that newly formed healthy mitochondria contribute to cellular health and healthy metabolism. Since healthy

mitochondrial function is essential after a period of ischemic/hypoxic stress, it is hypothesized that increased numbers of healthy undamaged mitochondria help tissues to recover from such stress faster and with less pathology by providing oxygen-deprived tissues with enough energy to sustain their survival upon return of oxygen (Li et al. 2016; Raefsky and Mattson 2017; Tian et al. 2017). Interestingly, some chemicals such as Glycogen synthase kinase 3 (GSK-3) inhibitors, besides restoring impaired mitochondrial biogenesis, also prevent reactive oxygen species (ROS) production and damage in neurons after onset of ischemia in rodents (Valerio et al. 2011). Furthermore, Stetler et al. (2012) showed that mitochondrial biogenesis contributes to ischemic neuroprotection afforded by lipopolysaccharide (LPS) preconditioning in rat cortical neurons. Likewise, Xie et al. (2014) demonstrated that after oxygen deprivation, rat neuronal cortex shows increased but limited natural mitochondrial biogenesis. Besides ischemia/reperfusion, there are numerous chemicals that may increase mitochondrial biogenesis; examples of such chemicals are NO, (an upstream PKG activator) and cGMP (direct PKG activator). These molecules are thought to induce PGC-1α and promote significant levels of mitochondrial biogenesis in mammalian *in vitro* and *in vivo* models as further discussed. In neuron-like PC12 cells, increased NO leads to mitochondrial biogenesis with higher respiration rates and elevated cellular energy production (Nisoli et al. 2004b). Similarly, it was found that in kidneys subjected to low oxygen followed by reperfusion, activation of the PKG signaling cascade stimulates mitochondrial biogenesis leading to protection of rodent kidneys from an acute injury (Whitaker et al. 2013).

Mitochondrial biogenesis in Drosophila

In *Drosophila*, mitochondrial biogenesis is regulated by *Spargel* gene, which is the fruit fly's homolog of mammalian PGC-1α (Mukherjee et al. 2014). Similar to its mammalian counterpart, *Spargel* controls nuclear transcription of mitochondrial genes. It has not been yet shown whether NO or cGMP-induced activation of PKG pathway in fruit flies induce mitochondrial biogenesis and whether increased mitochondrial density plays any role in fruit fly's anoxic tolerance. Nevertheless, it is currently known that overexpression of *Spargel* in fly's gut leads to increased mitochondrial metabolism, whereas the overexpression of mitochondria in stem cells and progenitor cells within the gut leads to an increased lifespan (Rera et al. 2012). For example, *Indy* (I'm Not Dead Yet) is *Drosophila* genetic model of longevity for which an increased mitochondrial biogenesis is a characteristic feature (Rogers and Rogina 2014). *Indy* is a gene that encodes plasma membrane transporter of intermediates of the TCA cycle; its decreased expression is usually associated with the increased lifespan, increased expression of dPGC-1, mitochondrial biogenesis, as well as reduced levels of ROS (Rogers and Rogina 2014).

It has not been yet shown whether NO or cGMP-induced activation of the cGMP/PKG pathway in fruit flies induces any mitochondrial biogenesis and whether an increased mitochondrial density plays any role in anoxia tolerance and neuroprotection. Currently, there are no reports of an anoxia-mediated increase of mitochondrial density in *Drosophila.*

SPECIFIC AIMS OF THE RESEARCH

1. Determine if natural variation of the *Drosophila melanogaster foraging* gene shows differences in mitochondrial dynamics and function upon anoxia/reoxygenation stress;
2. Develop an *in vivo* model of stroke using wild type *Drosophila* and test whether pharmacological activation of the cGMP/PKG is protective in these conditions;
3. Develop an *in vitro* model of low oxygen and oxidative stress using *Drosophila* S2 cells;
4. Establish whether an activation of the cGMP/PKG pathway leads to better survival of cultured *Drosophila* cells subjected to the stroke-like conditions and investigate the underlying molecular signaling mechanisms;
5. Investigate whether an activation of the cGMP/PKG pathway leads to better survival of mammalian neurons subjected to low oxygen and oxidative stress.

CHAPTER 1

Mitochondrial biogenesis in cGMP/PKG-regulated anoxia-tolerance in Drosophila melanogaster

1.1. Introduction

As it was previously discussed in the Introduction chapter, flies carrying the rover allele of the *for* gene show a PKG with high enzymatic activity, whereas the fruit flies with the sitter allele show a PKG with low enzymatic activity (Osborne 1997). It was shown that rover flies exposed to acute anoxia demonstrate higher survival rates upon return to normal oxygen levels than sitter flies (Dawson-Scully et al. 2010). This evidence suggests that the high activity of PKG (as in rover allele-carrying fruit flies) offers neuroprotection after onset of anoxia followed by reoxygenation. The existence of such protection from low oxygen and reoxygenation stress may also indicate the presence of a currently unknown antioxidant mechanism, and possibly, the involvement of mitochondria as they are known to be the centers of life and death decision-making within a cell (Petit et al. 1996; Zorov 1996; Hetts 1998). Mitochondrial biogenesis is an intracellular process by which new mitochondria are derived from the pre-existing mitochondria (Nisoli et al. 2004a; Marin-Garcia and Goldenthal 2000; Nisoli et al. 2004a). In mammalian cells, mitochondrial biogenesis is regulated by transcriptional co-activator peroxisome proliferator-activated receptor γ co-activator 1α (PGC-1α), which in turn, activates the transcription factors responsible for the downstream transcription of the mitochondrial DNA (mtDNA) and activation of antioxidant genes (Liang and Ward 2006; Houten and

Auwerx 2004; Li et al. 2017). Since healthy mitochondrial function is essential after a period of ischemic or hypoxic stress, it is hypothesized that increased numbers of healthy undamaged mitochondria help tissues to recover from the physiological insult faster and with less injury by providing the oxygen-deprived tissues with enough energy to sustain their survival upon reoxygenation (McLeod et al. 2005; Thornton et al. 2017). It is also possible that increased numbers of mitochondria lead to elevated levels of ROS and thus, result in cell damage and tissue pathology (Lehman et al. 2000; Russell et al. 2004). It is known that in mammals, NO signaling, which leads to cGMP synthesis and PKG activation, causes mitochondrial biogenesis (Nisoli et al. 2004a; McLeod et al. 2005; Shen et al. 2011). Since the role of mitochondrial biogenesis in *Drosophila* cGMP-dependent Protein Kinase (PKG)-regulated anoxia-tolerance is completely unknown, the main objective of this study was to determine whether a higher activity of PKG enzyme would result in increased levels of mitochondrial biogenesis in flies exposed to a non-lethal anoxic stress. In this study, mitochondrial biogenesis was characterized in two types of fruit flies: fruit flies whose PKG enzymatic activity is naturally high (rovers, for^{R}), and fruit flies whose PKG enzymatic activity is naturally low (sitters, for^{s}). The mitochondrial content was quantified biochemically by measuring whole fly citrate synthase enzymatic activity levels. The biochemical evaluation of mitochondrial content was accomplished by measuring differences in citrate synthase (CS) enzymatic activity in the protein extracts of rover and sitter fruit flies, which were later compared. CS, an essential TCA cycle enzyme and mitochondrial matrix protein that catalyzes a formation of citrate from oxaloacetate and Acetyl-CoA, is a known validator of the mitochondrial content as it is normally expressed at equivalent levels in the corresponding tissues of an animal (Eigentler et al.

2012; Charette et al. 2011). Furthermore, mitochondrial content was assayed molecularly by measuring the relative levels of mitochondrial protein cytochrome c by Western blotting. Additionally, to test whether the changes in mitochondrial density resulted in functional mitochondria, metabolic rate measurements of individual rover and sitter flies were performed. Since mitochondrial density as well as functionality is essential for animal survival upon anoxia, results of this study led to a better understanding of *Drosophila* innate anoxia-tolerance strategies as well the role of the PKG signaling in this resilience.

1.2. Materials and methods

1.2.1. Drosophila rearing and husbandry

Rover and sitter fruit flies were reared on standard corn food with 12 hours day: 12 hours night cycle at 25ºC for at least two weeks. After that, the food bottles with flies were cleared from any adult flies and left for up to 4 days to eclose. Then, males (0-4 day-old) were collected and transferred to plastic vials in groups of 40 individuals per vial containing standard fly food. Anoxia exposure experiments were performed on days when the flies were 5 to 9-days-old.

1.2.2. Anoxia induction

Argon gas anoxia was introduced for 1 hour at room temperature. For protein extraction experiments, during anoxia, vials with rover and sitter flies were placed in a clear plastic box with a closed lid. Each vial's open side was covered with two layers of cheesecloth material tightened with a rubber band. The plastic box was connected through a set of silicone tubing to a flask filled with DI water and to a flow meter attached to an argon gas tank. Argon gas was pumped through the box for 1 hour at a continuous rate. At the end of the cycle, argon was removed with a vacuum pump and the flies were left to

reoxygenate inside a standard *Drosophila* incubator. Oxygen amounts inside the anoxic box were tested using the Arduino oxygen sensor as well as the Arduino software to ensure that the oxygen levels were less than 0.1% during the anoxic treatment. Each set of flies was left to reoxygenate for a specific time: 1 hour, 4 hours, 8 hours, 12 hours, or 24 hours. In addition, there were control sets of both genotypes of flies that were not exposed to anoxia. At each corresponding time point, the flies were collected in 1.7mL Eppendorf tubes and frozen in a mix of dry ice and methanol, segmented, and stored at -80ºC until protein extraction procedures.

1.2.3. Protein extractions

Protein extractions were performed in a PBS-Tween-20 extraction buffer as described in Charette et al. (2011) containing 1 × SigmaFast protease inhibitor cocktail using a plastic pestle homogenizer and performing 30 strokes followed by the mechanical sonication for 5 seconds. The homogenates were then centrifuged at 13200 RPM at 4ºC for 10 minutes and the supernatant containing extracted proteins was collected and stored at -80ºC. To determine protein concentrations in homogenates, Pierce 660nm Protein Assay kit was used.

1.2.4. Citrate synthase enzymatic assays

To quantify the relative numbers of mitochondria in rover and sitter fruit flies subjected to anoxia/reoxygenation, citrate synthase enzymatic assays were carried out. The citrate synthase enzymatic assays were performed as described in Eigentler et al. (2012) but modified for a 96-well plate absorbance reader format. Briefly, 5µg of total protein per assay was used. Solutions of oxaloacetate, acetyl-CoA, and DTNB (5,5'-Dithiobis(2-nitrobenzoic acid)) were prepared beforehand. The absorbance of a resulting product was

measured at 412nm using a SpectraMax plate reader using the kinetic measurement option. The interval time was 15 seconds and total time of the assay was 120 seconds. All the measurements were conducted at room temperature. A regression equation was determined from the linear portion of the kinetic graph (Time vs. Absorbance at 412nm) and the graphs showing the relative reaction product absorbance values were constructed. N of 3 samples for each time point and fly type was assayed.

1.2.5. SDS-PAGE and Western blotting

To indirectly quantify the relative mitochondrial content in rover versus sitter fruit flies subjected to anoxia and reoxygenation, sodium dodecyl sulfate polyacrylamide gel electrophoresis (SDS-PAGE) and Western blotting procedure using anti-cytochrome c antibody were performed. For SDS-PAGE gel electrophoresis, 5µg of total protein was loaded into each lane of 4% acrylamide stacking/12% acrylamide resolving gels. Samples were prepared in 1 × Laemmli sample buffer and PBS-T extraction buffer; they were loaded in such way that all the rover and sitter samples for each specific time point were localized on the same gel. The gels were run for 1 hour at 120V. Resolved proteins were transferred to PVDF membranes for 1 hour at 0.3Amp at 4ºC. Membranes with transferred proteins were then blocked in 5% milk/ TBST buffer for 1 hour and incubated at 4ºC overnight in 5% fat-free milk/ TBST with cytochrome c antibody (Abcam, Cambridge, UK) at 1:3000 dilution. Next day, the membranes were washed three times in TBST buffer and incubated for 1 hour in 5% Milk/TBST buffer containing the corresponding 2º antibody. After the incubation, the membranes were washed with TBST (2 times, 5 minutes each time) followed by a TBS buffer wash (1 time for 5 minutes). Afterwards, the membranes were incubated with ECL reagent (Thermofisher, Waltham, MA) for 5 minutes

in the dark and imaged with the Li-Cor Odyssey fluorescence reading system with the chemiluminescence option on (LI-COR Biosciences, Lincoln, NE). For loading controls, Swift protein staining dye (G-Biosciences, St. Louis, MO) was used on the membranes, and fluorescent images were taken with the Li-Cor system. Finally, the resulting images were analyzed using ImageJ NIH software (Schneider et al. 2012).

1.2.6. In vivo metabolic rate measurements

To determine whether mitochondria generated upon the reoxygenation was functional, metabolic rates of rover and sitter fruit flies were assessed before and after anoxia. *In vivo* metabolic rate measurements were assessed using Sable CO_2 production measurement system (Sable Systems International, North Las Vegas, NV). The flies used in these assays were 5 to 9-days old grown at 25ºC in 12 hours light: 12 hours dark cycle. *Drosophila* activity monitoring assay (DAM) was performed simultaneously to determine the resting metabolic rates. Individual flies were loaded into cylindrical glass CO_2 chambers attached through the DAM system. The DAM system allowed for measuring activity of individual flies in the tubes when they crossed the DAM system, which emits infrared light that gets disrupted while a fly is located within the system; this gets counted as one movement (Pfeiffenberger et al. 2010). On each end of a chamber, there was a plastic plug hermetically connecting the chamber to the flow system. Each glass chamber had a small clear tube (about a 1cm-1.5cm-long) filled with 5% sucrose/red dye/1% agar attached to a Velcro tape. Before starting argon gas flow, the flies were allowed to adjust to room temperature and new environment for up to 2 hours. At the same time, CO_2 production and activity were recorded to determine baseline metabolic rates and activity differences between normoxic rover and sitter flies. Subsequently, anoxia was induced into each

chamber for one hour by pumping argon gas at a constant flow rate at room temperature. The activity monitoring showed that flies fell into locomotory coma within 1 minute from the start of anoxia and there was no additional locomotor activity until the reoxygenation/recovery phase. At least three flies of each genotype were assessed. The principle behind CO_2 measurement was that the plastic chambers housing individual flies collected CO_2 produced by *Drosophila* from respiration; the CO_2 contents of each of 8 the chambers were measured in a consecutive order by passing the gas contents of the chambers through a system containing a specific CO_2 gas probe. The analysis software (ExpeDataSetup_v1_8_4) translated the CO_2 measurements into ppm values, which then were expressed in units of µL of CO_2/fly/10 minutes. A macro was written to allow a faster rate of data analysis since the recordings were done for up to 24 hours with CO_2 being collected from each tube every 10 minutes. Further analysis was performed using Excel spreadsheets by aligning 10-minute batches of the CO_2 production values with the 10-minute batches of individual fly activity.

1.2.7. Statistics

The results were expressed as the means ± S.E.M. The statistical analysis was done using Student t-test or one-way ANOVA followed by Student-Newman-Keuls *post-hoc* test to determine significant difference between a group means. The quantitative results with the $P<0.05$ were considered statistically different.

1.3. Results and discussion

1.3.1. Citrate synthase activity measurements in rover and sitter Drosophila

From citrate synthase (CS) relative activity measurements at different post-anoxia time points, rovers and sitters showed a different mitochondrial dynamics pattern (Fig. 5).

Rover flies did not show any significant variation in citrate synthase during normoxia or upon reoxygenation. On the other hand, sitter flies CS enzyme showed a significant increase in activity at 8 hours of reoxygenation/recovery. In addition, at 24 hours of reoxygenation, sitter CS activity levels fell down to normoxic levels again. Unexpectedly, at 24 hours of reoxygenation, relative CS rates were not statistically different between the two fly types but sitter CS activity decreased significantly compared to 8 hours of reoxygenation/recovery. It is possible, that mitochondrial density increased but mitochondria were further degraded. Moreover, the CS activity rates of normoxic flies were not different between two genotypes and were indeed statistically different only at 8 hours post-anoxia. Interestingly, it has been previously reported that normoxic rover and sitter 3rd instar larvae do not show differences in basal metabolic rates as measured by oxygen consumption (Kaun et al. 2007). In this manner, if metabolic rates of the two genotypes are not different, then it is possible that the number of mitochondria is relatively the same during normoxia but may change upon physiological stress such low oxygen and reoxygenation; this needs to be further investigated in depth. It will be essential to further measure the CS activity in normoxic flies at different times of the day to ensure that there are no enzymatic activity fluctuations at different time points of a day thus indicating a potential circadian cycle influence on the CS activity.

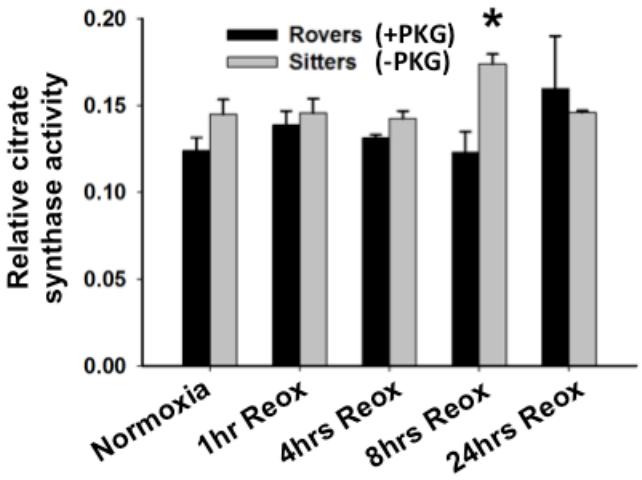

Figure 5. Relative citrate synthase enzymatic activity assay results for different time points before and after anoxia as determined by the formation rate of colored product (O.D. at 412nm). The star represents a statistical significance between a corresponding rover and sitter within a time point group, $P<0.05$, $N=3$.

1.3.2. Assessment of cytochrome c protein expression levels in rovers and sitters

To determine if differences in anoxia tolerance could be due to differences in mitochondrial density, relative cytochrome c protein expression level changes were assessed. The results of this study are shown in Fig. 6 and 7. I first studied the protein expression patterns in each individual fly type in normoxia as well as throughout recovery/reoxygenation time points (Fig. 6). When rover and sitter cytochrome c expression was determined and plotted on the same graph (rover normoxic cytochrome c expression was appointed as the control for image quantification purposes), there was a clear pattern of sitter cytochrome c expression increase at 8 and 24 hours of recovery but no statistical difference was found between the genotypes. The lack of statistical difference was due to very high protein density values in sitter post-anoxic samples, which resulted

in the variability. To bypass this problem, all the samples from each individual time point were run on the same gel (Fig. 7). There, normoxic rovers and sitters demonstrated similar cytochrome c protein expression levels. In addition to normoxic samples, almost all of the post-anoxic samples showed a high degree of variation and thus no statistical difference. On the other hand, at 8 hours of reoxygenation (recovery), there was a statistically significant difference in cytochrome c expression between rover and sitter flies. The difference between cytochrome c protein levels was almost 4-fold with sitters demonstrating the higher cytochrome c protein content and potentially higher mitochondrial density.

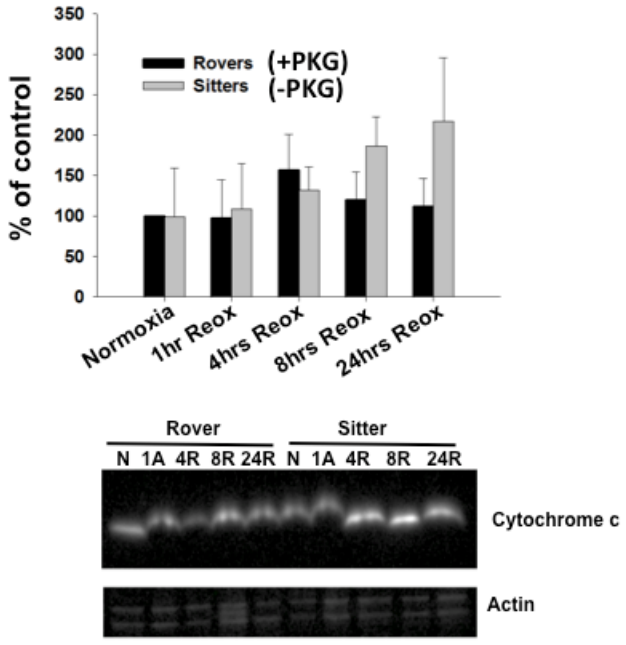

Figure 6. Western blot results and quantification showing expression of mitochondrial protein cytochrome c in whole fruit fly homogenates. A) Western blot quantification results showing the percent of control levels, N=4-5. Recovery means the time during which the flies were reoxygenated before sample collection. B) Representative Western blot image showing the cytochrome c protein levels and actin (as

loading control) levels. Rover normoxic cytochrome c levels were chosen as control. Flies were subjected to 1 hour of anoxia and reoxygenated (recovered) for different periods of time before they were collected and flash frozen for further protein analysis.

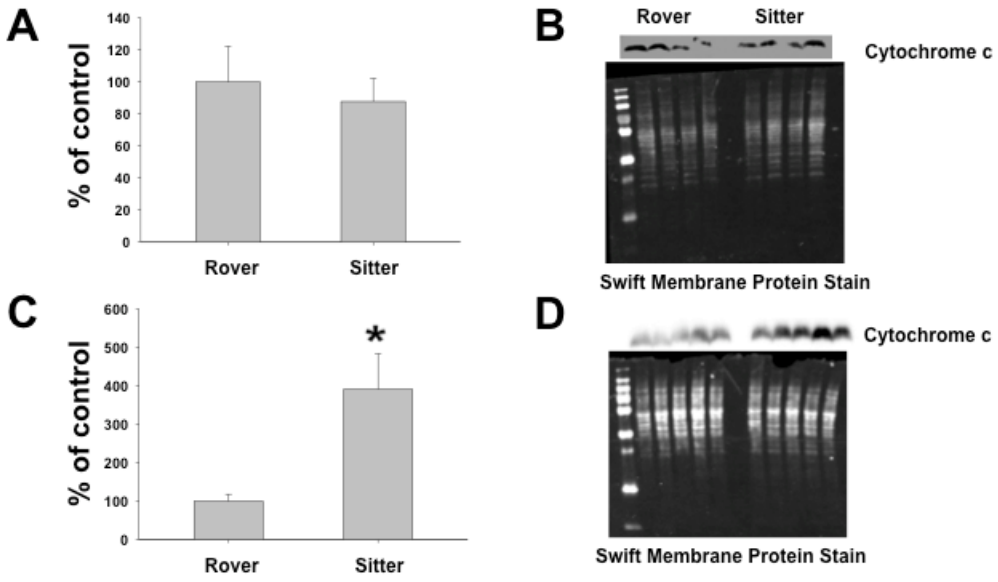

Figure 7. Western blot results and quantification showing expression of mitochondrial protein cytochrome c in whole fruit fly homogenates during normoxia and at 8 hours of reoxygenation. A), B) Western blot quantification results showing the percent of normoxic cytochrome c levels, N=4; C), D) Western blot quantification results showing percent of cytochrome c levels at 8 hours of reoxygenation, $P<0.05$, N=5. Different letters inside the bars designate the statistical difference between the groups. Swift membrane protein stain was used as a loading control to allow quantification of results. Western blot images show all rover sample bands followed by all sitter sample bands.

From both CS activity assays and Western blotting, it was determined that rovers and sitters did not have different basal levels of mitochondrial content. On the other hand, upon exposure to 1 hour of air anoxia and reoxygenation at 25ºC, the sitter relative CS activity

increased significantly possibly due to mitochondrial biogenesis or mitochondrial repair; conversely, the rover relative mitochondrial content stayed constant before and after anoxia up to 24 hours of reoxygenation. Further reoxygenation points must be investigated in future studies.

1.3.3. Assessment of metabolic rates of rovers and sitters

Since the previous quantification of mitochondrial biogenesis showed a potential increase in mitochondrial mass in sitters at 8 hours of reoxygenation, it was necessary to test if the new mitochondria were functional, suggested by the increased metabolic rates. I hypothesized that increased mitochondrial content would translate in higher metabolic rates of the whole animal as more mitochondria should generate more ATP by using more oxygen. The results of these experiments are shown in Fig. 8 and 9. The data demonstrated differences between the average metabolic rates of two *Drosophila* genotypes used. Significant differences in average metabolic rates between rover and sitter flies were found at 8 hours post-1 hour of anoxia. The DAM system fly data also demonstrated that rover and sitter flies displayed different levels of locomotor activity, though not significantly different, after the onset of anoxia at the equivalent time points (data not shown). Since an increased locomotor activity of an organism leads to an increased average metabolic rate, to account for the fly metabolic rates influenced by physical activity, the average resting metabolic rates corresponding to times of inactivity were determined (Speakman and Selman 2003). The data are shown in Fig. 9C. It was found that the average resting metabolic rates were consistently higher in sitters then in rovers upon reoxygenation but no statistical significance was displayed between the different genotypes at any of the assessed time points. From this, a higher number of trials should be performed to see if

there is any statistical difference between rover and sitter post-anoxic average resting metabolic rates, as an obvious trend was present in my study. Importantly, at about 21-hours of reoxygenation, sitter flies continued displaying higher resting metabolic rates than rovers. This phenomenon shows the opposite trend from the pre-anoxic resting metabolic rate pattern. Surprisingly, sitters consistently showed higher metabolic rates during one hour of anoxia. Anoxic metabolic rate values were the true reflections of metabolism at rest since the flies showed a complete absence of locomotion, which was typical of an anoxic coma. When the metabolic rate measurement results are compared to the citrate synthase activity and Western blot results, there were significant changes observed in all three measurements at 8 hours of reoxygenation displayed by sitter flies. More specifically, at 8 hours after anoxia, citrate synthase activity increased significantly, cytochrome c protein expression levels were raised, and these changes were reflected by the increased metabolic rates. From this, the newly generated mitochondria in sitter flies displayed functionality upon reoxygenation. A difference in post-anoxic metabolic rates in sitters and rovers could have indicated different levels of mitochondrial health. In this manner, sitter flies could have been making new mitochondria from old undamaged mitochondria thus preserving metabolic rate throughout almost half of the reoxygenation period. On the other hand, rover mitochondria could have been undergoing a process such as mitophagy or displayed a decreased functionality due to oxidative damage from reoxygenation.

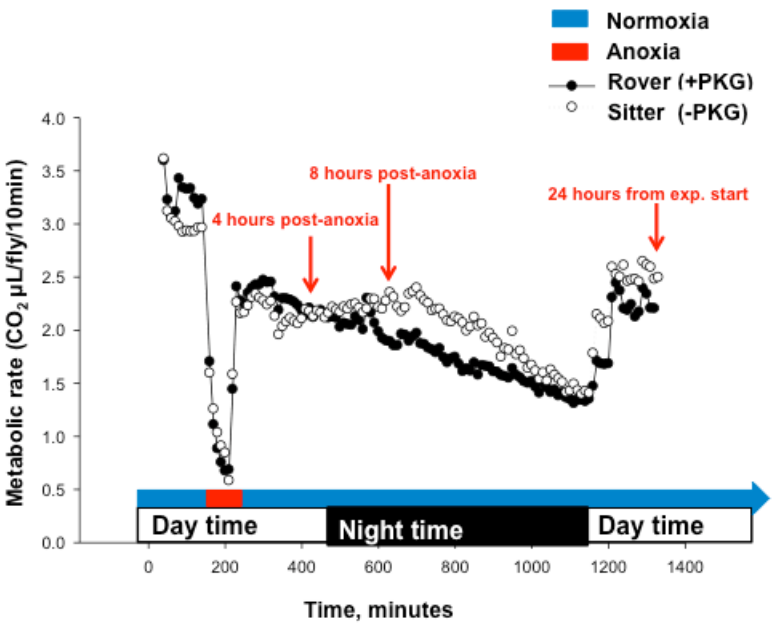

Figure 8. Average metabolic rate levels during experiments with 1 hour of anoxia. Rover and sitter fly metabolic rate measurements before and after exposure to 1 hour of anoxia. Statistical significance between rover and sitter flies was noted at around 8 hours of recovery ("post-anoxia" or reoxygenation), $P<0.05$ N=6-8.

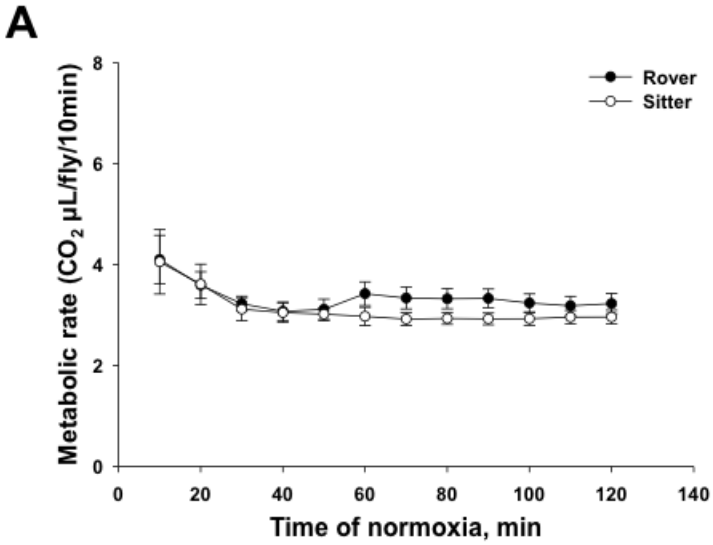

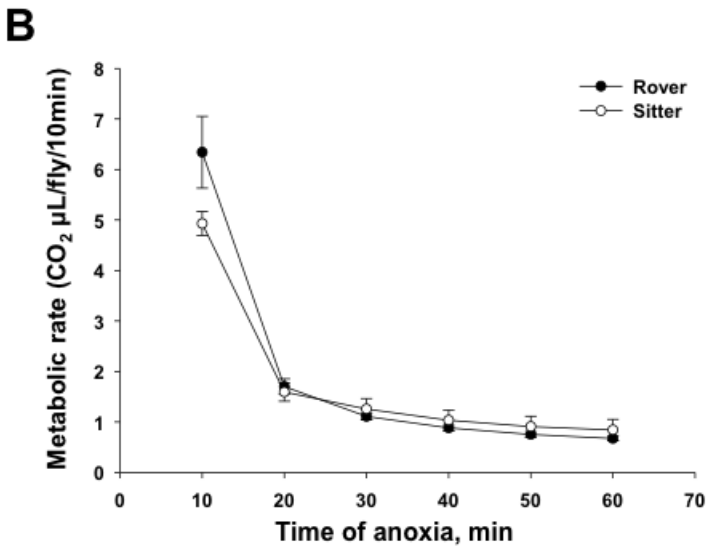
B
Rover
Sitter
Metabolic rate (CO_2 µL/fly/10min)
0
1
2
3
4
5
6
7
8
0
10
20
30
40
50
60
70
Time of anoxia, min

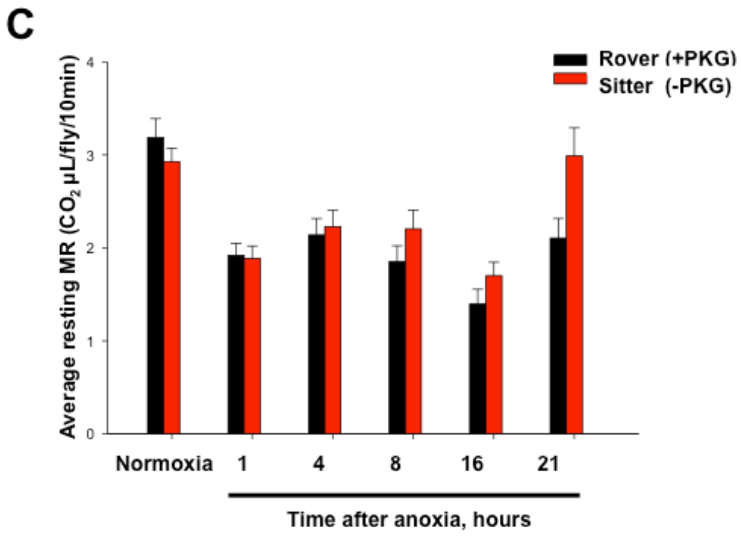
C
Rover (+PKG)
Sitter (-PKG)
Average resting MR (CO_2 µL/fly/10min)
0
1
2
3
4
Normoxia
1
4
8
16
21
Time after anoxia, hours

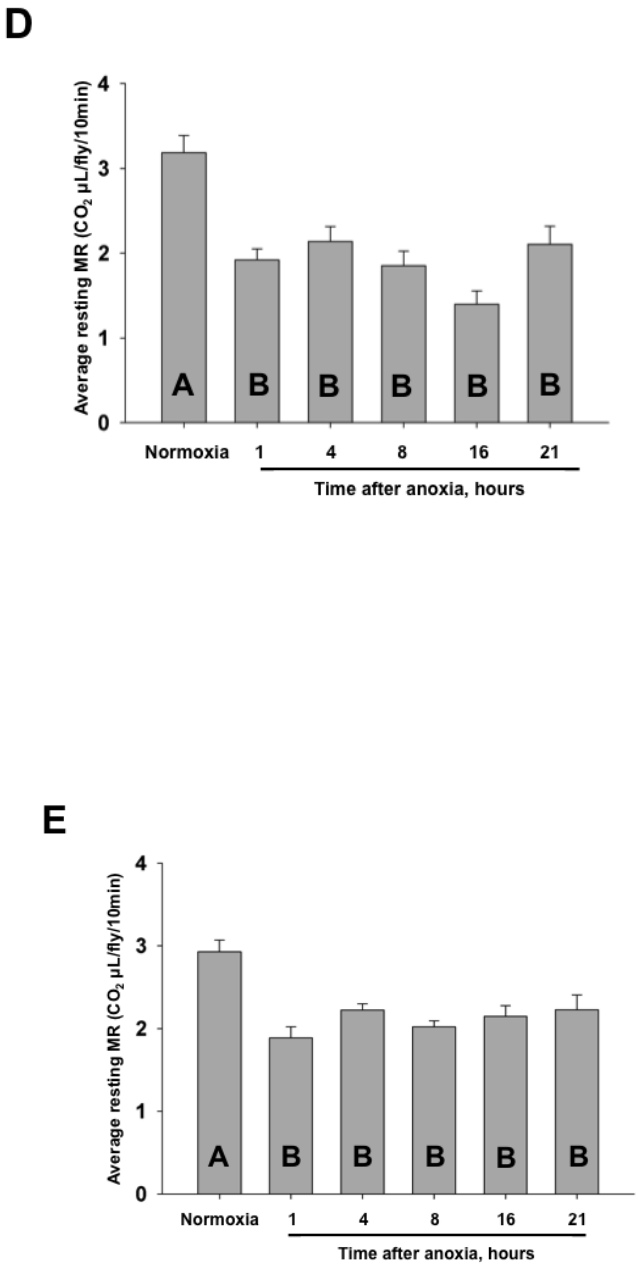

Figure 9. Average metabolic rate levels during 1-hour anoxia exposure experiments. A) Normoxia (pre-anoxic) metabolic rates of rover and sitter flies. B) Metabolic rates of rovers and sitters during the first hour of anoxia. C) Rover and sitter fly resting metabolic rates before and after exposure to 1 hour of anoxia as calculated from the periods of fly inactivity. D) Rover resting average resting metabolic rates at different

time points with statistical comparison. E) Sitter resting average resting metabolic rates at different time points with statistical comparison. Time after anoxia is equivalent to the time of recovery or reoxygenation period. No significant difference was detected at each time point comparison between the rover and sitter fruit flies, $P<0.05$, N=6-8.

Next, to "push the limit" of metabolic rate changes taking place during and after an anoxic exposure, flies of the two genotypes were exposed to 4 hours of anoxia. I hypothesized that the differences in metabolic rate patterns of rover and sitter fruit flies detected in the previous experiment would become statistically significant if the animals were exposed to a longer period of anoxia. To accomplish this, both genotypes of flies were exposed to 4 hours of anoxia and then were reoxygenated for up to 16 hours. It was critical not to expose the fruit flies to extended anoxic stress due to the high probability of animal death. Death would decrease the number of animals for which the average metabolic rates were calculated. The results of this experiment are shown in Fig. 10. Here, as hypothesized, longer exposure time to anoxia increased metabolic rate differences between rovers and sitters as observed in Fig. 8 and 9. Sitters demonstrated significantly higher anoxic metabolic rates than rovers during the exposure to anoxia. These metabolic rate differences became statistically significant at about 4 hours of anoxia. One possible explanation for this outcome is that rovers might be undergoing a deeper hypometabolic state leading to lower metabolic rates compared to sitters. Since rovers survive prolonged exposure to anoxia better than sitters, it is possible that the observed results were due to a better energy usage in which lower demand met the lower supply (Dawson-Scully et al. 2010). Moreover, this trend is reflected by the locomotory function difference between these two genotypes when exposed to anoxia. Rovers show a significantly quicker drop in locomotor

activity upon anoxia induction than sitters (Dawson-Scully et al. 2010).

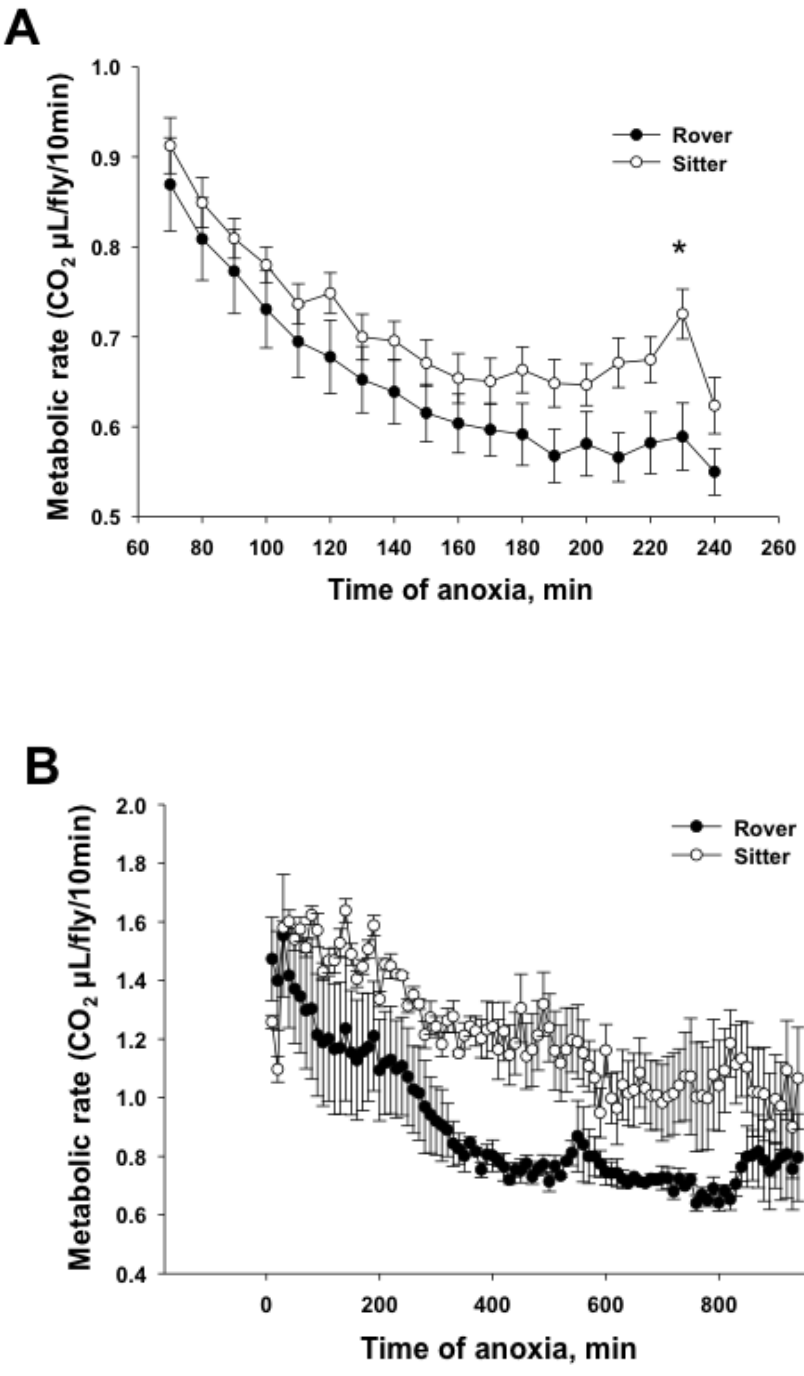

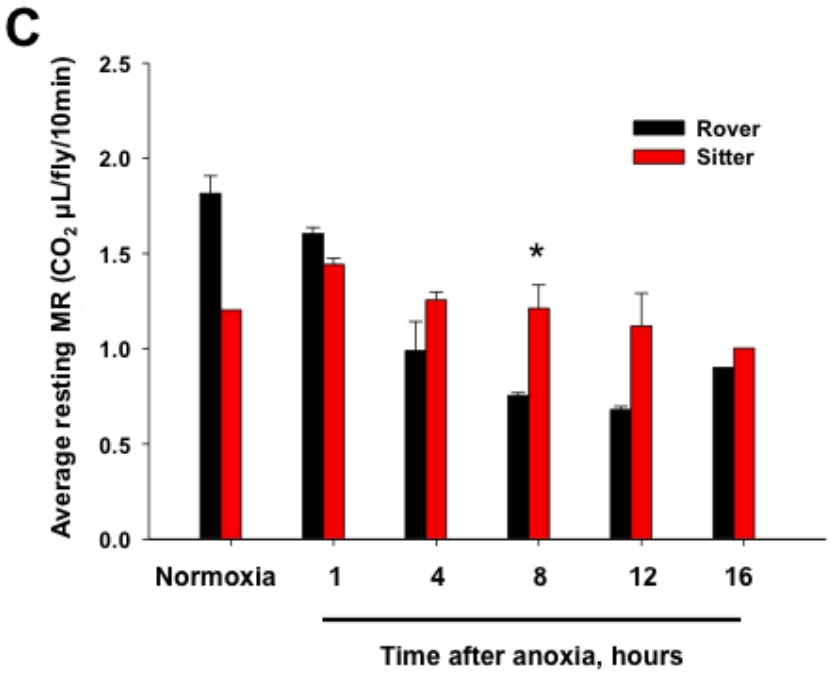
C
Average resting MR (CO_2 µL/fly/10min)
2.5
2.0
1.5
1.0
0.5
0.0
Rover
Sitter
*
Normoxia
1
4
8
12
16
Time after anoxia, hours

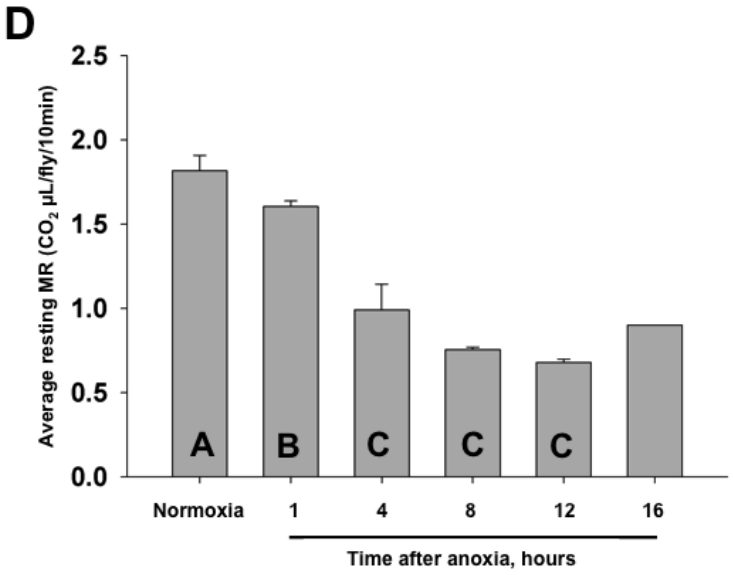
D
Average resting MR (CO_2 µL/fly/10min)
2.5
2.0
1.5
1.0
0.5
0.0
A
B
C
C
C
Normoxia
1
4
8
12
16
Time after anoxia, hours

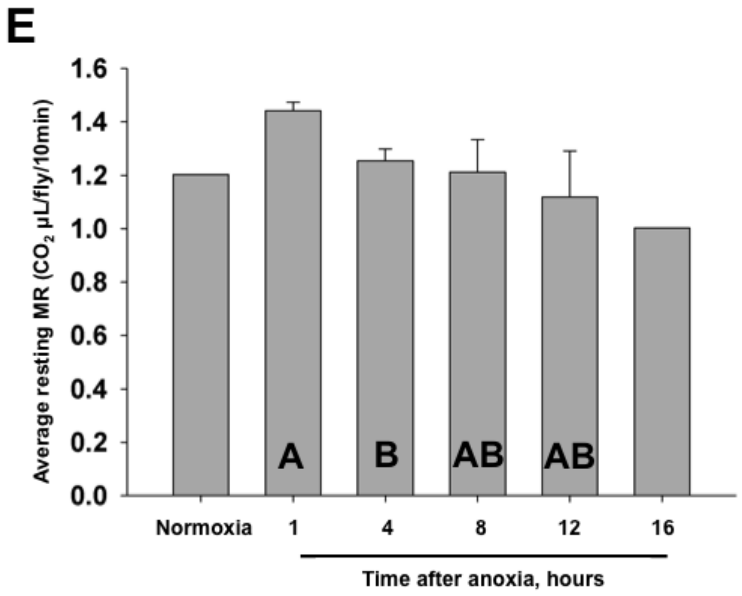

Figure 10. Metabolic rates in experiment with the 4 hours of anoxia exposure. A) Metabolic rates of rovers and sitters throughout 1 to 4 hours of anoxia. The values of metabolic rates for the first hour are not shown. B) Reoxygenation/recovery metabolic rates; C) Rover and sitter resting metabolic rates before and after exposure to 4 hours of anoxia as calculated from the periods of fly inactivity; D) Rover resting average resting metabolic rates at different time points with statistical comparison; E) Sitter resting average resting metabolic rates at different time points with statistical comparison. Time after anoxia is equivalent to the time of recovery or reoxygenation period, $P<0.05$, $N=3$.

Upon reoxygenation from the 4-hour anoxia, the flies with different genotypes showed exactly the same trend observed upon the recovery from the 1-hour anoxic treatment: sitters had significantly higher average metabolic rates then rovers throughout a considerable period of time that matched the metabolism of the flies exposed to 1 hour of

anoxia (Fig. 11). When the resting metabolic rates were calculated, a significant difference between rovers and sitters was found at 8 hours post-anoxia again. This is very interesting as it is possible that it did not matter if the flies were exposed to 1 hour or 4 hours of anoxia, as the expression of mitochondrial proteins was possibly triggered by reoxygenation and it was not dependent on flies' activity rates as shown by resting metabolic data; the increased metabolic rates in sitters were observed at 8 hours post-anoxia in both experiments. Further studies looking at the expression of mitochondrial proteins and enzymatic activities of mitochondrial marker enzymes should be performed to further confirm that mitochondrial biogenesis is independent of the anoxic exposure time, but is triggered by anoxia as long as there are enough of energy resources available for mitochondrial biogenesis to occur.

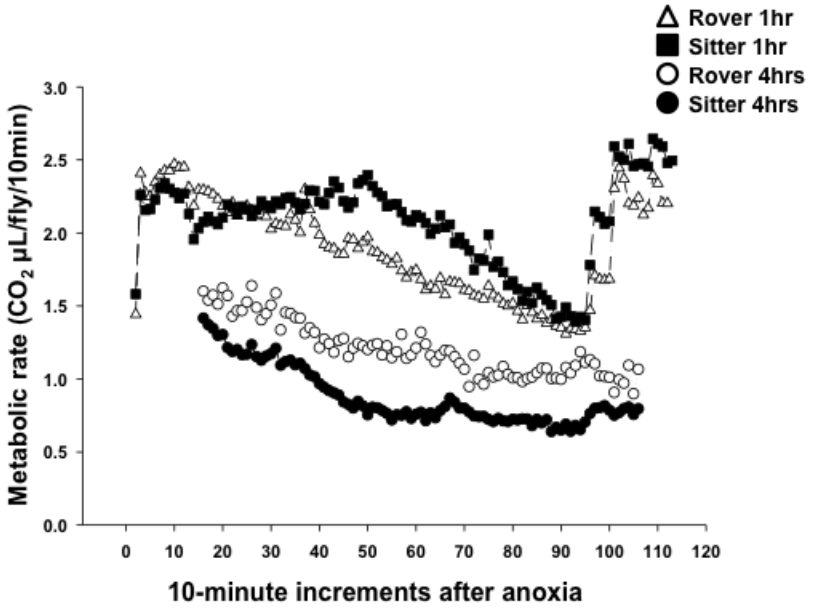

Figure 11. Comparison of average metabolic rates after 1 hour versus 4 hours of anoxia between rover and sitter flies. Times of the day are matched between the plots.

1.4. Conclusions

In conclusion, results from the citrate synthase enzymatic assays, Western blotting, as well as average resting metabolic rate measurements indicated that sitter flies exposed to anoxia demonstrated increased mitochondrial numbers and higher metabolic rates. Importantly, the newly formed mitochondria possibly possessed functionality as shown by sustained metabolic rates in sitters. Surprisingly, the increased duration of anoxia led to a dramatization of differences between average metabolic rates as well as between average resting metabolic rates of the fly genotypes during anoxia and upon reoxygenation. Upon longer anoxic treatment, both fruit fly genotypes were not able to recover their average metabolic rates to normoxic (pre-anoxic) levels within the period of measurement. This could possibly indicate a further rearrangement of metabolic signaling and dynamics, used up energy sources, a mitochondrial damage, or may be indicative of a protective mechanism turned on and being more efficient in rovers compared to sitters as shown in behavioral studies in Dawson-Scully et al. (2010). Since rover fruit flies survive better upon the recovery from an anoxic stress, it is likely that a downregulation of metabolism and indeed a preservation of mitochondrial mass resulted in the protection. Notably, in the above metabolic rate experiments, anoxia led to a significant drop in metabolic activity, which is similar to the drop observed during a night-time (about 0.5 µM of CO_2/mL/10min/fly); also, longer anoxia duration resulted in significant differences between rover and sitter fly average metabolic rates as well as average resting metabolic rates. From these results, it is tempting to hypothesize that the lower metabolic rates of rovers during anoxia may be reflective of a “deeper” protective hypometabolic state. This hypometabolic state may parallel or be the cause of the shorter time to onset of anoxic

coma (a decrease in locomotory function upon induction of anoxia) in rovers as well as in other anoxia-tolerant organisms such as *T. scripta* (Dawson-Scully et al. 2010; Benasayag-Meszaros et al. 2015; Perez-Pinzon et al. 1997). On the other hand, it is possible that increased respiration (metabolic function) post-anoxia in sitters is indicative of better overall health and fitness of sitter flies. Sitter flies may not survive long periods of anoxia but on average, they could be longer lived than rover flies as assessed by median lifespan (unpublished results). It is indeed very well known that increase in mitochondrial mass from for example intense exercise regimen leads to healthier muscles and brain in aging animals as well as prevents obesity (Miyashita et al. 2009; Wang et al. 2016). Further studies must be conducted inducing longer times of anoxia and measuring fruit flies' mitochondrial content as well as mitochondrial function. Moreover, it will be interesting to see if there are any mitochondrial number and function differences existing between aged rover and sitter flies. The information obtained throughout these experiments allows for further understanding of novel phenotypes regulated by cGMP/PKG signaling during and after physiological stress such as lack of oxygen, as well as possible protective mechanisms regulated by the *Drosophila foraging* gene. From this, the knowledge about underlying mechanisms of the cGMP/PKG-induced neuroprotection in *Drosophila* will allow for discovery of novel molecular and cellular targets that can be modulated to mimic the neuroprotection observed in fruit flies.

CHAPTER 2

Pharmacological PKG activation in vivo

2.1. Introduction

Besides mitochondrial dynamics and metabolism as phenotypes observed in rover and sitter fruit flies, survival upon anoxia and reoxygenation stress is another important phenotype which in turn possibly is dictated by differences in mitochondrial metabolism. In Dawson-Scully et al. (2010), it was shown that rover and sitter flies have different levels of PKG enzymatic activity and thus, have different levels of susceptibility to physiological stresses such as low oxygen stress and reoxygenation. From this, I hypothesized that pharmacological activation of the PKG pathway using sildenafil citrate, which is a specific inhibitor of the PDE5, an enzyme that hydrolyses cGMP leading to decreased cGMP/PKG molecular signaling, would result in better survival of flies subjected to anoxia and subsequent reoxygenation stress. In this part of my research, I investigated whether feeding Canton-S wild type *Drosophila* with sildenafil citrate added to fly food would result in an increased survival of flies subjected to anoxia followed by reoxygenation. Here, difference in post-anoxic survival was further compared between flies with chronic and acute PDE5 inhibitor exposure in their food. This study was designed to further investigate cGMP/PKG pathway activation potential in neuroprotection during anoxia and reoxygenation in adult flies using pharmacological approach instead of genetics.

2.2. Materials and methods

2.2.1. Drosophila rearing and husbandry

Canton-S wild-type fruit flies were reared on a standard corn food with 12 hours day : 12 hour night cycle at 25ºC. For experiments in which flies were subjected to drugs throughout their life cycle, Canton-S fruit flies were reared on standard food containing a range of concentrations of sildenafil citrate or a corresponding volume of deionized water for at least two weeks. After that, the food bottles with flies were cleared from all the adult flies (the adults were removed) and pupae within the food bottles were left for up to 4 days to eclose. Subsequently, male flies (0-4 day-old) were collected and transferred to plastic vials closed with cotton plugs in groups of 20 flies per vial. These vials contained either standard food (control) or standard food with the pharmacological compound at various concentrations. The flies then were aged to be 5-9-days old for the anoxia/reoxygenation experiments to match the age of rovers and sitters in the Dawson et al. (2010) study.

2.2.2. Fly food preparation

First, bottles with the standard food (about 50mL) were placed in a microwave to melt agar and liquefy food for more effective chemical mixing. Next, the bottles were cooled down to about 50ºC and an appropriate volume of sildenafil citrate solution was added and mixed using a vortex to ensure consistent homogenization. To prepare vials with food, the drug-containing food in the bottles was aliquoted using a hand-held automatic serological pipette. About 5mL of food were added to each vial. First, sildenafil citrate stock of 5mM was prepared and serial dilutions were performed to obtain the aforementioned concentrations of the drug. Vials and bottles with food were then left open but covered up with a cheesecloth (to prevent escaped flies entering the food) and were

placed in 18ºC, incubator overnight before the experimental flies were transferred into their corresponding containers (for mating- in bottles or for aging- in vials). Concentrations of sildenafil citrate in chronic drug treatment experiments were 1μM, 10μM, 100μM, and 500μM; the volume of the drug solution or distilled water added to the fly food bottles was always 1mL. Higher concentration of sildenafil citrate (1mM) resulted in no viable adults since all the flies died during the larval stage before reaching the pupation.

2.2.3. Induction of anoxia/reoxygenation and post-anoxic survival assessment

On the day of the anoxic experiment, the flies were transferred to empty vials and placed inside an "anoxia chamber". In this case, a plastic Ziploc bag was used as a chamber. A typical "anoxia chamber" setup is shown in Fig. 12. Then, a tube connected to an argon gas tank was inserted into the plastic bag, the tube was fixed in place, and the bag was tightly closed. Argon gas was pumped from a standard argon gas tank connected to a gas regulator turned on at 20in. Hg through a gas flow meter (Airgas, West Palm Beach, FL). Between the flow meter and Ziplock bag, a flask filled with DI water was connected to allow humidification of the flies exposed anoxia. Fish tank silicone tubing was used for all the connections of the anoxic gas setup. Anoxia experiments were performed at room temperature in daylight conditions. The effective length of anoxia was determined experimentally and was found to be 7 hours. After the anoxic treatment, flies were transferred back to the original vials containing standard fly food with or without drug and were placed in a 25°C incubator for 24 hours in a tilted position to avoid flies sticking to the food and become mechanically injured. Survival rates were determined and recorded by counting live and dead flies. It was essential to obtain survival that was less or equal to 50% in the control vials. Each vial represented one trial (N=1) and at least three 3 trials

were performed on different days. Importantly, each anoxic exposure was initiated between 12PM and 2PM (ET) to ensure that the results were independent of circadian rhythm influences. A typical experimental timeline for acute drug treatment experiments is shown in Fig. 13.

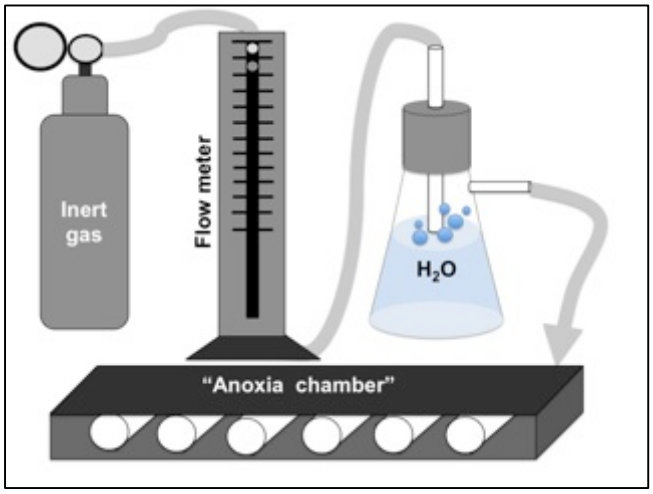

Figure 12. A schematic representation of a typical anoxia chamber setup. An inert gas, such as argon, was pumped at a controlled rate into a glass flask filled with DI water and connected to an "anoxia chamber" (a tightly closed container).

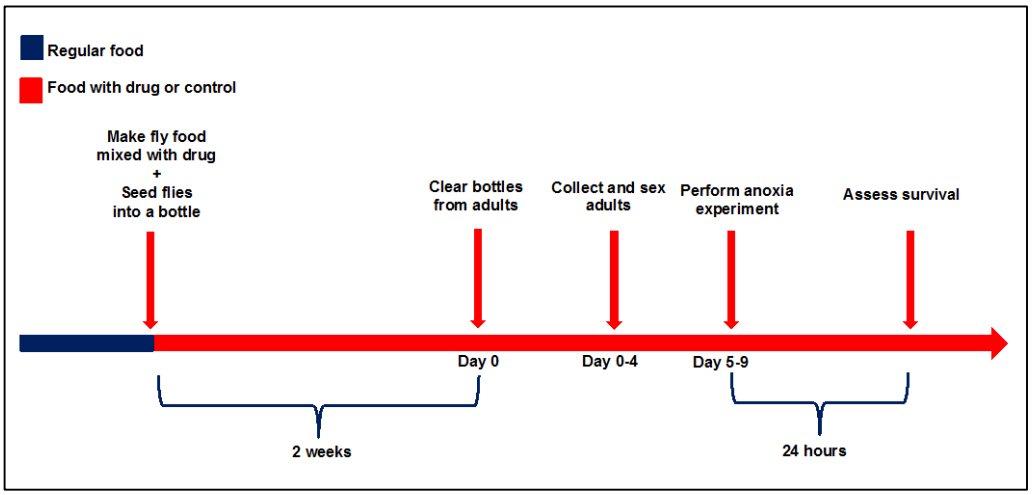

Figure 13. Schematic representation of *Drosophila* rearing, feeding, and anoxic stress induction timeline. Flies were fed sildenafil citrate chronically from the beginning of their life cycle until their death or survival after anoxia/reoxygenation stress.

2.2.4. CAFE assay

The Canton-S flies were grown inside plastic bottles containing about 50mL of standard corn food. The bottles were incubated at 12hrs day : 12hrs night cycle at 25ºC temperature. The bottles were cleared of live adults when enough old-stage pupae were present. After clearance, the bottles were left in the incubator for 2 days until newly-eclosed male flies were collected and transferred into vials containing regular solid food where they stayed until they were 5-7 days old (aging period). There, the flies were aged to match the age of rover and sitter *in vivo* experiments described in Dawson-Scully et al. (2010). After aging, flies were transferred into CAFE chambers in groups of 8 flies per chamber (Ja et al. 2007). Each CAFE chamber was made of a standard fly plastic vial with 4 holes made with a hot metal wire (Fig. 14). These holes ensured an equal and continuous air exchange between the outside and the inside of the chambers. On the bottom of each vial, there was

1% solidified agar dissolved in water present. The agar solution was poured one day prior to the experiment to avoid agar desiccation. The purpose of this agar layer was to provide water to the flies, thus preventing fly dehydration and thirst (not to be confused with liquid food, which is consumed when flies are hungry). The agar was poured up to about 1cm below the gas exchange holes to reduce drying of the agar. On the top of each vial, there was a tight rubber plug. The plug had two pierced holes through which 200μL plastic pipette tips were inserted. The pipette side of the smallest diameter was facing down; the pipette downward tips were cut off to allow for insertion of calibrated microcapillaries. On the first day of each experiment, two calibrated 5μL microcapillaries containing less than 1μL of sterile mineral oil on the top and 5μL of 5 % sucrose with 5% yeast extract (dissolved in DI water and filter-sterilized after preparation) were inserted into the 200μL plastic pipette holders. The mineral oil on the top of the fly liquid food ensured that the liquid food would not evaporate through the top openings of the microcapillaries. Importantly, the top of the oil meniscus was marked with a black marker after capillary insertion into chambers. About 1cm of each glass microcapillary was exposed below the rubber plug (Ja et al. 2007). After each 24-hour period, distance traveled by liquid food towards the bottom of the chambers was measured with a metal ruler and then an estimated average food volume eaten by a fly per day was calculated. Before each experiment, flies were habituated to the liquid food for 24 hours and then were treated with sildenafil citrate or control for a subsequent 24-hour period. After the 24 hour-long drug treatment, capillaries from all the experimental CAFE chambers were removed, and the estimated food consumption was assessed. Subsequently, the chambers were placed inside a plastic Ziplock bag in a horizontal position. The nitrogen gas setup was constructed in the same

manner as in the experiments with argon gas in one of the previous sections; nevertheless, the flies were exposed to 4 hours of anoxia to cause at least 50% death. Surprisingly, the flies lost their locomotor activity at about 30-45 minutes from the start of gas pumping, whereas in the chronic drug feeding anoxia experiments, the flies would fall into anoxic coma within 15 minutes from the start of gas pumping. This difference may be attributed to differences in gas properties, potential nitrogen gas reactivity, as well as differences in anoxia-tolerance adaptation of flies during the time between the two sets of experiments. After 4 hours of anoxia, the CAFE chambers were taken out of the plastic bag; the rubber plugs were opened and then closed again to ensure homogeneous reoxygenation throughout different chambers. Next, capillaries containing fresh liquid food without the drug were inserted into the rubber plugs and the flies were left inside of a 25ºC incubator for 24 hours, until the fly survival rates were assessed. Each vial was considered N=1 with total of N=6. Importantly, each anoxic exposure was initiated between 12 PM and 2 PM to ensure that the results are independent of the circadian rhythm influences. A typical experimental timeline for the CAFE experiments described here is shown in Fig. 14. Moreover, to make sure that the flies were actually eating the food, the measurements of food consumption were taken and resulted in no significant differences between the control and the sildenafil citrate-containing CAFE chambers (Fig. 17).

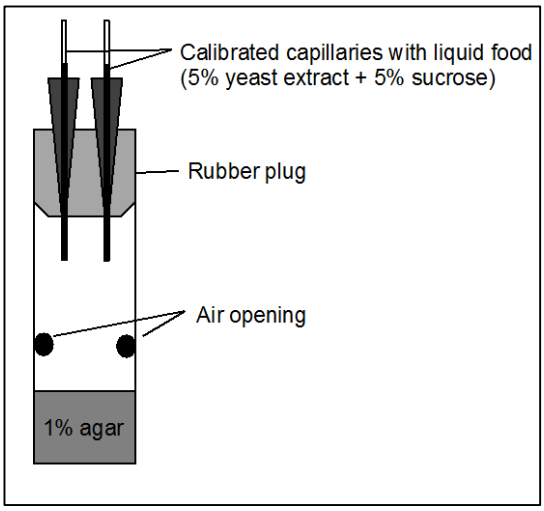

Figure 14. Schematic representation of a typical CAFE chamber setup. Calibrates capillaries contained liquid food with or without sildenafil citrate.

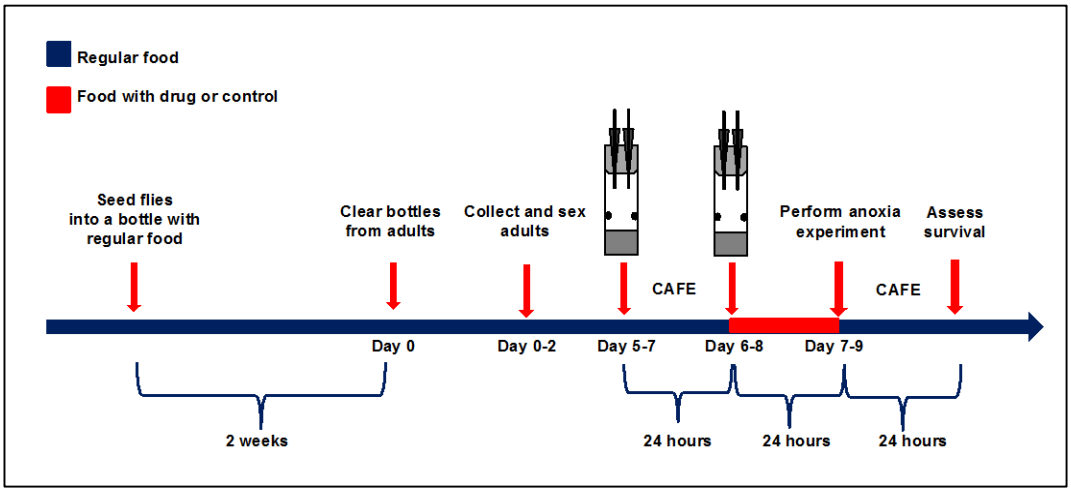

Figure 15. Schematic representation of *Drosophila* rearing, feeding, and anoxic stress induction timeline. CAFE assay was used to treat flies with sildenafil citrate acutely as well as to determine any taste aversion or increased appetite possibly induced by the drug ingestion.

2.2.5. Statistics

Statistical analysis was carried out by Student t-test. This was done using SigmaPlot Statistical Analysis Software (Systat Software, Inc., San Jose, California). A result was considered statistically different when $P<0.05$. Significant differences between groups were represented on graphs by different letters. If there was no statistical difference between two groups, then the letters inside the bars under comparison were identical. The data were represented as means ± S.E.M.

2.3. Results and discussion

2.3.1. Chronic sildenafil citrate exposure and post-anoxic survival

In the chronic drug feeding experiments, sildenafil citrate administered to flies at concentrations of 10μM and 100μM induced a significant protection from death after anoxia/reoxygenation as shown in Fig. 16. The survival rates were about 20% and 25% higher than of the control flies (sham, treated with DI water instead of sildenafil citrate). From this, when the flies were exposed to sildenafil citrate at the intermediate concentrations, there was an increase in survival rates. It is possible that the chronic exposure to the drug resulted in long-term effects that were not identified due to the lack of an easily observed phenotype. It also is possible that the chronic activation of the PKG pathway led to changes in the gene expression profiles of the flies. Moreover, the development of flies may have been affected by the chronic drug exposure. This should be further assessed by measuring dry fly weight, wet fly weight, and developmental parameters. In addition, the chronic sildenafil citrate-feeding assay demonstrated that low concentrations of sildenafil citrate (e.g. 1μM), as well as high concentrations of sildenafil citrate (500 μM), did not offer a protection of the wild type flies from anoxia and

subsequent reoxygenation (Fig. 16). Since the intermediate sildenafil concentrations (10 µM and 100µM) resulted in significant protection, it is possible that the 1µM of sildenafil citrate was not enough to induce activation of the PKG enzyme. On the other hand, 500µM of sildenafil citrate potentially resulted in increased toxicity possibly along with some protection since the average survival rates were higher than those of controls but lower than those of 10µM and 100µM treatments. Interestingly, when adult flies were seeded on food containing sildenafil citrate at concentration of 1mM, the flies died at larval stage of development with no flies maturing to the pupal stage. This was potentially due to toxicity induced by the activation of PKG or of cGMP-gated ion channels. It is also possible that the toxicity resulting from sildenafil citrate emerged due to products of the drug degradation. As described in the Methods section, sildenafil citrate solutions were added to the molten fly food before it solidified to allow for better homogenization. It is possible that the high temperatures during the dissolution process led to hydrolysis of the pharmacological compound; it is possible that some of the products of the hydrolysis were toxic, and more so at higher concentrations. Besides, the sildenafil citrate present in this food was at least 2-3 weeks old, and the bottles containing the flies and the food were incubated at 25ºC. Time-lapse and temperature may have an effect on the drug stability.

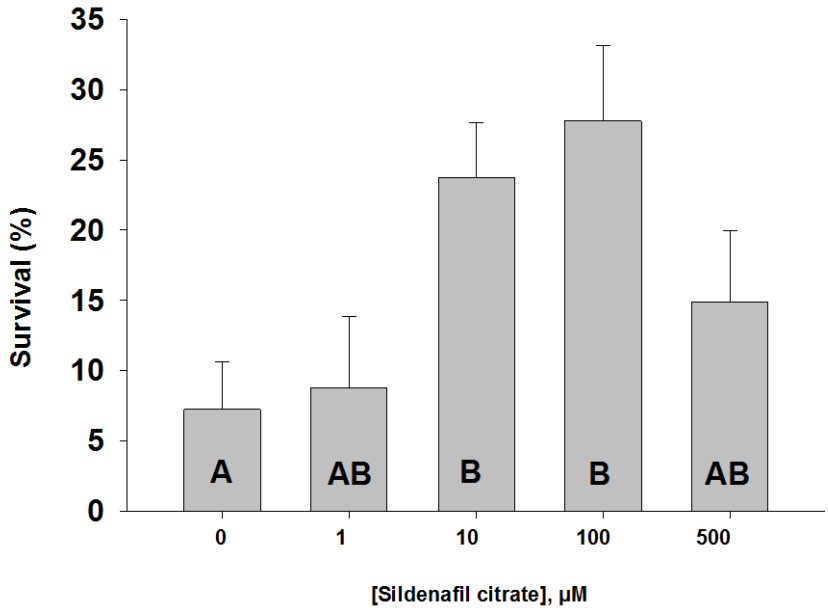

Figure 16. Survival graph of adult flies treated with sildenafil citrate and subjected to anoxia and reoxygenation. 5-9-day old wild type Canton-S flies were raised on food containing either 0µM, 1µM, 10µM, 100µM or 500µM of sildenafil citrate and were treated with 7 hours of anoxia and then reoxygenated for 24 hours. Survival rates were assessed by counting dead and live animals and then calculating percent survival. Different letters indicate a statistical difference between two groups as assessed by Student t-test, $P<0.05$, N=3, each N is a representative of one vial.

2.3.2. Acute sildenafil citrate exposure and post-anoxic survival

Next, I investigated if flies fed with sildenafil citrate for 24 hours only would result in protection from death upon exposure to anoxia and reoxygenation. Since the mechanism of the PKG-induced protection in flies subjected to anoxia and reoxygenation is not clear, it was important to investigate the efficacy of sildenafil citrate administered for a relatively short period. The administration of the pharmacological compound was carried out using the CAFE chambers. The CAFE chambers were used as described in Ja et al. 2007. In this

experimental system, the PKG activation did not influence the fly development and did not incur any long-term effects on normal physiology. This was due to the fact that the flies were treated when they were already in the adult stage (5-9 days-old). It was found that 10μM of sildenafil citrate was enough to induce significant protection from anoxia/reoxygenation stress in adult flies (Fig. 18). It is important to mention that the sildenafil citrate stock solution was prepared fresh, immediately before the feeding experiments. Furthermore, the treated flies did not have a taste aversion or an increased appetite due to ingestion of the sildenafil citrate-containing liquid food tested in this study.

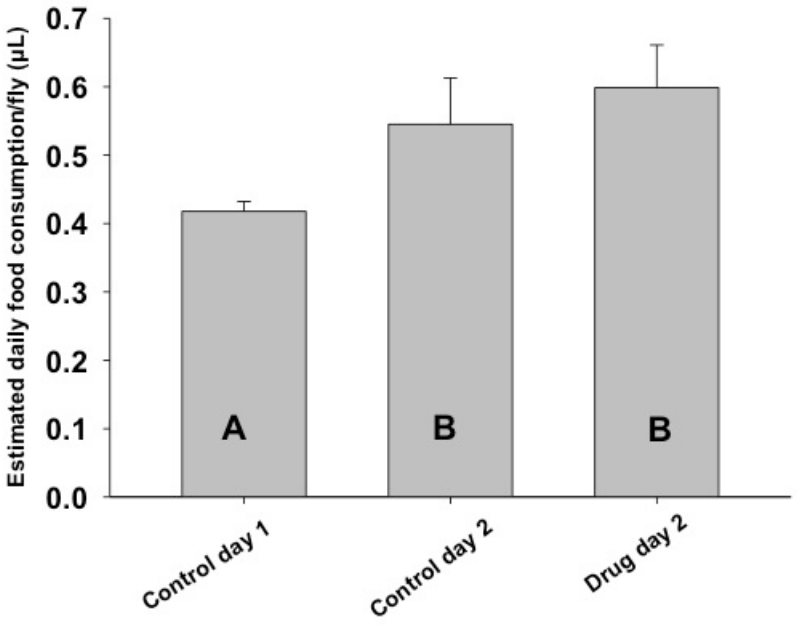

Figure 17. Estimated daily food consumption in microliters per fly. The flies were fed a control or a drug-containing liquid food. "Control day 1" represents estimated daily food consumption per fly during the first 24 hours of exposure to the liquid food (solid to liquid food adjustment period). "Control day 2" represents the estimated daily food consumption per fly during 24 hour-period before anoxic stress in the CAFE vials containing control liquid food. "Drug day 2" represents the estimated daily food consumption per fly during

the 24 hour period prior to an anoxic stress; the food in CAFE vials contained 10µM of sildenafil citrate dissolved in regular liquid food. Different letters indicate a statistical difference between two groups as assessed by Student t-test, P<0.05, N=8-24, each N is a representative of one vial.

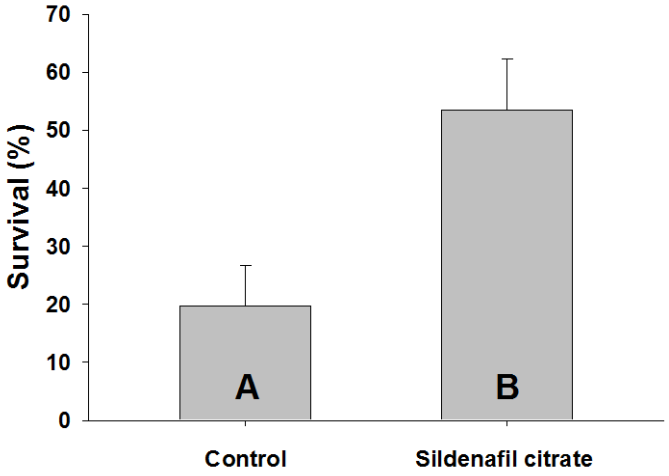

Figure 18. Survival graph of adult flies acutely treated with sildenafil citrate and subjected to anoxia and reoxygenation. 5-9-day old wild type Canton-S flies were treated with the liquid food containing either 0µM or 10µM of sildenafil citrate for 24 hours prior to anoxia. After the drug treatment, flies were subjected to 4 hours of anoxia and then were reoxygenated for 24 hours until the survival assessment. Different letters indicate a statistical difference between two groups as assessed by Student t-test, P<0.05, N=6, each N is a representative of one vial.

Even though the results were similar in both assays (both types of drug administration were protective to flies subjected to anoxia/reoxygenation), one needs to be careful in interpreting them. Acute feeding potentially led to short-term protective gene expression and physiological changes (opening of potassium ion channels, increased levels of neuronal excitability, changes in metabolism, etc.), whereas chronic feeding potentially

led to developmental changes and long-term changes in the fly gene expression. *Drosophila* in the chronic feeding assay potentially was preconditioned to stress as it was previously shown that an activation of the PKG pathway in mammalian cells results in increased ROS-induced stress (Oldenburg et al. 2004; Costa et al. 2008). As a future direction, it will be critical to develop a simple and fast assay to measure PKG enzyme activity since it is important to ensure that changes taking place upon sildenafil citrate treatment are from the increase in the enzyme activity and not due to another pathway activated by the increased availability of cGMPs. In addition, setting up a PKG enzymatic activity profile of rovers and sitters throughout development and adulthood will be interesting since the PKG signaling during a specific developmental stage could be of exclusive importance in the post-anoxic fly survival. For chronic feeding assay, it will be critical to assess amounts of ingested food by adding a colorful dye to the food and measuring optical density of the fly homogenates. Likewise, it will be necessary to test shorter times of the drug exposure in the acute feeding assay (e.g., 12hours, 4hrs, 2hrs etc.). Not to mention, treating flies with sildenafil citrate only post-anoxia will help to determine if the PKG pharmacological pathway activation offers a protection from an oxidative stress induced by the reoxygenation. Furthermore, additional phenotypes besides fly survival can be tested. Examples of such phenotypes are fly motor function (climbing assay) post-anoxia, time of locomotion failure after start of anoxia, as well as the time until recovery from an anoxic stress. To further dissect the cGMP/PKG pathway, it will be necessary to use other pharmacological compounds besides sildenafil citrate. Examples of such compounds include potassium ion channel blockers (general, plasma membrane, or mitochondrial), inhibitors of PP2A, as well as NO donors such as DETA NONOate. By

using combinations of these drugs together with sildenafil citrate, it might be possible to narrow down the upstream and downstream molecular participants of the pathway. Besides, it is possible to use pharmacology in mutant flies, in which *foraging* gene is expressed at different "dosages" (Allen et al. 2017). In conjunction, potassium ion channel mutants could be treated with PKG-modifying pharmacological compounds to further narrow down the pathway's downstream targets of the observed anoxic tolerance.

2.4. Conclusions

From the above results, it was determined that sildenafil citrate dissolved in fly food was protective from animal death and possibly neuronal damage in both chronic as well as acute feeding assays. The effective concentrations were 10µM and 100µM. The chronic feeding was started from the beginning of fruit fly life cycle until 24 hours post-anoxia when the fly survival rates were assessed. Acute feeding was also performed on adult flies but lasted for 24 hours before the induction of anoxia. It is important to note that the two different treatment assays were employed to determine the extent of protection provided by sildenafil citrate, if any. Due to the nature of the acute treatment, it was possible to assess the estimated amounts of food eaten by one fly per day (estimated daily food consumption/fly, measured in µL). The chronic feeding assay did not allow for an estimation of food consumption without actually measuring the nutrient intake in *Drosophila* living on the drug-containing food. Consequently, it was impossible to know how much food the flies were ingesting. It is very likely that the flies ate the drug-containing food since their approximate developmental rates (time until pupariation and number of flies eclosed) was not different from the flies fed with the control food. Using the capillary feeding assay (CAFE) during the acute drug treatment allowed to

determine if the flies had any taste aversion or increased appetite to the food mixed with sildenafil citrate. This control eliminated any other factors that could affect flies during their food ingestion. Such factors could be starvation, caloric restriction, as well as a neurobiological stress induced by food aversion or increased appetite. In future experiments, it will be interesting to investigate if the sildenafil citrate-offered protection could be induced through a shorter time exposure to the drug. This would allow for determining the exact timing when the sildenafil citrate protection occurs or is effective ("window of protection").

CHAPTER 3

Development of an in vitro model of chemical hypoxic and oxidative stress

3.1. Introduction

Since *in vivo* cGMP/PKG pathway activation using pharmacological compound sildenafil citrate resulted in protection from anoxia and reoxygenation-induced injury, I hypothesized that if *Drosophila* cell cultures were similarly protected, it could provide means to determine the pathways and downstream effectors of the sildenafil citrate protection. First, it was important to ensure that *Drosophila* cells were protected from anoxia and reoxygenation-induced cell death by pharmacological activation of the cGMP/PKG pathway. To perform these experiments, *Drosophila* S2 cell line was used. This cell line was developed from an embryonic fruit fly tissue by Schneider (1972) and has been used in molecular and cell biology studies to investigate cellular and molecular processes such as ones induced by a hypoxic exposure (Dekanty 2005; Dijkers and Farrell 2009; Utani 2010). To induce low oxygen stress there were two options: exposing the S2 cells to low oxygen environment followed by reoxygenation or using hypoxia mimetics, which are the chemicals that inhibit production of ATP; to induce an oxidative or a reoxygenation-like stress, hydrogen peroxide was used (Dawson et al. 1993; Lu et al. 2010; Liu et al. 2015). Numerous literature sources suggest that sodium azide and cobalt

chloride are hypoxia mimetics and can be used as such in mammalian *in vitro* studies (Chandel et al. 1998; Chachami et al. 2004; Higgins et al. 2009; Bae et al. 2012). These chemicals are inorganic compounds that inhibit mitochondrial cytochrome oxidase (Complex IV) by binding to the heme groups and interrupting the electron transport (Robertson and Boyer 1955; Vijayasarathy et al. 1999). As a result, the compounds seize mitochondrial function and stop production of ATP, causing cellular death (Robertson and Boyer, 1955). There are additional mechanisms by which sodium azide and cobalt chloride induce cell death. For instance, sodium azide is known to inhibit function of cellular catalases and thus, it induces oxidative stress; similarly, $CoCl_2$ increases intracellular ROS and induces HIF-alfa stabilization, which is a typical cellular protective response to hypoxia in mammalian cells (Nag and Resnick 2017; Tedesco et al. 2001; Zou et al. 2001; Zeeshan et al. 2017). Use of hypoxia mimetics may be preferred for studying *in vitro* models due to their low economic cost and reproducibility. In addition to the hypoxia mimetics, hydrogen peroxide was used to induce acute oxidative stress. Hydrogen peroxide is a known reactive oxygen species (ROS), which induces intracellular organelle, plasma membrane oxidation and damage eventually leading to cell death (Yokomizo and Moriwaki 2006; Zmijewski et al. 2010). One of the toxic effects of H_2O_2 is its induction of intracellular calcium overload, which consequently results in mitochondrial calcium overload, mitochondrial permeability transition pore (MPTP) formation, and cytochrome c leak (Josephson et al. 1991; Stridh et al. 1998; Herson et al. 1999; Smith et al. 2003; Palumbo et al. 2012; Gutiérrez-venegas et al. 2015).

In order to test the protective effects of pharmacological compounds such as PKG activators on D*rosophila* cell survival, it was critical, first, to develop culture models of

chemical hypoxia and oxidative stress injury using the S2 cell line. In order to accomplish this, I first assessed effects of different concentrations of known hypoxia mimetics NaN_3 and $CoCl_2$ as well as of an ROS molecule H_2O_2 on S2 cell death. Next, I investigated potential mechanisms of toxicity underlying the above cell treatments. This was accomplished by performing various cell-based assays that evaluated cellular health. Even with all the present knowledge about cytotoxic effects of the hypoxia mimetic compounds in mammalian cells, it was crucial to develop a cell culture model of chemical hypoxia and oxidative stress injury specifically in *Drosophila* S2 cells, since use of these chemicals with *Drosophila* S2 cells has never been reported before. I hypothesized that sodium azide and cobalt chloride inhibit mitochondrial production of ATP, and this drop in ATP eventually results in *Drosophila* S2 cell death. I further hypothesized that cobalt chloride, in addition to mimicking hypoxia chemically, also induces ROS production by mitochondria. This dual stress characteristic would make cobalt chloride an attractive compound to induce low oxygen as well as reoxygenation-like stress simultaneously mimicking a air hypoxia and reoxygenation. One of the main cytotoxic effects of hydrogen peroxide, the calcium influx and resulting cell death, was also investigated briefly in the acute oxidative stress experiments.

3.2. Materials and methods

3.2.1. Cell culture protocol

The *Drosophila* Schneider 2 (S2) cell line (Invitrogen, Carlsbad, CA) whose origin is from a primary culture of late-stage embryos was used as a generalized *Drosophila* cell type. S2 cells were grown at room temperature in Schneider's *Drosophila* medium containing $NaHCO_3$ (Sigma Aldrich), supplemented with 10% fetal bovine serum (FBS,

Atlanta Biological, Flowery Branch, GA and Sigma Aldrich), 50 units/ml penicillin and 50 µg/ml streptomycin (Invitrogen, Waltham, Massachusetts) in T-25 cm^2 or T-75 cm^2 tissue culture flasks. The cells were split in a 1:2 or 1:3 ratio every 2-5 days. Before each experiment, the cells were centrifuged at 1000 × g for 3 minutes at room temperature; the supernatant was replaced with fresh *Drosophila* Schneider's medium, and a 1×10^6 cells/ml cell suspension was prepared. The cell suspension then was divided into equal-volume aliquots to perform treatments with subsequent measurements.

3.2.2. Determination of cell toxicity from NaN_3, $CoCl_2$, and H_2O_2 treatments

To determine cell toxicity levels caused by NaN_3, $CoCl_2$, and H_2O_2 treatments, 1mL S2 cell suspensions at 1×10^6 cells/mL density were treated with different concentrations of the above chemicals for 4 hours. At the end of the incubation period, cell death assessment by trypan blue exclusion method and morphological cell counting with Bright-Line hemocytometer (Improved Neubauer, 0.100 mm deep) and a compound light microscope (Swift Instruments International S.A.) was performed. About 400-600 cells total were counted in at least three separate counts for each treatment and then cell death percentage was calculated and averaged between trials.

In these experiments, NaN_3 and $CoCl_2$ (Sigma Aldrich, St. Louis, MO) were used at the following concentrations: 0mM (sham control with equivalent volume of water), 1mM, 2mM, and 4mM. H_2O_2 (Sigma Aldrich, St. Louis, MO) was used at the concentrations of 0mM, 6mM, 10mM, 25mM, and 50mM.

3.2.3. ATP measurements

ATP measurements were performed in order to investigate changes to the metabolic output in S2 cells treated with cobalt chloride and sodium azide, since both compounds are

known to be potent mammalian metabolic disruptors, which reduce cellular ATP production (Massie et al. 2003; Chachami et al. 2004; Bae et al. 2012). First, the cells were spun down for 3 minutes at 1000 × g and supernatant was removed. Next, the cells were diluted in a fresh complete *Drosophila* Schneider's medium to generate a suspension of 100,000 cells/mL. Next, 90µl of suspensions were added to corresponding wells marked as follows: medium - no cells, 0mM $CoCl_2$, 0.1mM $CoCl_2$, 0.2mM $CoCl_2$, 0.4mM $CoCl_2$, 1mM $CoCl_2$, 2mM $CoCl_2$, 4mM $CoCl_2$, 10mM $CoCl_2$, 0.2mM, 0.4mM NaN_3, 1mM NaN_3, 2mM NaN_3, 4mM NaN_3, 10mM NaN_3. Sham control (0mM $CoCl_2$) did not have any drug treatment; instead, an equivalent volume of DI water was added to a cell suspension since $CoCl_2$ and NaN_3 stokes were prepared in water. Furthermore, each assay plate had background interference controls - medium with and without a lysis buffer (used for intracellular ATP release, Promega, Madison, WI) and medium with $CoCl_2$ and NaN_3 treatments of the above concentrations but without cells. It is also important to note that each trial had an "all dead" control where the lysis buffer was added. Each of the treatments was performed in at least 2 wells, in at least three independent trials (cells at different passages used) and each individual ATP value from a well was considered as N=1.

After the chemicals were added to corresponding wells, the assay plate was incubated at room temperature for 4 hours. After the incubation time, cells were lysed for 1 minute on the rocker and cell lysates were homogenized by pipetting. Then, 90µL of ATP reaction mix composed of DI water, 20 × reaction buffer, DTT, luciferase, and luciferin were added to each well of a white opaque plate and 10uL of cell lysates were subsequently added to each corresponding well of this white plate. ATP standards (0µL, 0.1µL, 0.25µL, 0.5, 1µL) were used to determine absolute values of ATP. This step was

performed in dark to avoid any loss of the luciferase activity; the plate was wrapped in aluminum foil and luminescence was measured from the top setting of the SpectraMax M2 plate reader (Molecular Devices, Sunnyvale, CA) and SoftMax Pro software (Molecular Devices). To determine the absolute levels of ATP in the samples, an ATP standard regression equation was calculated. At least 8 independent wells containing S2 cells were tested. The actual number of trials for a specific experiment is shown in a figure legend of a corresponding graph.

3.2.4. Relative levels of metabolic activity assays

To confirm the results obtained in the ATP assays, the relative levels of metabolic activity were measured using AlamarBlue reagent (Thermofisher Scientific, Waltham, MA), a chemical, which, when reduced by electrons in the medium, changes its absorbance and fluorescence qualities. The AlamarBlue reagent accepts electrons, which are products of oxidative metabolism, and this is accompanied by a change in fluorescence as well as absorbance. For these assays, the S2 cells were plated in the same manner as for the ATP assays in a 96-well plate format. After plating the cell suspension, $CoCl_2$ or NaN_3 and 10µL of AlamarBlue reagent were added to each well and incubated for 4 hours at room temperature wrapped in aluminum foil to protect from light to avoid loss of fluorescence. After the incubation period, the plate was read at 550 excitation/590 emission wavelengths using the SpectraMax M2 plate reader. The relative metabolic rates were expressed in arbitrary fluorescence units. The experiment was performed independently in total of 8 wells.

3.2.5. pH measurements

After carrying out the ATP and AlamarBlue assays, I hypothesized that the observed unexpectedly high ATP levels in cobalt chloride-treated *Drosophila* S2 cells may be due to an increase in pH levels from the $CoCl_2$ being added to the cell cultures. The pH was measured using a glass pH probe (Hanna Instruments, Woonsocket, RI). The 2mL suspensions of S2 cells at 1×10^6 cells/mL cell density were incubated with different final concentrations of $CoCl_2$ (0-10mM) for 0 or 4 hours at room temperature. At each corresponding time point, the pH was measured three times per treatment.

3.2.6. Acidosis experiments

To further test the idea that *Drosophila* S2 cells were protected by the increased levels of acidity of the medium, the following experiments were performed. First, S2 cells were resuspended either in insect hemolymph-like solution HL3 saline (Feng et al., 2004) or in complete Schneider's insect medium containing penicillin/streptomycin and FBS at cell density of 1×10^6 cells/mL. Then, the cell suspension was distributed between 15mL Falcon centrifuge tubes in 2-mL aliquots. Next, pH values of the cell suspensions were changed according to the treatment (a range of pH values: 2.8, 6.2, 7.2, 7.8) using HCl or NaOH solutions, and were measured with a glass pH probe as described in 3.2.5. Cell damage and cell death were assessed using bright-field and fluorescent settings of Zeiss Axiovert microscope (Karl Zeiss Meditec, Dublin, CA). The images were subsequently taken using Olympus camera (Olympus Corporation, Shinjuku, Japan). In bright-field microscopy, the plasma membrane-damaged cells appeared to have disintegrated plasma membrane; conversely, the healthy cells appeared to keep their plasma membrane integrity. In fluorescence microscopy, dead cells were stained with propidium iodide (PI) stain and all the cells were co-stained with Hoechst 33342 nucleic acid stain. Dead/total cell ratios

represented on the graphs were determined from the ImageJ NIH software-aided manual cell count procedure. Minimum of 3 independent trials was performed with 3 images per treatment captured.

3.2.7. Oxidative stress assay

After determining that NaN_3 and $CoCl_2$ can be used on *Drosophila* cell cultures to mimic decrease in ATP production, I tested whether these chemicals also induce oxidative stress as was shown in mammalian studies (Tedesco et al. 2001; Zou et al. 2001). Oxidative stress levels were determined using OxiSelect^{TM} Intracellular ROS Assay Kit - Green Fluorescence (Cell Biolabs, San Diego, CA). In brief, cells were pelleted and diluted in Schneider's *Drosophila* medium without FBS at about 0.5-1 × 10^6 cells/mL. Then, the cell suspension was incubated in the 100μM 2', 7'-Dichlorohydrofluorescein diacetate (DCFH-DA) for 1 hour, cells were pelleted and washed with Hank's Balanced Salt Solution (HBSS) 3 times and re-suspended in Schneider's medium without FBS (to prevent oxidation of the dye by FBS) at 0.5-1 × 10^6 cells/mL cell density. Next, 90μL of cell suspension were transferred to a dark 96-well plate and 10μL of dilutions resulting in different final concentrations NaN_3 (0-10mM), $CoCl_2$ (0-10mM) were added. The plates were incubated at room temperature for 4 hours in the dark. After incubation, the cells were gently washed 2 times with HBSS and green fluorescence from each well was read at the following parameters: excitation 485nm, emission 538nm. Each treatment was done in triplicate and repeated independently at least three times on different days. The results were expressed as a percent of the control fluorescence reading.

3.2.8. H_2O_2 intracellular calcium overload experiment

To test if the H_2O_2 treatment results in influx of calcium from the medium into *Drosophila* S2 cell cytosol, calcium imaging was performed using an intracellular calcium indicator. In the calcium overload experiment, the S2 cells were first attached to a $10cm^2$ plastic dish coated with Concanavalin A (Con A, Sigma Aldrich, St. Louis, MO) at concentration of 0.5mg/mL (Buster et al. 2010). Con A is a protein lectin that helps in attachment of cells to growth substrates as it binds to extracellular sugar-containing molecules (Rizki et al. 1977; Ahn et al. 2014).

After cell attachment, the complete Schneider's medium in the dishes was replaced with Locke's buffered saline and fluo-3AM dye (Sigma Aldrich, St. Louis, MO) was added for at least 30 minutes to load the cells. Then the cells were washed with Locke's buffer and treated with either DI water or 10mM hydrogen peroxide for 4 hours and subsequently incubated at room temperature protected from light. After the incubation period, the cells were stained with propidium iodide (Sigma Aldrich) for detection of dead cells and observed under Zeiss Axiovert microscope (Karl Zeiss Meditec, Dublin, CA). Green fluorescence (intracellular calcium) and red fluorescence (propidium iodide) were imaged using Olympus camera (Olympus Corporation, Shinjuku, Japan) and Qcapture software (QImaging, Surrey, Canada).

3.2.9. Statistics

Statistical analysis was carried out by performing a Student t-test or one-way analysis of variance (ANOVA) followed by a *post-hoc* multiple comparisons procedure, the Student-Newman-Keuls (SNK) test. This was done using SigmaPlot Statistical Analysis Software (Systat Software, Inc., San Jose, California). A result was considered statistically different when $P<0.05$. Significant differences between groups are represented

on graphs as different letters inside the bars, with the same letters indicating no significant differences between compared groups. Also, in some figures, statistical differences are represented as stars, when results of chemical treatments were compared with a control treatment or between specific groups, only if indicated. The data are represented as means ± S.E.M.

3.3. Results and discussion

3.3.1. Assessment of mechanism of action of NaN_3

3.3.1.1 Assessment of cytotoxicity from different concentrations of sodium azide

To assess cellular death upon NaN_3 treatment, trypan blue exclusion method was used. Trypan blue is a dark blue-colored dye that penetrates cells that have lost their membrane integrity, whereas live cells exclude the dye (Levin 1913). From this, live cells appear as bright circles, whereas dead cells turn blue. In these experiments, it was found that NaN_3 induced cell death in a concentration-dependent manner (Fig. 19). Interestingly, this hypoxia mimetic induced significant cell death at 1mM concentration but higher concentrations did not seem to dramatically increase cell death compared to 1mM. Some cell types such as PC-12 cell line, also show high resistance to the sodium azide treatment. In one study, it was shown that 30mM sodium azide incubation for 3 hours led only to about 45% cell death (Shan et al., 2017). Hepatocytes treated with 20mM sodium azide for 2 hours resulted in about 10% cell death (Dawson et al., 1993). In this study, researchers also used cyanide and at 2.5mM concentration of this metabolic disruptor, hepatocytes die at the same rate as when treated with the above concentration of sodium azide. From this, different hypoxia mimetics may possess different levels of permeability and specificity. Importantly, higher concentrations of sodium azide could disrupt the osmotic balance of

the solution leading to cell death through an ATP-independent mechanism.

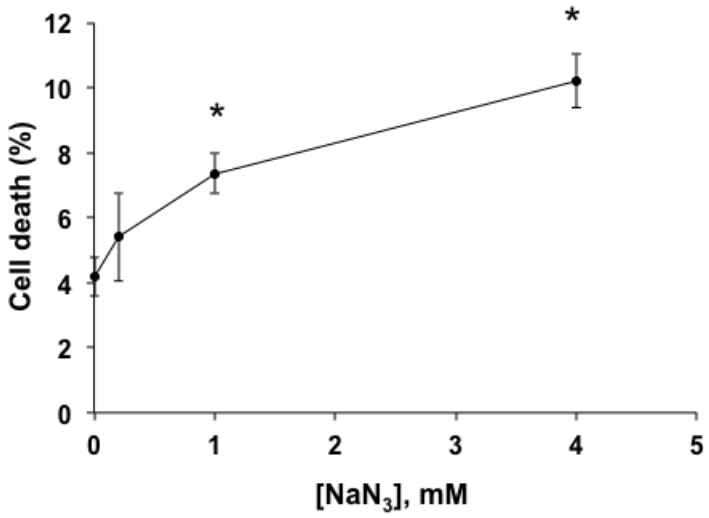

Figure 19. Increasing concentrations of metabolic disruptor NaN_3 induced *Drosophila* S2 cell death. P<0.05, N=3.

3.3.1.2. Metabolic function measurements upon NaN_3 treatment

Furthermore, to test the hypothesis that NaN_3 acts on *Drosophila* S2 cells as a true hypoxia mimetic, thus by decreasing ATP production, ATP assays were performed (Fig. 20). It was found that NaN_3, at 0.1mM concentration and above, decreased *Drosophila* cellular ATP production significantly (Fig. 20A). At 0.4mM of NaN_3, the ATP levels were reduced two-fold. At the same time, I measured relative metabolic rates in cells treated with different concentrations of chemicals mimicking hypoxia to see if the results replicate the ATP assay data (Fig. 20A). To measure relative metabolic rates, AlamarBlue assay was used and fluorescence of the medium upon its reduction by metabolically active cells was measured. It was found that NaN_3 significantly decreased relative metabolic rates in a

concentration-dependent manner (Fig. 20B). At 1mM concentration, the cells reached the minimum reduction capacity and stayed at the same level throughout the treatments with higher NaN_3 concentrations. Consequently, the ATP assessment and the AlamarBlue assay showed similar results and together suggest a significant downregulation of oxidative metabolism in the cells; notably, each of the assays depends on unrelated chemical reactions (ATP-powered luciferase reaction versus number of electrons accepted by the AlamarBlue dye). Interestingly, when the control S2 cells were treated with a lysis buffer at the beginning of the 4 hour incubation period, the ATP levels, as well as metabolic levels, were very low and close to 0. The decomposing matter (as in cells treated with lysis buffer) after 1-4 hours of incubation did not produce a significant change in the AlamarBlue fluorescence (results not shown). From this, NaN_3 acted on S2 cells as a true hypoxia mimetic in a sense that it significantly decreased the ATP production and decreased reduction capacity of the cell cultures. At higher concentrations, starting at 1mM, NaN_3 treatment led to ATP depletion that was comparable to a nearly complete lack of oxygen or anoxia. An important point to note is that complete inhibition of ATP production did not mean that cells were dead. From the cell death assessment, 1mM NaN_3 4-hour treatment only resulted in about 13% cell death, even though the ATP production was nearly at 0. From studies on mechanisms of apoptosis and necrosis, it was found that intracellular ATP is necessary for a cell to undergo and complete apoptosis whereas necrosis occurs when there is a lack of ATP (Tsujimoto 1997). From this, it is possible that this decrease in ATP is protective until a specific point in time when cells cannot sustain their basal low-metabolic state and finally, undergo necrosis, which is hallmarked by plasma membrane rupture (Shimizu et al., 1996).

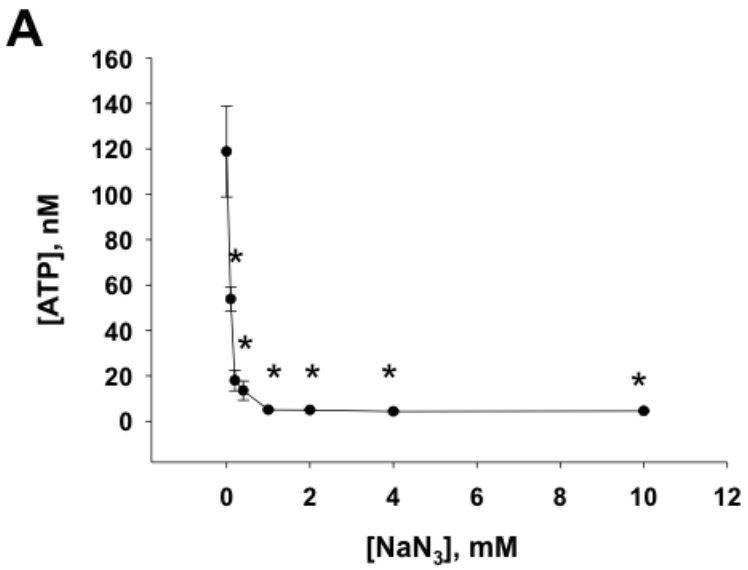
A
160
140
120
100
80
60
40
20
0
[ATP], nM
*
*
*
*
*
*
0
2
4
6
8
10
12
[NaN3], mM

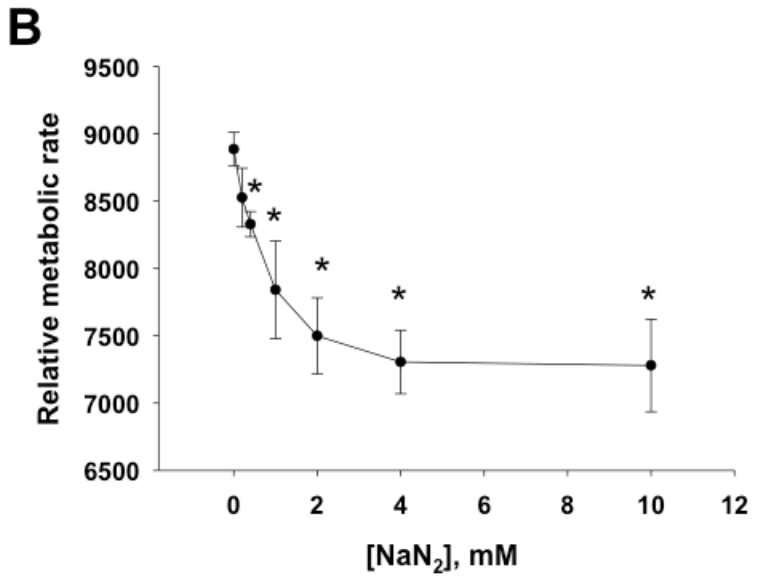

Figure 20. Increasing concentrations of metabolic disruptor NaN_3 decreased *Drosophila* S2 cellular metabolic rates after 4 hours of incubation. A) ATP production; B) Alamar blue reduction. A "*" represents a significant statistical difference between a treatment and the control, $P<0.05$, $N\geq8$.

3.3.1.3. Quantification of ROS production upon NaN_3 treatment

Moreover, the effect of increasing concentrations of NaN_3 on intracellular ROS production was also investigated to further determine the mechanism of action of this chemical (Fig. 21). From the data, there was no significant increase in ROS production from NaN_3 treatments. On one hand, this was expected since ATP production and thus ETC of mitochondria were inhibited; in this manner, there was a decreased passage of electrons through ETC and less leaked electrons to generate ROS. On the other hand, it was unexpected since oxygen was still present in the air and was available to accept electrons passing through the ETC before reaching the inhibited complex IV. Leaked electrons accepted by oxygen could lead to formation of free radicals. Furthermore, sodium azide is a known cellular catalase inhibitor (Tedesco et al. 2001). That by itself would

indirectly increase the rate at which ROS such as hydrogen peroxide are cleared from cells. But since it is possible that ROS were not produced at all, catalase inhibition may not have been detrimental to the cells. In a study where hepatocytes treated with 20mM sodium azide for 2 hours resulted in about 10% cell death, azide showed 3 times higher ROS production than cyanide (Dawson et al. 1993). This discrepancy in mechanisms of action of the two common metabolic disruptors potentially points out at the existence of an additional molecular target and or different potency in disrupting ETC and flow of electrons (Stannard and Horecker, 1947). Furthermore, it is possible that only high concentrations of sodium azide induce ROS production since there is a trend towards increasing ROS with increased sodium azide concentration. Conversely, catalase of human erythrocytes is inhibited significantly by 10μM sodium azide (Aksoy et al. 2004). From these findings, it is possible to conclude that there might be parallel mechanisms of ROS production: catalase dependent (due to a decrease in antioxidant function) and catalase independent (interfering with iron in heme groups and possibly donating electrons to oxygen), but it needs to be further investigated in *Drosophila* S2 cells.

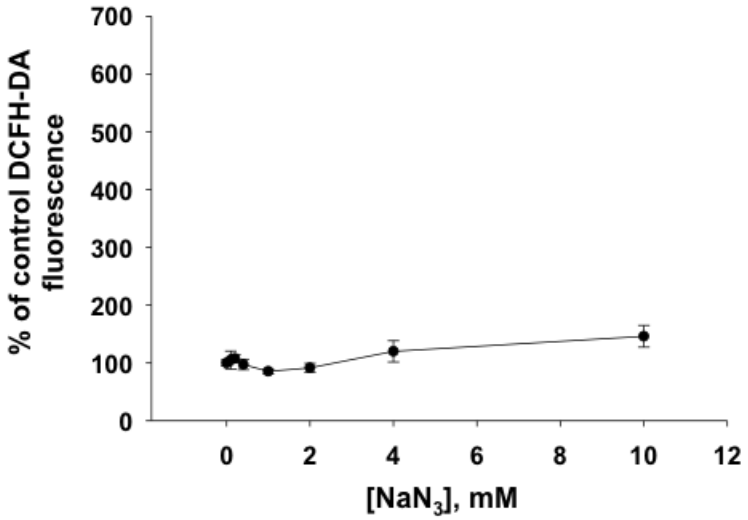

Figure 21. Intracellular ROS levels do not increase significantly upon NaN_3 *Drosophila* S2 cell treatment for 4 hours. A "*" represents a significant statistical difference between a treatment and the control; no significant difference was found, N=3.

From the above experiments, it was determined that NaN_3 was cytotoxic to *Drosophila* S2 cells and caused cell death in a concentration-dependent manner. Moreover, NaN_3 was acting as an anoxia mimetic when used at concentrations equal or higher to 1mM. Below this concentration, the cells decreased their ATP production significantly but not fully potentially being in a metabolic state equivalent to hypoxia. Experiments measuring the relative reducing capacity of the S2 cell cultures also showed decreased levels of molecular reduction capacity upon treatment with NaN_3. Notably, *Drosophila* S2 cells seemed to be relatively resistant to the lack of ATP when treated for 4 hours. However, longer exposure times such as 24 hours caused up to 100% cell death (data not shown). It will be critical to determine mechanisms behind such resistance as it could uncover yet another mechanism *Drosophila* uses to withstand a lack of energy production. Moreover, the present data showed that NaN_3 did not induce oxidative stress in *Drosophila* S2 cells, at least at the concentrations that were tested in the above studies. To further investigate the mechanisms of action of sodium azide on S2 cells, it will be critical to induce chemical hypoxia using higher concentrations of the chemical and determine the resultant ROS production and possible the sources of ROS being produced.

3.3.2. Assessment of mechanism of action of $CoCl_2$

3.3.2.1. Assessment of toxicity by $CoCl_2$

To assess cellular death upon $CoCl_2$ treatment, similar to NaN_3 experiments, trypan blue exclusion method was used. From the studies, it was found that $CoCl_2$ induced cell

death in a concentration-dependent manner (Fig. 22). Similar to NaN_3, this hypoxia mimetic induced significant cell death at 1mM concentration but higher concentrations did not dramatically increase cell death as compared to 1mM. In human hepatocellular carcinoma cell HepG2, 4 hours of incubation with 0.8mM $CoCl_2$ caused about 40% cell death whereas 2mM caused 15% cell death (Liu et al. 2015). In retinal ganglion cells, 0.4mM $CoCl_2$ caused about 30% cell death after 24 hours of incubation (Tulsawani et al. 2010). Interestingly, 10mM $CoCl_2$ with pH equal to the Schneider's medium (pH 7.0±0.2) caused about 30% cell death after 4 hours of incubation (Fig.27). From this, *Drosophila* S2 cells possess a lower degree of resistance to cell death from $CoCl_2$ than retinal ganglion cells. In a study where osteoblast-like MG-63 cell line was treated with 0.2mM CoCl2 for 24 hours, there was 50% cell death observed after 24 hours of incubation (Li et al. 2017a). In Drosophila, the S2 cells, on the other hand, after incubation for 24 hours with 0.2mM CoCl2, showed cell proliferation, which was expected since this concentration did not cause complete inhibition of ATP production as demonstrated by the results of the next section. From this, different types of cells exhibit different levels of resistance to CoCl2 treatment in mammals, thus it is possible that Drosophila cells of different embryonic origin also show different levels of resistance depending on the molecular profile of a cell type and this needs to be further investigated.

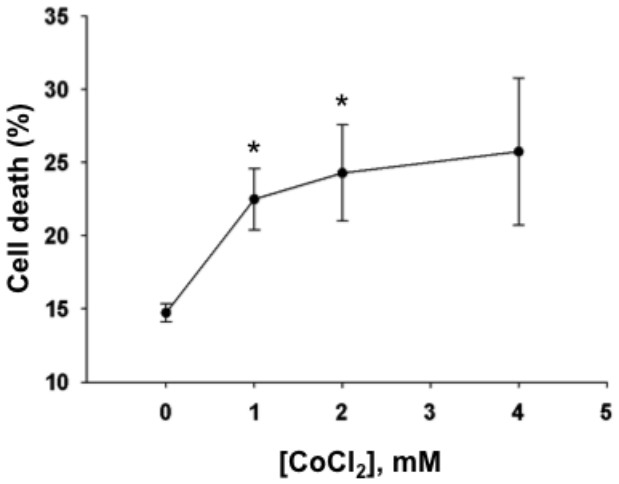

Figure 22. Increasing concentrations of metabolic disruptor $CoCl_2$ led to *Drosophila* S2 cell death. $P<0.05$, N=3.

3.3.2.2. Metabolic function measurements upon $CoCl_2$ treatment

As with NaN_3, increasing concentrations of the metabolic disruptor $CoCl_2$ lowered ATP concentration and relative metabolic rates in S2 cells. However, at low $CoCl_2$ concentration, an interesting pattern became apparent (Fig. 23A). First, at very low concentrations, $CoCl_2$ lowered the ATP production (though not significantly). At cobalt chloride concentrations of 0.4mM to 2mM, there was an increase in ATP production with 2mM producing a statistically significant ATP rise, when compared to a control. Furthermore, treatments at 4mM and above decreased ATP; 10mM $CoCl_2$ showed statistical difference from the 2mM treatment as well as from the control treatment. Results of the AlamarBlue assay showed a similar pattern of metabolic changes at the low, intermediate, and high concentrations of $CoCl_2$ (Fig. 23B).

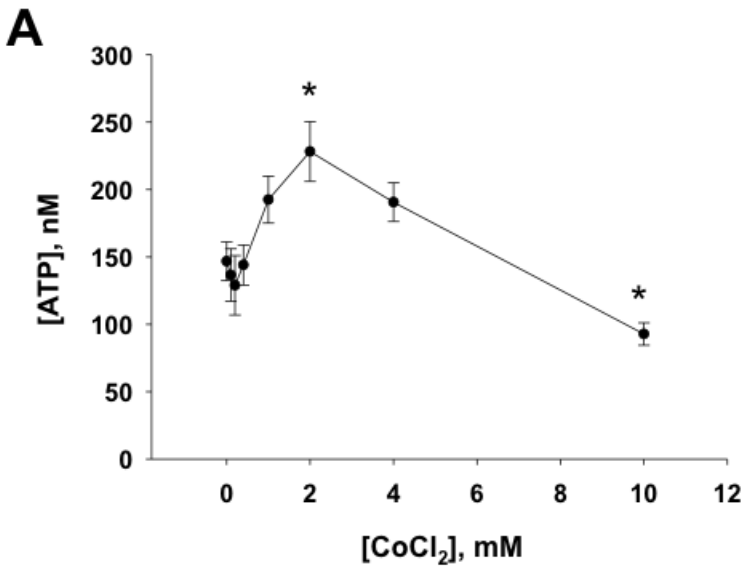
A
300
250
200
150
100
50
0
[ATP], nM
*
*
0
2
4
6
8
10
12
[CoCl2], mM

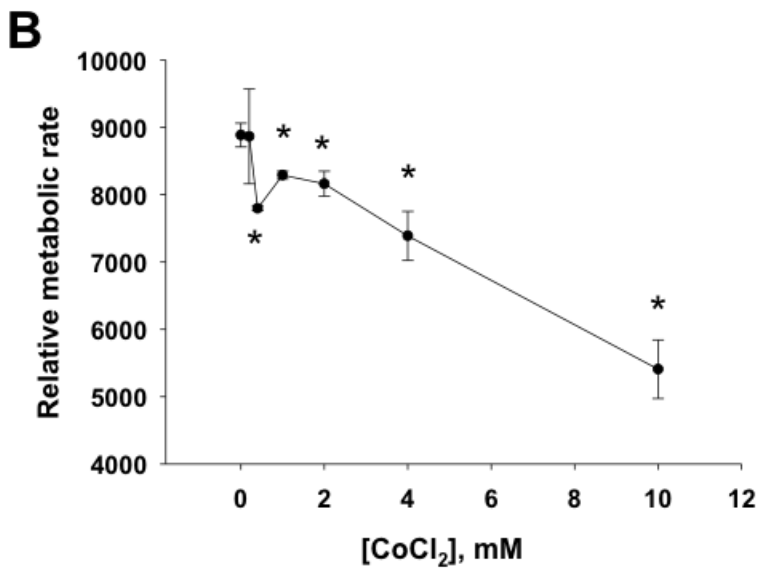

Figure 23. Increasing concentrations of metabolic disruptor $CoCl_2$ led to decrease and increase of metabolic rates in *Drosophila* S2 cells after 4 hours of incubation. A) ATP production; B) AlamarBlue reduction. A "*" represents a significant statistical difference between a treatment and the control, $P<0.05$, N=8-16.

The above experiments led me to hypothesize that pH of high concentration $CoCl_2$-treated cells could be acidic, since ATP levels may increase in acidic environments (Trafton et al. 1996). When the pH of cell suspensions treated with $CoCl_2$ at different concentrations was measured, high concentrations of $CoCl_2$ were significantly acidic compared to the pH of the medium alone or control cell suspensions (Fig. 24). If acidity was toxic (cell death-inducing) then it was surprising that there was no additional increase in cell death at 4mM $CoCl_2$ compared to 1mM $CoCl_2$. A similar phenomenon of ATP levels preservation in an acidic environment has been previously observed in studies performed on mammals in heart muscle, neurons, liver, and cancer cells (Bing et al. 1973; Currin RT, Gores GJ, Thurman RG 1991; Morimoto et al. 1997; Khacho et al. 2014). It is

also known that cobalt ions inhibit calcium influx unspecifically binding to calcium ion channels (Moger 1983; Abernethy et al. 1995). One possibility is that a decreased pH (increased acidity) may be protective to cells due to increased concentration of H^+ as this leads to increased proton gradient (increased mitochondrial membrane potential) and as a result ATP production continues since there is a constant supply of electrons from the nutrient-abundant medium. Since at 10mM there was a significant drop in ATP production observed (compared to control value), this could be due to increased acidity as well as other cytotoxic effects that compensated for the increased ATP. Moreover, these cells might have been undergoing through early stages of apoptosis, which eventually resulted in cell death.

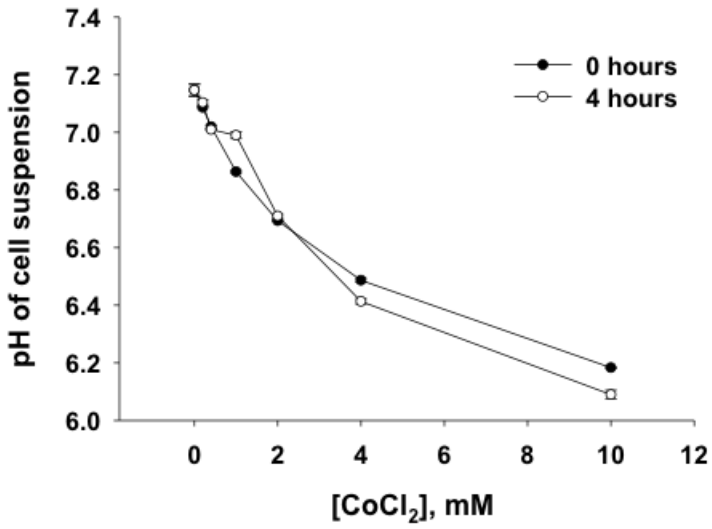

Figure 24. *Drosophila* S2 cell suspension pH values in the beginning and at the end of the 4-hour incubation period after addition of $CoCl_2$. N=3.

To test if the "acidosis" hypothesis was feasible, pH of the medium containing $CoCl_2$ at different concentrations was changed to the one of complete Schneider's insect medium

with constant pH buffered to pH of 7.0±0.2, ATP production levels decreased significantly with increasing concentrations of $CoCl_2$ without a "bump" observed in the previous study (Fig. 25). From this, the hypothesis that acidosis prevented a cellular ATP drop from a hypoxia mimetic-induced ATP reduction is a potential explanation.

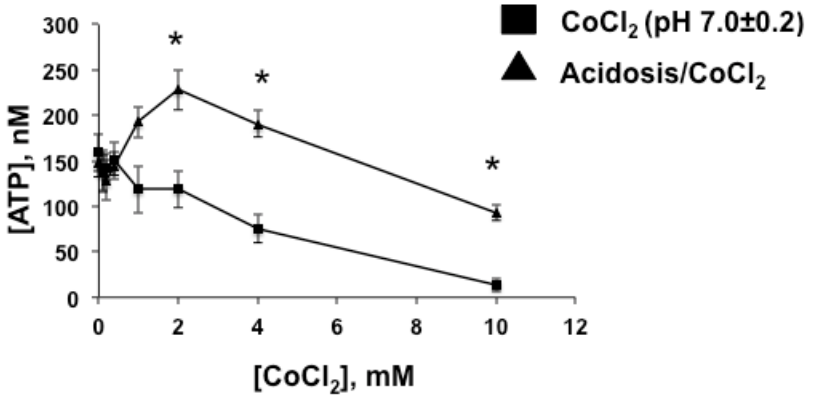

Figure 25. Effect of increasing concentrations of metabolic disruptor $CoCl_2$ on *Drosophila* S2 cellular ATP production after 4 hours of incubation and the protection offered by acidosis (Schneider's complete medium pH plot is shown by black square markers). A "*" represents a significant statistical difference between the treatments of equivalent concentration, $P<0.05$, N=8-16.

Since acidosis led to increased ATP production in *Drosophila* S2 cells, I decided to test if S2 cells survive better in a more acidic environment compared to mammalian cells (mammalian normal pH ranges around 7.4). For this purpose, *Drosophila* cells were resuspended in HL3 saline (hemolymph-like solution), pH 7.2 (Stewart et al. 1994). Next, the pH of the cell suspensions was changed by adding small amounts of HCL or NaOH to create a range of pH from pH of 2.8 to pH of 7.8. The cells were plated in ConA-coated

wells of a tissue culture plate. After 4 hours of incubation, bright-field and fluorescent images (PI staining) of the resulting cells were obtained. The results of this experiment are shown in Fig.26A (bright-field representative images) and 26B (propidium iodide fluorescence). There, cells at pH of 7.2 and 7.8 experienced higher cell death and plasma membrane disintegration compared to cells incubated at the pH of 6.2. This was interesting but not surprising due to my previous results with elevated ATP production from acidity produced by $CoCl_2$ solutions. It seems that lower pH (less than 7.0) medium or buffered saline might be optimal for *Drosophila* cell survival, especially in stress-like conditions such as hypoxia. In addition, the effect of significantly lower pH on S2 cell survival and morphology was tested. It was found that pH of 2.8 caused cell detachment from ConA-coated plastic wells. This extremely low pH may have also resulted in cell death but interestingly the whole cells were stained mildly and diffusely with red fluorescent marker, which is atypical for dead cells (PI usually binds irreversibly to DNA and this event increases stain's fluorescence). Surprisingly, plasma membrane of the cells was fully preserved. It will be further important to look at effects of low pH on *Drosophila* S2 cell survival and mitochondrial function during various environmental and physiological stresses.

Furthermore, S2 cells were resuspended in HL3 saline and treated with the stock $CoCl_2$ resulting in different final concentrations to see if cellular membrane would be preserved (Fig. 26C). Control cells, which were treated with the corresponding volume of DI water, showed a high degree of plasma membrane disintegration. On the other hand, cells treated with 2mM and 10mM $CoCl_2$ showed healthy cellular morphology and normal cell attachment to the substrate. Next, the S2 cells were resuspended in complete

Schneider's insect medium (pH 7.0±0.2) and treated with 10mM $CoCl_2$ and the pH was changed to a range of values. I found that if the cells were treated with the $CoCl_2$ at physiological pH (pH of the complete Schneider's insect medium), cellular death significantly increased almost 6-fold compared to the control cell death as assessed by PI/Hoechst 33342 stain (Fig. 27). On the other hand, acidosis (pH ~6.2) led to an extreme cell protection as the cell death upon this treatment was statistically equivalent to the control cell death levels (cells incubated at pH of 7.0±0.2 and not treated with $CoCl_2$).

The above acidity and $CoCl_2$ studies, together suggest that a decreased pH led to the *Drosophila* S2 cell protection through increased ATP production. In mammalian studies employing neuronal cells as well as cancer cells, the benefit of mild acidosis has also been shown. In rodent hippocampal brain slices, it was determined that acidosis (pH 6.4 or 6.7) leads to prolonged survival of neurons (Yao et al. 2007). In cortical neurons, mild acidosis resulted in delayed ATP depletion, mitochondrial rearrangement and elongation (Khacho et al. 2014). Surprisingly, in these cortical neurons, pH of 6.0 resulted in mitochondrial fragmentation, which could potentially lead to less efficient mitochondrial metabolism. In hepatocyte cultures, extracellular acidosis (pH 6.1-6.5) results in a significantly delayed cell death in a model of chemical hypoxia with KCN and iodoacetate (Gores et al. 1988). In this manner, a mild acidosis as a part of ischemic physiological environment could be potentially considered as an unexpected positive "side effect" of stroke-like conditions. It will be interesting to see the effects of acidosis, if any, in fruit flies subjected to anoxia/reoxygenation stress *in vivo*. It is possible that the acidosis may offer increased neuroprotection to flies fed with acidic food and subsequently exposed to gas anoxia. In a similar manner, it was previously shown that flies fed acidic diet survive longer than the

flies consuming food of regular or alkaline pH (Deshpande et al. 2015). As a result, extracellular pH could be a potential therapeutic target for treatment of stroke-like conditions, metabolic dysfunctions, as well as for extending organism's life expectancy. Furthermore, it is well understood that glycolysis is one of the major mechanisms of cancerous cell improved survival (Steliou et al. 2009; Bonuccelli et al. 2010; Marino et al. 2012). In these cells, acidosis is a byproduct effect of lactate production during glycolysis. In turn, this "side effect" may be protective to the cancer cells due to modification of their metabolism (when sugar substrates are present) as well as due to easier cell detachment from substrate tissues, which leads to metastasis, a similar phenomenon to what was observed in S2 cells incubated at extremely low pH (Rofstad et al. 2006; Ibrahim-Hashim et al. 2017; Wu et al. 2017). Since it is also known that acidosis leads to degradation of extracellular matrix in tumor models, the fruit flies could be used as models for studying cancer metabolism and cancer metastasis *in vitro* and potentially *in vivo* (Gatenby et al. 2006).

A

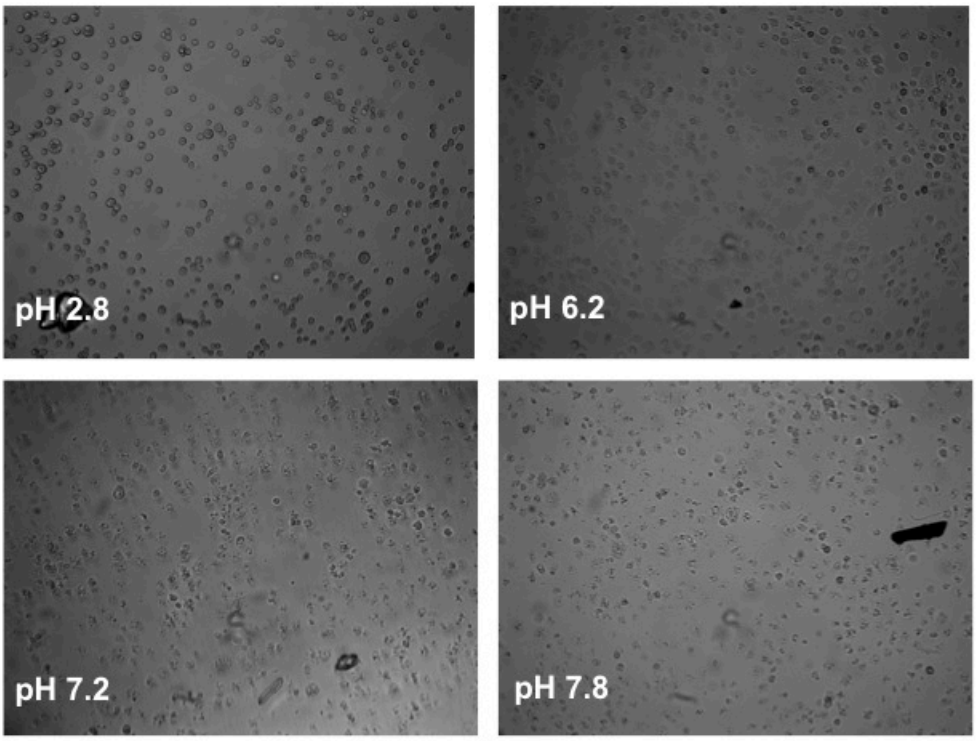

B

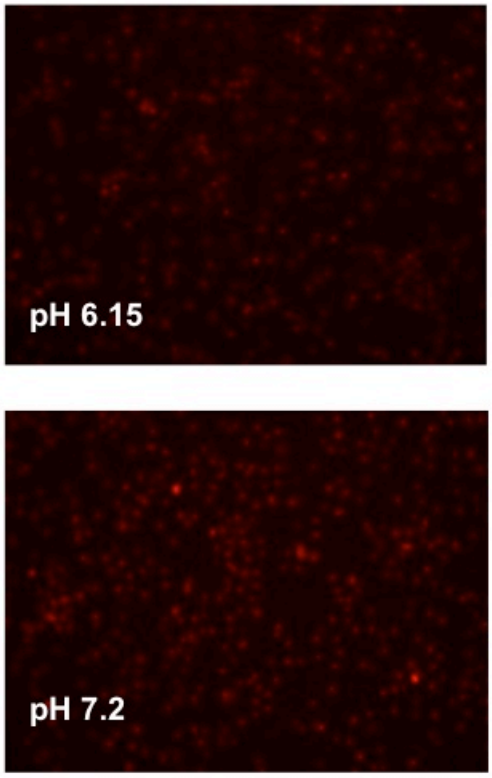

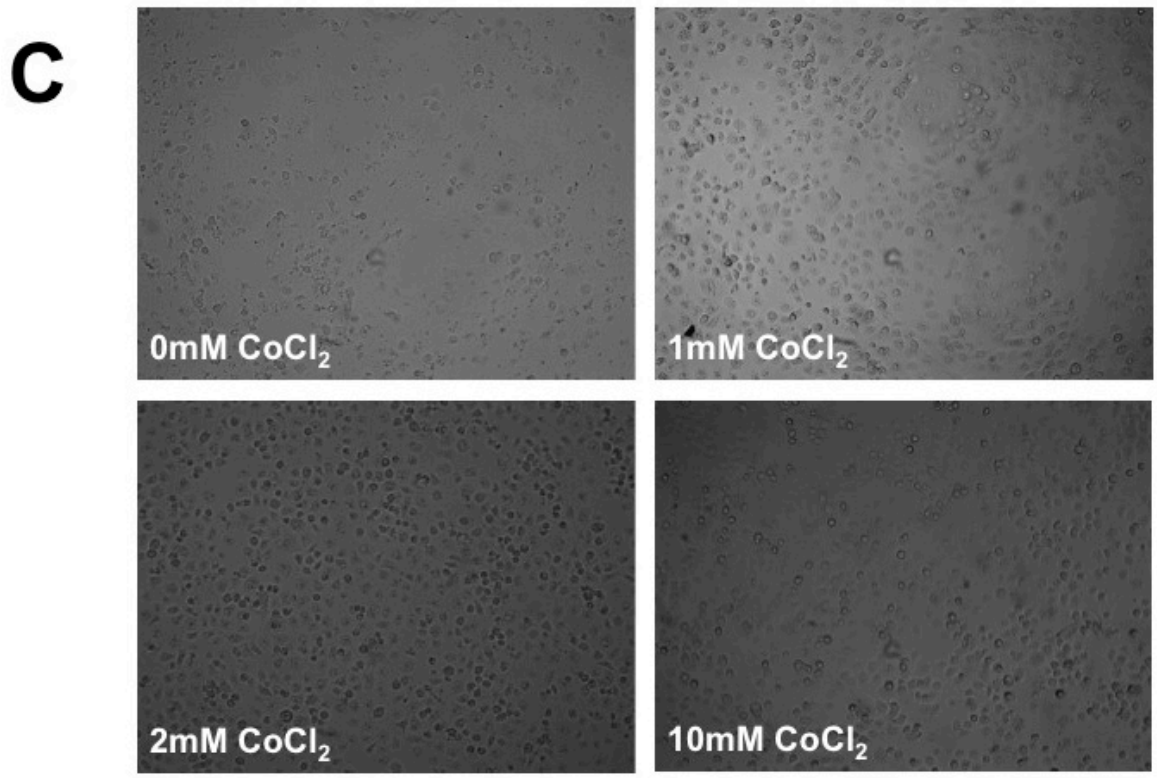

Figure 26. Protective effect of acidosis on *Drosophila* S2 cell morphology and death as assessed by microscopy. A) Bright field images of cells resuspended in HL3 saline. pH was subsequently changed to values shown inside of each image. B) Fluorescence images of cells resuspended in HL3 saline of different pH values and stained with the propidium iodide. C) Bright field images of cells resuspended in HL3 saline and treated with $CoCl_2$ stock (pH of the cells suspension was as shown in Fig. 24). Images represent the typical results.

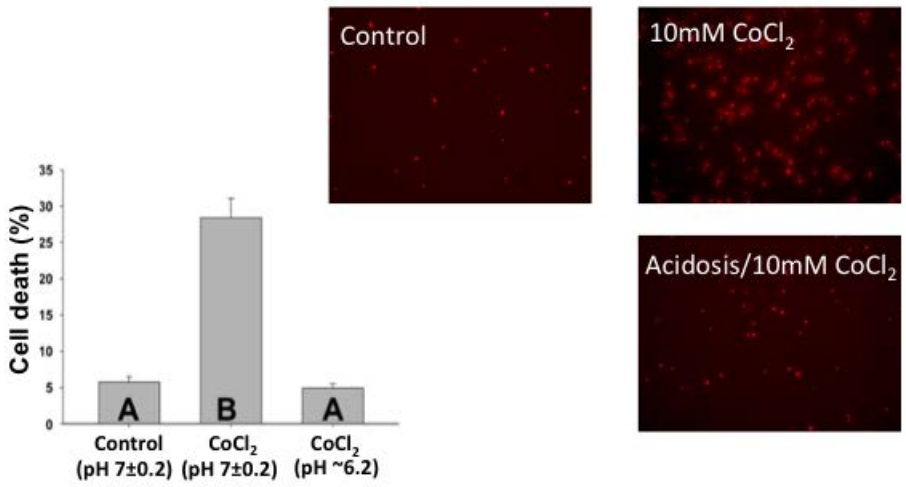

Figure 27. Protective effect of acidosis on $CoCl_2$-induced cell death in *Drosophila* S2 cell line. Acidosis refers to pH of ~6.2. Red cells on images are stained with cell death indicator propidium iodide. Different letters refer to significant differences between the treatment groups, $P<0.05$, $N=3$.

3.3.2.3. Assessment of cellular ROS content upon $CoCl_2$ treatment

Since there are reports that $CoCl_2$ induces oxidative stress, intracellular ROS measurement assay was performed in *Drosophila* cells to further investigate the mechanism of action of this chemical on the cells. In this assay, ROS oxidize DCFH fluorescent marker loaded inside the cells (LeBel et al. 1992). $CoCl_2$ at concentrations equal or higher than 1mM after 4 hours of incubation caused a significant increase in intracellular ROS production (Fig. 28). 1mM $CoCl_2$ increased the amount of intracellular ROS levels more than 2 times compared to control, while 10mM increased ROS concentrations 5-fold. A possible explanation for the results could be that the $CoCl_2$ blocked ETC function leading to an increased leak of electrons in addition to decreased proton gradient. It is also possible that $CoCl_2$ inhibited function or expression of some of *Drosophila* antioxidant enzymes by a yet unknown mechanism that should be further

investigated.

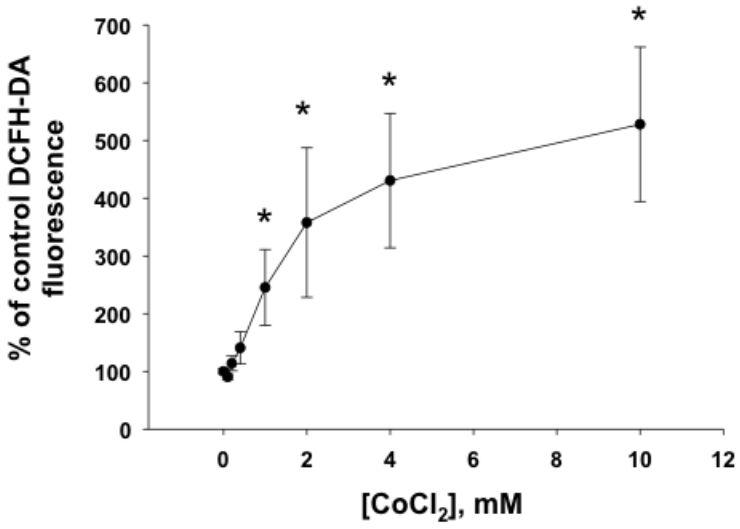

Figure 28. Intracellular ROS levels increased upon $CoCl_2$ *Drosophila* S2 cell treatments. A "*" represents a significant statistical difference between a treatment and the control, $P<0.05$, $N=3$.

To test if the "acidosis" observed in the previous section was protective due to decreased intracellular ROS production, pH of the medium containing $CoCl_2$ at different concentrations was changed to the one of the complete Schneider's insect medium (pH 7.0±0.2) (Fig. 29). When the pH was changed to the control physiological levels, ROS production increased significantly by a factor of two compared to the acidosis-treated cells. This suggests that acidosis protected cells by decreasing the intracellular ROS concentrations or by inhibiting the ROS formation.

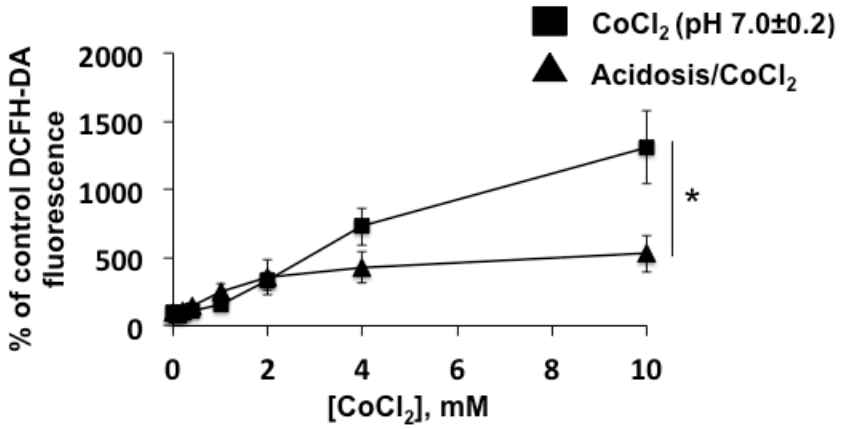

Figure 29. Intracellular ROS levels decreased upon $CoCl_2$ *Drosophila* S2 cell treatment and pH decrease. A "*" represents a significant statistical difference between two treatments at equivalent $CoCl_2$ concentrations, $P<0.05$, $N=3$.

In this set of experiments, it was shown that $CoCl_2$ inhibited ATP production at higher concentrations (above 1mM) and also induced significant ROS production. On the other hand, acidosis (pH of ~6.2), allowed for complete protection from cell death induced by 10mM $CoCl_2$ treatment, ATP level preservation, as well as significant decrease in ROS production.

3.3.3. Assessment of hydrogen peroxide effects on Drosophila S2 cells

3.3.3.1. Assessment of cytotoxicity of different concentrations of hydrogen peroxide

To expand on the observation that increased cell survival was associated with reduced ROS and vice versa, the cells were treated with H_2O_2 to test the hypothesis that oxidative stress would affect survival. As expected, hydrogen peroxide-induced cell death in *Drosophila* S2 cells, which was directly proportional to the concentration of the chemical being used. Surprisingly, relatively high concentrations of hydrogen peroxide

(50mM) were needed to induce ~50% of cell death. This was not expected, as in mammalian studies hydrogen peroxide concentrations causing equivalent levels of death are significantly lower; mammalian cells such as of epithelium as well as macrophages (maximum concentration 1mM) are sensitive to much lower concentrations of peroxide (Mulier et al. 1998; Maeda Yasuhiro Yoshioka et al. 2006; Okahashi et al. 2013). This resistance or tolerance to a H_2O_2-induced cell death could be the result of *Drosophila* cells employing unique cytoprotective strategies that are downregulated or absent in mammalian cells.

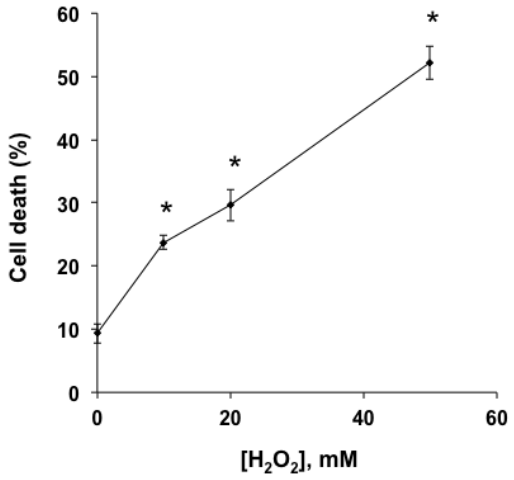

Figure 30. Increasing concentrations of H_2O_2 resulted in *Drosophila* S2 cell death. P<0.05, N=3.

3.3.3.2. Assessment of intracellular calcium and cell death upon hydrogen peroxide treatment

Since it is known from mammalian research that hydrogen peroxide induces an influx of calcium leading to cell death, next, I determined if hydrogen peroxide treatment resulted

in calcium influx or overload in *Drosophila* cells (Thomas et al. 1998; Bruce and Elliott 2007; Zhang and Ma 2008; Nakamura et al. 2009). Because it was previously found that 10mM hydrogen peroxide treatment showed a minimum significant cytotoxic treatment, it was decided to test if this concentration of hydrogen peroxide induces the cell toxicity by means of inducing calcium overload. To do so, S2 cells were loaded with Fluo-3AM fluorescent indicator of calcium ions and treated with 10mM hydrogen peroxide for 4 hours in a calcium-containing buffer (Fig. 31). It was found that there was an increased Fluo-3AM-positive fluorescence in wells treated with hydrogen peroxide compared to the sham control wells. When the same cells were stained with propidium iodide cell death marker, some of the green fluorescent cells were not co-stained with propidium iodide. Lower green fluorescence of the cells in the hydrogen peroxide treatment images indicated loss of intracellular calcium potentially due to the loss of membrane integrity towards the end of 4-hour incubation period. This result means that in *Drosophila* S2 cells, the acute H_2O_2 treatment caused an influx of calcium and subsequently led to cell death but the intermediate mechanism needs to be further investigated.

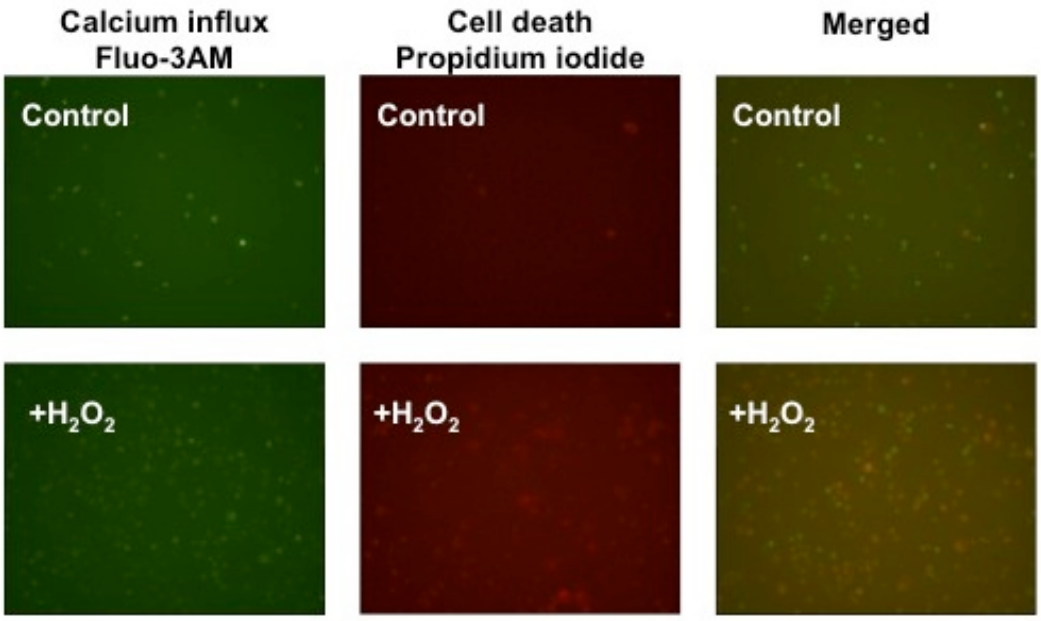

Figure 31. Images showing the effect of 10mM hydrogen peroxide on intracellular calcium concentration and cell death. Cell death occurred after calcium influx reached its maximum and dissipated possibly due to plasma membrane disintegration. Representative images are shown.

3.4. Conclusions

In conclusion, $CoCl_2$, NaN_3, and H_2O_2 caused cell death in a concentration-dependent manner. As expected, mechanisms and extent of cytotoxicity of these chemicals were different for each as well as from mechanisms determined in mammalian studies as described in the literature. In this set of experiments, it was found that $CoCl_2$ and NaN_3 caused a decrease in metabolic function and caused ATP depletion. In addition to its effect on cellular ATP, cobalt chloride also led to intracellular ROS production. Moreover, in *Drosophila* S2 cells, H_2O_2 caused calcium influx followed by plasma membrane disintegration, which potentially indicated mitochondrial involvement and cytochrome c leakage. In this set of studies, it was also discovered that *Drosophila* S2 cells can be

significantly protected from cobalt chloride-induced stress by inducing mild acidosis. At high concentration of $CoCl_2$, upon induction of acidosis, cell morphology and ATP levels were preserved and ROS levels decreased. It will be necessary to further investigate the protective mechanisms behind this unexpected and interesting phenomenon. This particular novel finding could uncover one of the important mechanisms of anoxia-tolerance in *Drosophila* since, in general, insect hemolymph is significantly more acidic (pH 6.4-6.8) than the blood and the interstitial fluid of mammals (Wyatt and Meyer 1959; Xylander 2009). There is also a wide discrepancy in the ability of different insects to tolerate anoxia. For example, *Locusta migratoria* can only survive up to 4 hours of anoxia whereas *Manduca sexta* can survive up to 24 hours of complete anoxia (Wegener and Moratzky 1995). Differences in anoxia-tolerance capabilities between different insect species should be further investigated specifically comparing pH values of insect hemolymph. Moreover, the *Drosophila in vitro* models of chemical hypoxia and oxidative stress developed in this research could potentially be used to test different pharmacological compounds as well as RNAi gene silencing systems to further uncover potential mechanisms of the unique hypoxia tolerance observed in fruit flies.

CHAPTER 4

Effects of cGMP/PKG signaling on survival and metabolism of Drosophila S2 cells

4.1. Introduction

It was previously reported in mammalian studies that the activation of the cGMP/PKG pathway is protective from low oxygen and oxidative stress. For example, it was shown that a Phosphodiesterase 5 (PDE5) inhibition by administration of sildenafil citrate (PDE5 inhibitor) leads to brain protection in mice subjected to chronic 8-day hypoxia (Caretti et al. 2008). In addition, it was demonstrated that PKG activation protects human neuroblastoma cells from oxidative damage and apoptosis (Andoh et al. 2003). In cortical neurons, cGMP/PKG pathway activation also leads to cytoprotection from oxidative stress (Fernández-Tomé et al. 1999; Abdul and Butterfield 2007). Since the pharmacological activation of the cGMP/PKG pathway showed to be protective from anoxia/reoxygenation stress in *in vivo* studies in adult *Drosophila* (Chapter 2), it was tempting to investigate if a pharmacological activation of the cGMP/PKG pathway in *Drosophila* cell culture would lead to protection from low oxygen and oxidative stress. Since in the previous chapter, important aspects of NaN_3, $CoCl_2$, and H_2O_2 toxicity in *Drosophila* S2 cell line were investigated, the effects of cGMP/PKG-targeting

pharmacological compounds on the stressed *Drosophila* S2 cell survival and health were investigated next. After the effects of the cGMP/PKG activation and inhibition were assessed, potential downstream targets of the cGMP/PKG signaling were determined using combinations of pharmacological PKG activators and inhibitors of downstream molecular targets under question. Various pharmacological activators and blockers affecting specific molecular targets of the hypothesized cGMP/PKG pathway were used on *Drosophila* S2 cells treated with cobalt chloride and hydrogen peroxide and their effects on cytotoxicity were determined by the trypan blue exclusion method. Fig. 32 displays some of the chemical activators and inhibitors of the pathway of interest that were employed in the experiments.

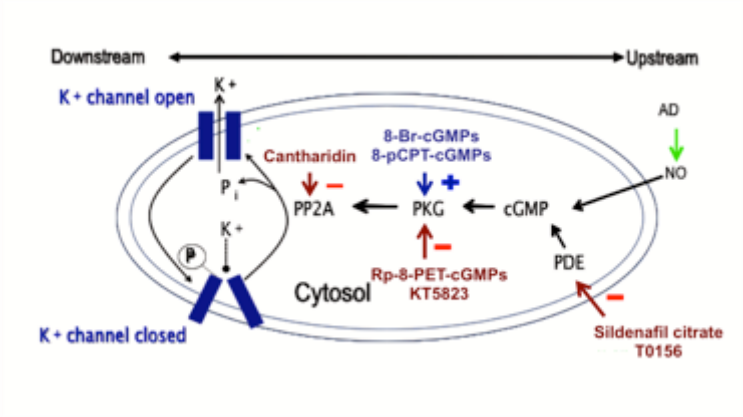

Figure 32. Diagram of the cGMP/PKG pathway with pharmacological agents that target specific molecules of the pathway (adapted from Dawson-Scully et al. 2010). "+" means activation, "-" means inhibition.

4.2.1. Cell culture protocol

Drosophila S2 cells were cultured as described in the section 3.2.1. After the centrifugation step, the supernatant was exchanged for an appropriate volume of fresh complete *Drosophila* Schneider's medium (containing 10% FBS and 1% penicillin/streptomycin antibiotics) to generate 1×10^6 cells/ml suspension. The cell suspension then was divided into 1 ml aliquots to perform pharmacological treatments with subsequent cell counting.

4.2.2. Physiological stress induction: NaN_3, $CoCl_2$, and H_2O_2

In order to determine effects of the activation and the inhibition of the cGMP/PKG pathway during metabolic and oxidative stresses, a pharmacological approach was used. To induce metabolic stress, NaN_3 or $CoCl_2$ stock solutions were added to the cell suspensions to generate a final concentration of 1 mM. Since a PKG activation treatment (see next section) was more effective during $CoCl_2$-induced stress, the remainder of the experiments was performed solely utilizing $CoCl_2$ to induce chemical hypoxia. To induce acute oxidative stress, H_2O_2 was added to the cell suspensions to a final concentration of 10mM. For those experiments, the H_2O_2 aqueous solution was made fresh before each individual trial to avoid H_2O_2 degradation and the rest of pharmacological treatments were performed immediately before stress induction. The cells were incubated with stressors and pharmacological compounds for 4 hours at room temperature.

4.2.3. Pharmacological cGMP/PKG pathway manipulation

4.2.3.1. PKG activation

Manipulation of the cGMP/PKG signaling was achieved using chemicals that target upstream and downstream components of the pathway. Different known activators and

inhibitors of the cGMP/PKG pathway, as well as activator and inhibitors of the potential downstream targets of the cGMP/PKG signaling, are shown in Fig. 33. First, it was necessary to test if an activation of the cGMP/PKG pathway led to cytoprotection from $CoCl_2$- and H_2O_2- induced stresses, as was seen *in vivo*. The cGMP/PKG pathway was activated by direct PKG kinase activation via 8-Br-cGMP (40µM) or by indirect PKG activation via upstream inhibition of PDE5 by sildenafil citrate (10µM). It was hypothesized that both a direct and an indirect activation of the PKG enzyme would result in increased survival upon induction of the physiological stresses. 8-Br-cGMP was dissolved in sterile DI water and sildenafil citrate was dissolved in dimethyl sulfoxide (DMSO). DMSO constituted up to 0.05% (v/v) maximal final concentration.

4.2.3.2. PKG inhibition

After determining that 8-Br-cGMP and sildenafil citrate offered protection during aforementioned stresses, inhibition of the cGMP/PKG pathway was induced by direct inhibition of the PKG enzyme by Rp-8-Br-PET-cGMP (50µM) and KT5823 (1µM). It was hypothesized that direct inhibition of the PKG enzyme would result in decreased survival upon induction of the physiological stresses. Rp-8-Br-PET-cGMP was dissolved in either dimethyl sulfoxide (DMSO) or sterile DI water. DMSO constituted up to 0.05% (v/v) maximal final concentration.

4.2.3.3. Non-specific potassium ion channel blocking

Next, a general potassium ion channel blocker tetraethylammonium (TEA) was used in both metabolic disruption by $CoCl_2$ and acute oxidative stress by H_2O_2 to dissect potential signaling targets downstream of PKG; this was done since there are reports that the cGMP/PKG activates potassium ion channels in plasma membrane or mitochondrial

inner membrane in mammals (Zhang et al. 2008; Behmenburg et al. 2015; Khavandi et al. 2016; Frankenreiter et al. 2017). In these experiments, TEA was dissolved in deionized sterile water. A concentration versus cell death plot was constructed to determine the toxicity of TEA by itself without induction of stress to determine an effective and nontoxic concentration of TEA to be used in the co-treatment experiments. Next, combinations of the co-treatments of TEA, 8-Br-cGMP, and physiological stressors were administered to the *Drosophila* S2 cells. This was done to determine if the 8-Br-cGMP-induced activation would be inhibited by the co-administration of TEA, which targets K^+ ion channels, the potential downstream targets of the cGMP/PKG (Dawson and Routledge 1995; Doggrell and Bishop 1996; Luzhkov and Åqvist 2001). In both chemical hypoxia and acute oxidative stress experiments, TEA was added to cell suspensions before adding 8-Br-cGMP.

4.2.3.4. Specific mitochondrial ATP-sensitive potassium ion channel blocking

After inconclusive results from the administration of TEA to cells co-treated with $CoCl_2$ or H_2O_2 and the PKG activator 8-Br-cGMP, it was decided to use a more specific potassium ion channel blocker 5-HD at 100µM concentration. 5-HD is a specific inhibitor of mitochondrial ATP-sensitive potassium ion channels that was used together with 8-Br-cGMP during stress-inducing conditions to determine if there is an abrogation of 8-Br-cGMP-induced protection due to a downstream target blockade (in this case, mitochondrial K^+ ion channels are the potential downstream targets) (Liu et al. 2001). The 5-HD solution was prepared in sterile deionized water and was administered to the *Drosophila* S2 cells similar to TEA, before the 8-Br-cGMP co-treatment.

4.2.3.5. Specific mitochondrial ATP-sensitive potassium ion channel activation

To further confirm the involvement of mitochondrial ion channels in one of the cytotoxic treatments, 1µM, 10µM, and 100µM diazoxide (DZX) was used upon induction of stress without co-administration of 8-Br-cGMP. If mitochondrial ATP-sensitive ion channels were involved in protective signaling, then the activation of this ion channel with DZX would result in protection from $CoCl_2$- and or H_2O_2-induced cell death. The DZX solutions were prepared in DMSO and were administered to the *Drosophila* S2 cells immediately before a cytotoxic treatment.

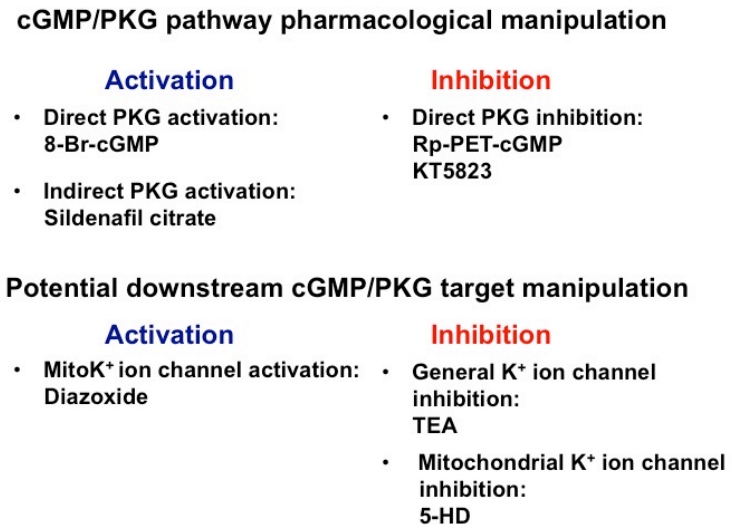

Figure 33. Pharmacological compounds used in this research in *Drosophila* S2 cell death assessment.

4.2.3.6. Control pharmacological treatments

To ensure that the pharmacological agents used to modulate the cGMP/PKG pathway did not have independent toxic effects on S2 cells, 8-Br-cGMP, 5-HD, Rp-8-Br-PET-cGMP, DMSO, and sildenafil citrate were tested independently and control treatments were not subjected to any pharmacological treatments except the equivalent volume of DI water (Fig. 34). These treatments did not induce cytotoxicity in *Drosophila* S2 cells at tested concentrations in the absence of a physiological stress. TEA treatment, on the other hand, induced toxicity in a concentration-dependent manner with 0.250mM demonstrating the lowest cytotoxic effect (Fig. 35).

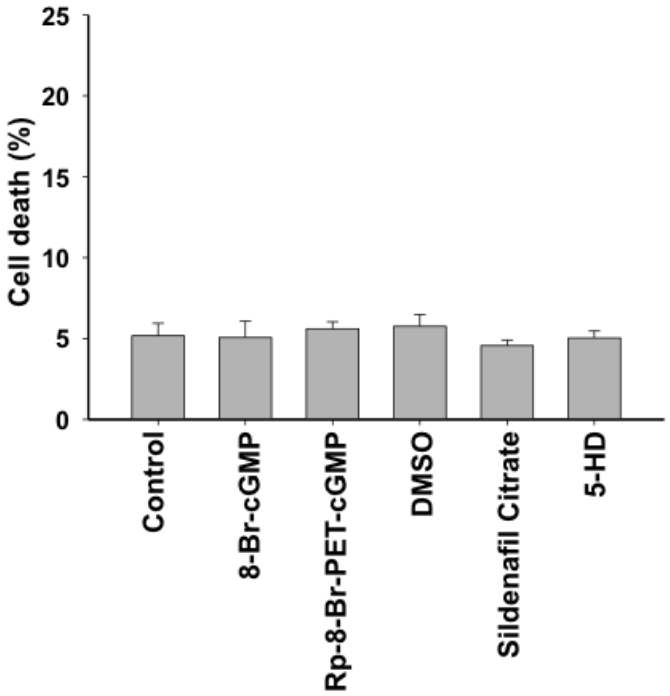

Figure 34. Pharmacological compounds did not induce a significant *Drosophila* s2 cell death in the absence of a physiological stress. S2 cells were treated with DI water (control), 40μM 8-Br-cGMP, 50μM of Rp-8-Br-cGMP, 0.05% (v/v) DMSO, 100μM 5-HD, 10μM of sildenafil citrate. Cells were incubated at

room temperature for 4 hours without additional pharmacological stress. No statistical difference was found between these treatments, P>0.05, N=5-6.

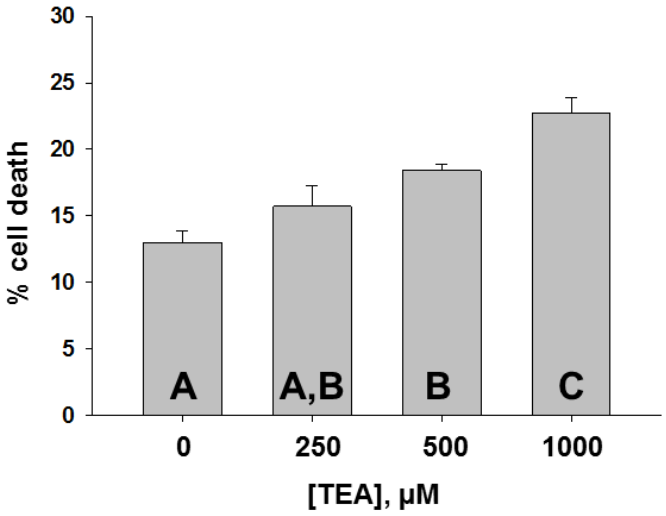

Figure 35. Increasing concentrations of TEA caused *Drosophila* S2 cell death. Cells were treated either only with DI water or TEA. Different letters indicate there is a significant statistical difference between the compared experimental groups, P<0.05, N=3.

4.2.3. Cell death assessment by trypan blue exclusion method

Determination of cell death was done using the trypan blue exclusion method with live and dead cell counting with a Bright-Line hemocytometer (Improved Neubauer, 0.100 mm deep) and a compound light microscope (Swift Instruments International S.A.). About 400-600 cells total were counted in at least three separate counts for each treatment and then the percent of cell death was calculated and averaged between trials.

4.2.4. Oxidative stress measurements

After determining that the activation of the cGMP/PKG pathway was protective during metabolic stress and that this protection was potentially a result of mitochondrial ATP-sensitive K^+ ion channel activation downstream of PKG enzyme, it was rational, next, to investigate the biochemical mechanism, through which *Drosophila* S2 cells were protected upon the cGMP/PKG pathway activation and mitochondrial potassium ion channel inhibition. In order to carry this out, first, it was tested whether cGMP/PKG pathway activation leads to a decrease in ROS formation since one of the main mechanisms of $CoCl_2$- induced toxicity was oxidative stress induction, as shown in Chapter 3.

The levels of reactive oxygen species oxidative stress in S2 cells were determined by OxiSelect^{TM} Intracellular ROS Assay Kit - Green Fluorescence. First, 100µL of S2 cells were plated in black 96-well plates (coated with conA), treated and incubated with $CoCl_2$, 8-Br-cGMP, 5-HD, and combinations of these chemicals for 4 hours at room temperature. After the incubation, the cells were washed gently two times with a saline solution to remove a complete Schneider's medium, which produces green autofluorescence; the extent of green fluorescence was determined using SpectraMax M2 plate reader at 485nm excitation/538nm emission wavelengths. The relative intracellular DCFH fluorescence values were expressed as percent of the control level of green fluorescence.

4.2.5. Mitochondrial membrane potential measurements

Since the source of 8-Br-cGMP-induced protection was found not to be a reduction in intracellular ROS concentrations, mitochondrial membrane potential was tested next. It is possible that the opening of mitochondrial potassium ion channels leads to a decrease in mitochondrial inner membrane electric potential, only if the potassium current is directed

inwards, into the mitochondrial matrix. Similarly, from electrophysiological experiments done in *Drosophila* larvae, upon induction of low oxygen stress, neuronal synaptic failure at a neuromuscular junction (NMJ) occurs faster in larvae with higher PKG enzymatic activity upon oxidative stress (Caplan et al. 2012). This could also be due to a decreased mitochondrial membrane potential and interruption of ATP production to power the propagation of action potentials.

Here, the mitochondrial membrane potential was assessed using CMH_2-XRos MitoTracker red dye. *Drosophila* S2 cells were seeded on 1cm × 1cm glass slides inside of 6-well plate wells coated with Con A at the concentration of 0.5mg/mL (Buster et al. 2010) for at least 30 minutes to allow for their attachment to the glass coverslips and then were treated with combinations of chemicals. At the end of the 4-hour incubation period, the cells were washed 2 times with a Schneider's insect medium without FBS (to avoid false-positive results due to oxidation of the FBS) and loaded with MitoTracker Red CM-H_2XRos dye (the highly functional mitochondria showed higher level of fluorescence) for 30 minutes, fixed in fresh 4% paraformaldehyde in Schneider's medium, washed two times in 1 × PBS. Then, a drop of a mounting media containing DAPI stain was added separately onto a glass slide and a coverslip containing treated cells were placed upside down (cells were facing the glass slide) and clear nail polish was used to seal the coverslip. The slides then were stored at 4˚C until images were taken using a confocal Carl Zeiss Microimaging LSM 700 laser scanning system/Zen 2009 software and an Axio Observer Z1 inverted microscope). All the images were taken using the same microscope settings throughout and within all the trials to allow for comparison but the results were always compared to the control results for each specific trial.

4.2.6. ATP experiments

After assessing the modulating effect of cGMP/PKG activation on *Drosophila* S2 cell mitochondrial membrane potential during $CoCl_2$-induced stress, it was critical to determine if the mitochondrial inner membrane potential changes detected would translate into equivalent changes in the ATP production. To accomplish this, intracellular ATP assays were performed in *Drosophila* S2 cells treated with $CoCl_2$ with or without PKG activator 8-Br-cGMP. Furthermore, the effect of 5-HD on the metabolically stressed cells was also investigated to see if 5-HD would abrogate the 8-Br-cGMP-induced effect, if any, on *Drosophila* cells subjected to the cobalt chloride treatment. This would further confirm the results obtained from the cell death assessment experiments. The ATP assays were performed as described in Chapter 3 but with a slight modification. The relative ATP production was assessed instead of the actual values of the intracellular ATP levels. The values were expressed as percent of the control (DI water-treated cell samples). At least 3 independent trials were performed with each treatment per trial carried out in a triplicate.

4.2.7. Statistics

Statistical analysis was carried out by performing Student t-tests and one-way ANOVA with Student-Newman-Keuls *post-hoc* test. This was done using SigmaPlot Statistical Analysis Software (Systat Software, Inc., San Jose, California). A result was considered statistically different when $P<0.05$. Significant differences between groups are represented on graphs as stars (*) above bars or as different alphabetical letters inside the bars. The data are represented as means ± SEM.

4.3. Results and discussion

4.3.1. PKG activation during metabolic stress

First, cell death assessment upon activation of the PKG pathway was performed in cells undergoing metabolic stress from NaN_3 and $CoCl_2$ treatments. From Chapter 3, induction of either stress should result in a significant cell death when compared to the controls, which were treated with DI water. To induce a metabolic stress and, in case of the cobalt chloride, also an oxidative stress, the *Drosophila* S2 cell cultures were treated either with 1mM sodium azide or 1mM cobalt chloride as shown in Fig. 36. Both treatments resulted in an increased cell death compared to the untreated control cell cultures. Furthermore, the specific PKG activator, 8-Br-cGMP, was used to pharmacologically activate the cGMP/PKG pathway. Functionally, 8-Br-cGMP is analogous to the natural signaling molecule cGMP but with some of its functional groups being replaced (Wyatt et al. 1991). From the data shown in Fig. 36, the activation of the PKG pathway resulted in a significant decrease in a cell death with either stress being applied.

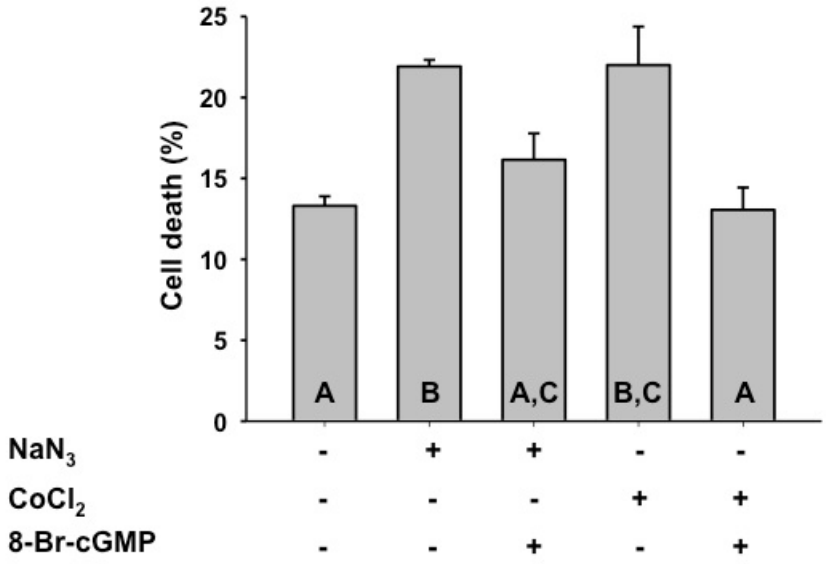

Figure 36. Metabolic disruptors sodium azide and cobalt chloride induced cell death whereas cGMP/PKG activation protected *Drosophila* S2 cells. Control cell cultures were not treated with pharmacological compounds. Different letters refer to a significant difference between treatment groups, $P<0.05$, N=3.

4.3.2. PKG activation and inhibition during acute oxidative stress

Upon an acute oxidative stress treatment with 10mM H_2O_2 and simultaneous activation of the PKG pathway, there was a decrease in cell death. The results of the experiment are shown in Fig. 37. Activation of the cGMP/PKG pathway with 8-Br-cGMP led to decreased cell death suggesting that the direct activation of PKG enzyme offered a cytoprotection in the *Drosophila* S2 cell culture (Fig. 37A). Moreover, an indirect activator of the PKG pathway, sildenafil citrate, was used at 1µM and 10µM concentrations during the acute induction of oxidative stress. This chemical compound specifically inhibits phosphodiesterase 5 (PDE5), a molecule that enzymatically hydrolyzes endogenous cGMPs (Moreland et al. 1999). As in case of the direct PKG activation, indirect activation of the cGMP/PKG pathway also led to cytoprotection from the acute oxidative stress although higher concentration demonstrated increased effectiveness as determined by statistical analysis (Fig. 37B).

To inhibit the cGMP/PKG pathway, specific blockers of PKG enzyme Rp-8-PET-cGMPs (50 µM) and KT5823 (1 µM) were used (Fig. 37A, 38). It was found that the inhibition of the PKG pathway by these chemicals did not result in increased cell death, which was unexpected and could be due to the short time of incubation (4 hours only). The 0.05% dimethyl sulfoxide (DMSO) control treatment was also carried out since the 8-Br-PET-cGMPs were dissolved in DMSO. The DMSO treatment did not result in any further

increase in cellular death, which means that at this particular concentration, it was not toxic to the *Drosophila* S2 cells. An additional explanation for such results could be the fact that PKG inhibition using direct pharmacological inhibitors did not proceed in full, meaning that PKG was still functional enough to fulfill its physiological roles. On the other hand, during a time of stress or a pathological event such as apoptosis or necrosis, decreased PKG function may be detrimental to cells. It will be further necessary to test different concentrations of PKG inhibitors and simultaneously measure levels of PKG activity.

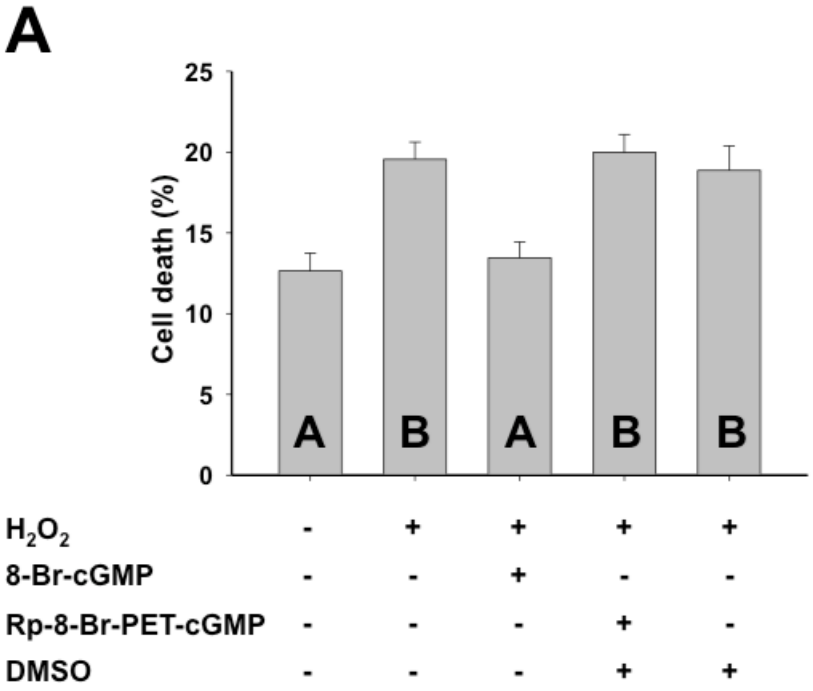

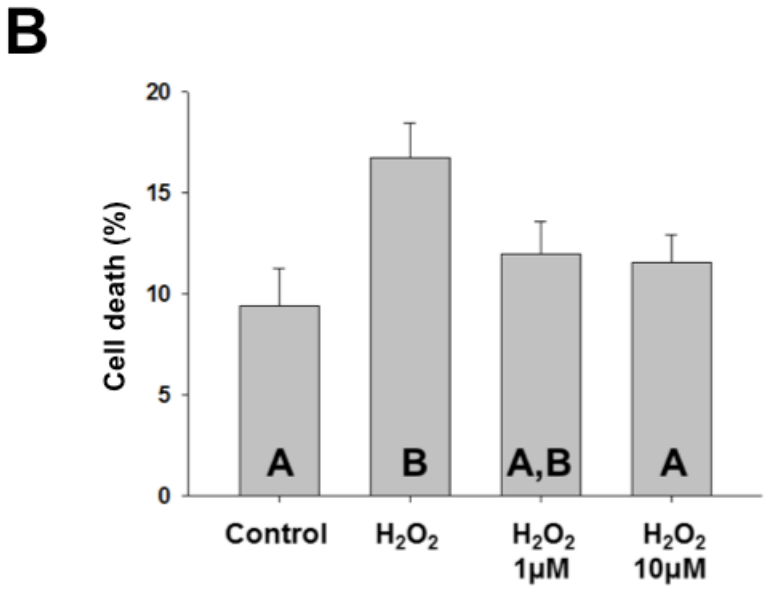

Figure 37. Effect of an acute oxidative stress and cGMP/PKG pathway manipulation on *Drosophil*a S2 cell death. A) Direct activation and inhibition of PKG; B) Indirect activation of PKG with sildenafil citrate at two different concentrations. Different letters refer to significant differences between the treatment groups, $P<0.05$, N=3-8.

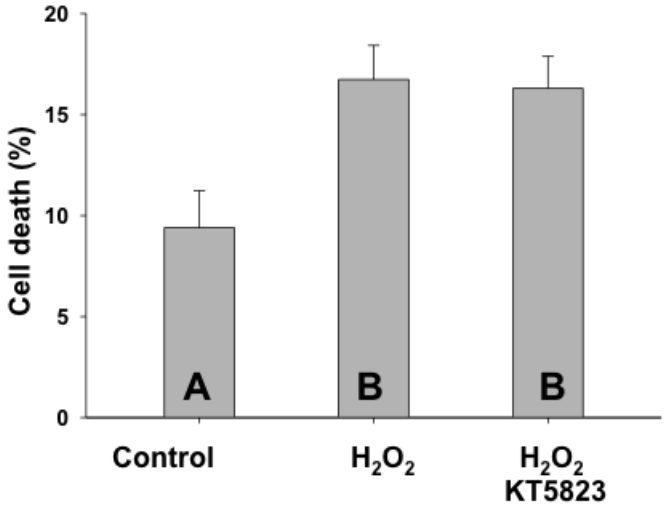

Figure 38. cGMP/PKG pathway inhibition with 1uM KT5823 did not result in further *Drosophila* S2 cell death. Different letters refer to significant differences between the treatment groups, P<0.05, N=3-5.

4.3.3. Potassium ion channel blocking and activation during a metabolic stress

Since it was determined that activation of the PKG pathway led to cell protection during the metabolic stress, I next tested whether the PKG pathway ultimately acts on a specific type of potassium ion channels, thus changing membrane potential. Some of the potential downstream targets of the PKG pathway are plasma membrane potassium ion channels and mitochondrial potassium ion channels. The opening of either one of the channels would result in changes in membrane potential depending on the subcellular localization and potassium ion current direction. To test this hypothesis the following chemicals were used: tetraethylammonium (TEA), 5-hydroxydecanoate (5-HD), and diazoxide (DZX). TEA is a non-specific blocker of the K^+ ion channels in the cells. It was previously found by our lab that 0.250mM TEA specifically inhibits plasma membrane K^+

ion channels (Caplan et al. 2012). On the other hand, 5-HD is a specific mitochondrial ATP-sensitive potassium ion channel blocker that was shown to block potassium currents through the inner mitochondrial membrane in isolated mitochondrial fractions (Assad et al. 2009). The downstream blocking experiments and cell survival assessment were performed with $CoCl_2$ (Fig. 39, 40). The obtained results demonstrated an interesting and unexpected pattern. *Drosophila* S2 cells exposed to $CoCl_2$, TEA, and 8-Br-cGMP simultaneously still showed a trend of protection although minimal and statistically not significant. This protection could be from the TEA-induced stress or from the $CoCl_2$-induced stress. In order to further narrow down the effects of potassium ion channel blockade, it was necessary to use a more specific potassium ion channel-blocking agent upon cobalt chloride treatment.

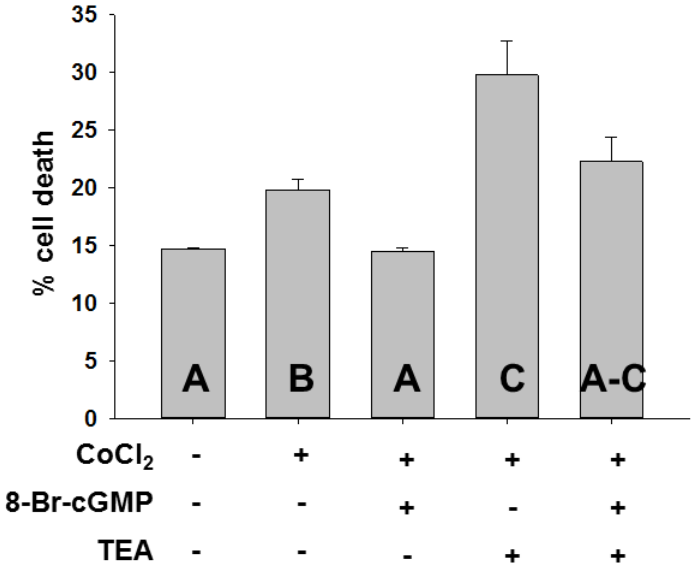

Figure 39. Effect of metabolic disruption, cGMP/PKG pathway activation, and plasma membrane potassium ion channel blockade on *Drosophila* S2 cell death. Different letters refer to significant differences between the treatment groups, P<0.05, N=3.

Next, the effect of a mitochondrial potassium channel blocking on the 8-Br-cGMP-offered protection during the metabolic stress was tested (Fig. 40). In cells co-treated with $CoCl_2$, 8-Br-cGMP, and 5-HD there was an abrogation of protection potentially by the mitochondrial ATP-sensitive potassium ion channel blocker 5-HD during the stress. This means that the molecular targets of 5-HD, potentially the mitochondrial ATP-sensitive potassium ion channels, are involved downstream of the cGMP/PKG signaling.

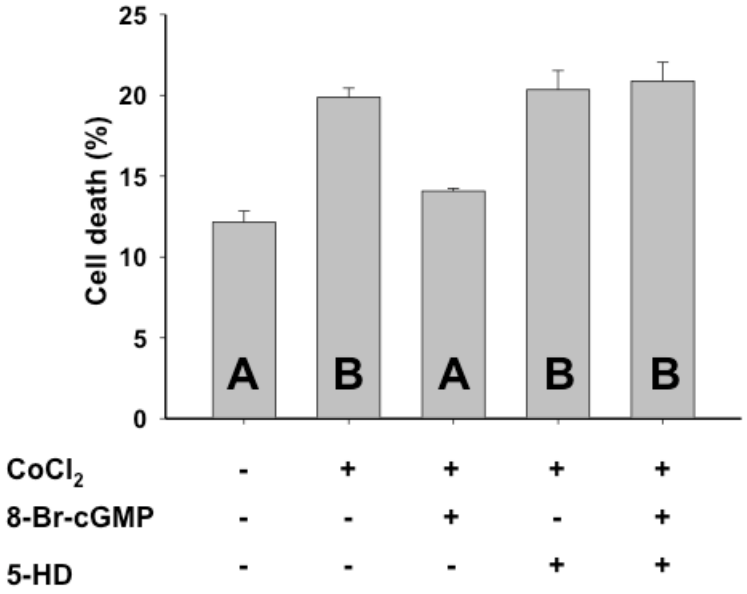

Figure 40. MitoK$_{ATP}$ channel blockade abrogated PKG-induced protection in *Drosophila* S2 cells subjected to cobalt chloride-induced stress. Different letters refer to significant differences between the treatment groups, $P<0.05$, N=3-5.

Moreover, to confirm that an activation of the mitochondrial ATP-sensitive ion channels is indeed protective in *Drosophila* S2 cells during the $CoCl_2$-induced stress, DZX (diazoxide) was used at different concentrations to find an effective range of protection.

The results of this experiment are shown in Fig. 41. When the cells were co-treated with DZX (1µM and 10µM) and cobalt chloride, there was a decrease in cell death compared to the cobalt chloride treatment alone. From this, it was confirmed that an activation of the mitochondrial ATP-sensitive potassium ion channels was protective in *Drosophila* S2 cells subjected to the cobalt chloride-induced stress. It is important to note that the existence of mitochondrial potassium ion channels in *Drosophila* is yet to be confirmed, but interestingly, both, the pharmacological activator DZX and the inhibitor 5-HD target a process, which when modulated, is protective during $CoCl_2$-induced stress (Domoki et al. 1999). In mammals, the existence of potassium ion channels targeted by the inhibitor 5-HD and the activator DZX is indeed confirmed by electrophysiological studies in isolated mitochondria (Inoue et al. 1991). It is possible that the mitochondrial potassium ion channels *in vivo* function differently from the proposed mechanism since physiological environment inside a cell is not exactly the same as in these electrophysiological experiments.

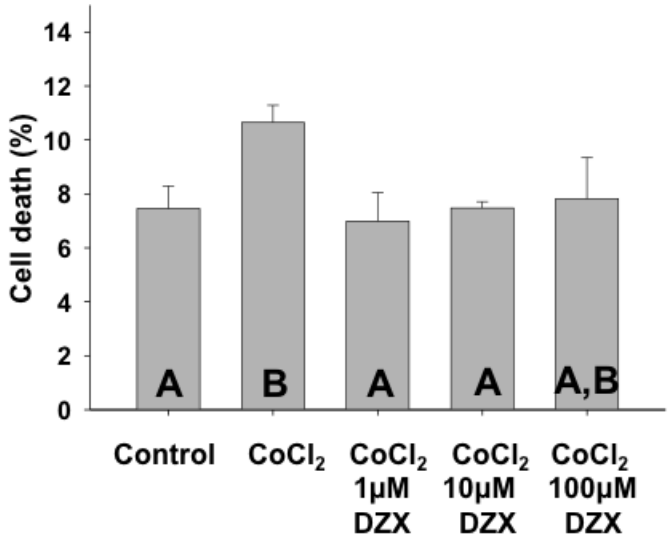

Figure 41. Mitochondrial potassium ion channel activation resulted in *Drosophila* S2 cell protection from cobalt chloride-induced stress. Different letters refer to significant differences between the treatment groups, $P<0.05$, $N=3$.

The above results demonstrated that an activation of the cGMP/PKG pathway with cGMPs membrane permeable analogs led to a cellular protection in the S2 cell line treated with the metabolic disruptors sodium azide or cobalt chloride. One possible mechanism of the cGMP/PKG-mediated protection includes a cytoprotection from calcium overload caused by the reduced ATP production and the subsequent influx of Ca^{2+} into the cells, since the medium, in which the S2 cells were incubated, contained high concentrations of $CaCl_2$. Calcium could enter the cells through oxidatively damaged ion channels, as cobalt chloride induced ROS production significantly (Chapter 3). From this, a potential effect of the pathway activation could be linked to a protection from the elevated intracellular calcium concentrations observed by Whittemore et al. (1995) in neurons exposed to an

oxidative stress.

4.3.4. Potassium ion channel blocking and activation during acute oxidative stress

Next, the downstream cGMP/PKG target-blocking and -activating experiments were performed with H_2O_2 -induced acute oxidative stress and cell death was assessed (Fig. 42, 43, 44). *Drosophila* S2 cells exposed to H_2O_2, TEA, and 8-Br-cGMP simultaneously, as shown in Fig. 42, did not demonstrate any significant protection, similar to the co-treatment with the metabolic stressor $CoCl_2$. This possibly was due to the fact that TEA is a non-specific potassium ion channel blocker and has many unspecific targets and is toxic to *Drosophila* cells by itself. Alternatively, it is possible that the activation of one type of a potassium channel is protective but the activation of another potassium ion channel leads to a cell death. Moreover, the expression patterns or the density of different types of potassium ion channels in *Drosophila* S2 cells is not currently known. From this, it will be important to assess the gene expression of ion channel subtypes to further confirm the identity of the potassium ion channels playing role in the cGMP/PKG pathway in this cell line.

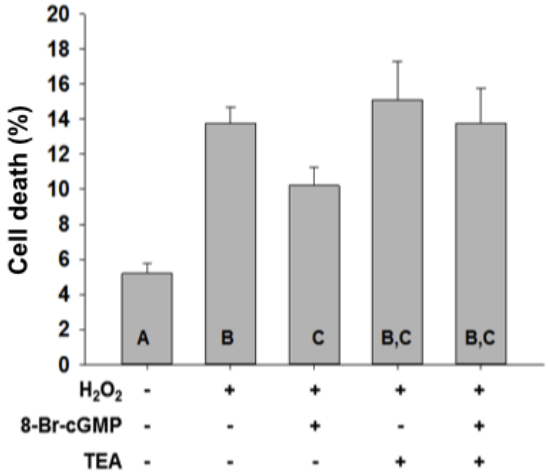

Figure 42. Effect of acute oxidative stress, cGMP/PKG pathway activation, and plasma membrane potassium ion channel blockade on *Drosophila* S2 cell death. Different letters refer to significant differences between the treatment groups, $P<0.05$, N=7-8.

Next, the effect of the mitochondrial potassium channel blocker 5-HD on the 8-Br-cGMP-offered protection was tested during the acute oxidative stress (Fig. 43). In cells co-treated with H_2O_2, 8-Br-cGMP, and 5-HD, there was no abrogation of protection by the mitochondrial ATP-sensitive potassium ion channel blocker during the stress. In other words, co-administration of 5-HD with the PKG activator during the acute oxidative stress still resulted in protection. From this, it was hypothesized that *Drosophila* S2 cells were protected by the cGMP/PKG activation from H_2O_2-induced injury by a mechanism independent of the mitoK_{ATP} ion channels. It is possible that there is another molecular target of the pathway possessing antioxidant capabilities; in addition, another ion channel not specific to 5-HD action could be targeted downstream of PKG enzyme.

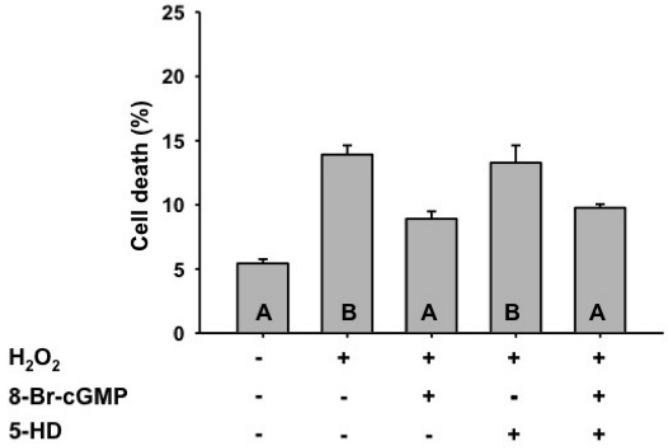

Figure 43. MitoK$_{ATP}$ channel blockade did not abrogate PKG-induced protection in *Drosophila* S2 cells subjected to hydrogen peroxide-induced stress. Different letters refer to significant differences between the treatment groups, P<0.05, N=4.

To further confirm the hypothesis that mitochondrial ion channels were not involved in the cGMP/PKG-offered protection during the H_2O_2 treatment, diazoxide was used upon induction of the stress. If mitochondrial ATP-sensitive ion channels were involved in the protective signaling, then activation of these ion channels with DZX at 1µM -100µM range would result in protection from H_2O_2-induced cell death. The results of this study are shown in Fig. 44. It was found that upon hydrogen peroxide treatment, DZX did not offer any significant protection to *Drosophila* S2 cells. This was not completely unexpected since when the mitochondrial potassium ATP-sensitive ion channel blocker 5-HD was used, it did not abrogate the cGMP/PKG-mediated protection during peroxide-induced stress. This set of experiments further confirmed that the activation of the mitoK$_{ATP}$ ion channels in inner membrane is not protective during oxidative stress. As a result, the cGMP/PKG protective signaling during the acute oxidative stress targeted

another molecular entity. It is possible that during the addition of the cGMP analog 8-Br-cGMP, cGMP-gated ion channels were activated and this resulted in protection (Dijkers and Farrell 2009).

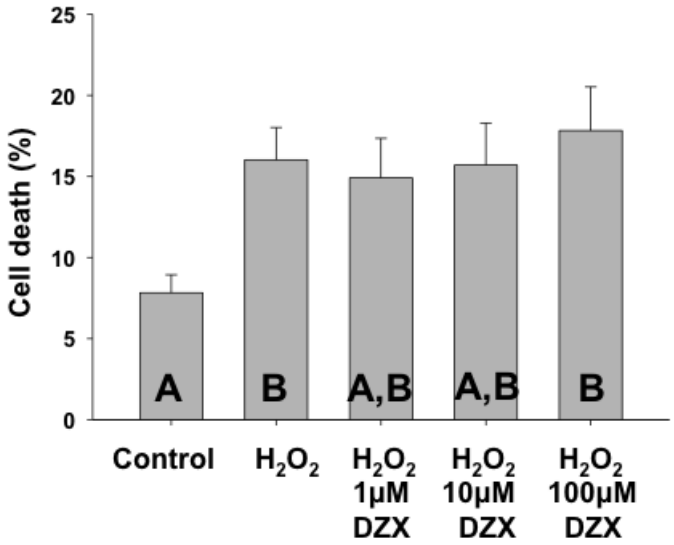

Figure 44. Mitochondrial potassium ion channel activation did not result in *Drosophila* S2 cell protection from hydrogen peroxide-induced stress. Different letters refer to significant differences between the treatment groups, $P<0.05$, $N=3$.

4.3.5. Measuring ROS production in cells with activated cGMP/PKG pathway during $CoCl_2$-induced stress

Since the $CoCl_2$ treatment led to a significant ROS production in *Drosophila S2* cells, as demonstrated in Chapter 3, changes in ROS content upon different treatment combinations were assessed next; more specifically, this was done to determine if the PKG

induced protection in the $CoCl_2$-treated cells was mediated by a decrease in ROS production. It is important to note that an intrinsic ROS stress induced by disrupted mitochondria leaking free electrons might activate and work through different signaling pathway from the ROS stress induced by acute treatment with hydrogen peroxide. In these ROS quantification studies, intracellular ROS levels did not decrease upon addition of 8-Br-cGMP during the metabolic stress but ROS levels slightly increased whenever 5-HD was present in a cell suspension. The results of this study are shown in Fig. 45. The data also confirmed that 1mM $CoCl_2$ treatment led to the formation of twice as much ROS as in control untreated cells, as was previously demonstrated in Chapter 3. It is possible that 8-Br-cGMP induced the cell protection through a mechanism that downregulated the flow of electrons through the electron transport chain of mitochondria or reduced membrane potential. A decrease in membrane potential would result in a decreased metabolic function, which could be potentially protective (Dey and Moraes 2000; Visch et al. 2006).

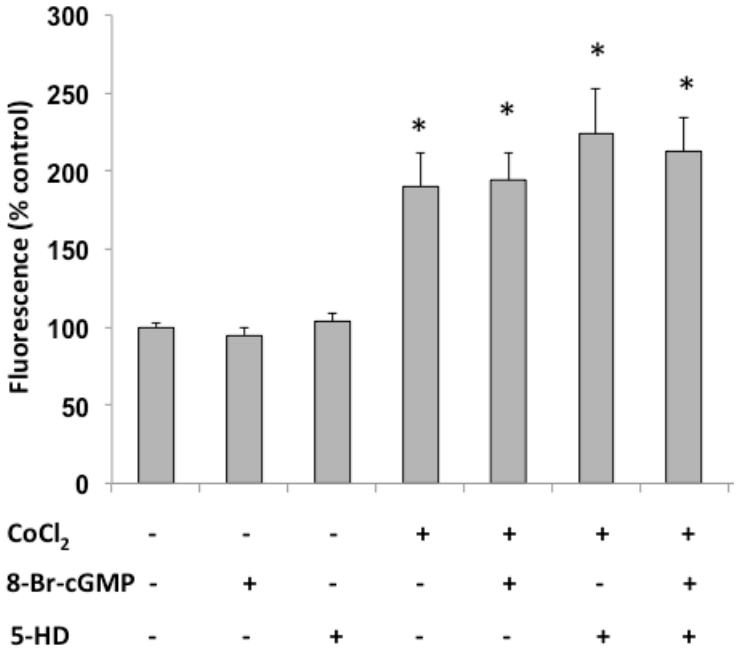

Figure 45. cGMP/PKG pathway activation did not lead to decreased ROS production upon $CoCl_2$ treatment in *Drosophila* S2 cells. Star "*" refers to significant differences between treatment and control, $P<0.05$, $N=3$.

4.3.6. Assessment of mitochondrial inner membrane potential in cells with the activated cGMP/PKG pathway during $CoCl_2$-induced stress

Since the 8-Br-cGMP treatment did not reduce ROS stress generated by the cobalt chloride incubation, changes in mitochondrial membrane potential upon different treatment combinations were assessed next. It was hypothesized that the cGMP/PKG pathway activation may preserve the mitochondrial membrane potential and thus, also the energy production. The results of this study are demonstrated in Fig. 46 representing typical images since the patterns of mitochondrial potential change were constant from one experiment to another. Activation of the PKG pathway using 8-Br-cGMP led to a

significant decrease in mitochondrial membrane potential as shown by the reduced intensity of MitoTracker Red dye fluorescence. Addition of 5-HD resulted in increased mitochondrial aggregation but decreased area of cells with fluorescing mitochondria. It is possible that some of the mitochondria lost their mitochondrial membrane potential but other fraction of mitochondria became functionally overloaded or damaged and thus aggregated. Addition of $CoCl_2$ led to a decrease in mitochondrial potential as expected since one of the toxic effects of $CoCl_2$ is the reduction of ATP production due to decreased number of protons pumping into mitochondrial intermembrane space (Bae et al. 2012). Combinations of these pharmacological compounds gave surprising results. Co-treatment of $CoCl_2$ with 8-Br-cGMP resulted in healthy-looking cells (area-wise) with higher MitoTracker Red fluorescence than controls or $CoCl_2$ – treated cells. This could be reflective of cells in which ATP is continuously made, possibly by decreasing cobalt chloride binding or modifying the tertiary structure of proteins playing a functional role in ETC. It is also possible that the addition of $CoCl_2$ and PKG activation led to mitochondrial biogenesis resulting in higher mitochondrial numbers and higher fluorescence that was not due to an increased mitochondrial membrane potential. On the other hand, co-treatment of cells with $CoCl_2$ and 5-HD resulted in intermediate mitochondrial fluorescence (compared to $CoCl_2$ and 5-HD alone) with some mitochondrial aggregation reflected by high-intensity MitoTracker red fluorescence. Addition of all three chemicals led to decreased fluorescence possibly due to decreased mitochondrial membrane potential and decreased mitochondria-filled area of the imaged cells. This is interesting but not totally unexpected. It is possible that the effect of 8-Br-cGMP on $CoCl_2$-treated cellular mitochondria was blocked by addition of 5-HD since it was previously demonstrated here that the activation

of the PKG pathway upon the stress led to an increased MitoTracker fluorescence and healthier-looking cellular morphology.

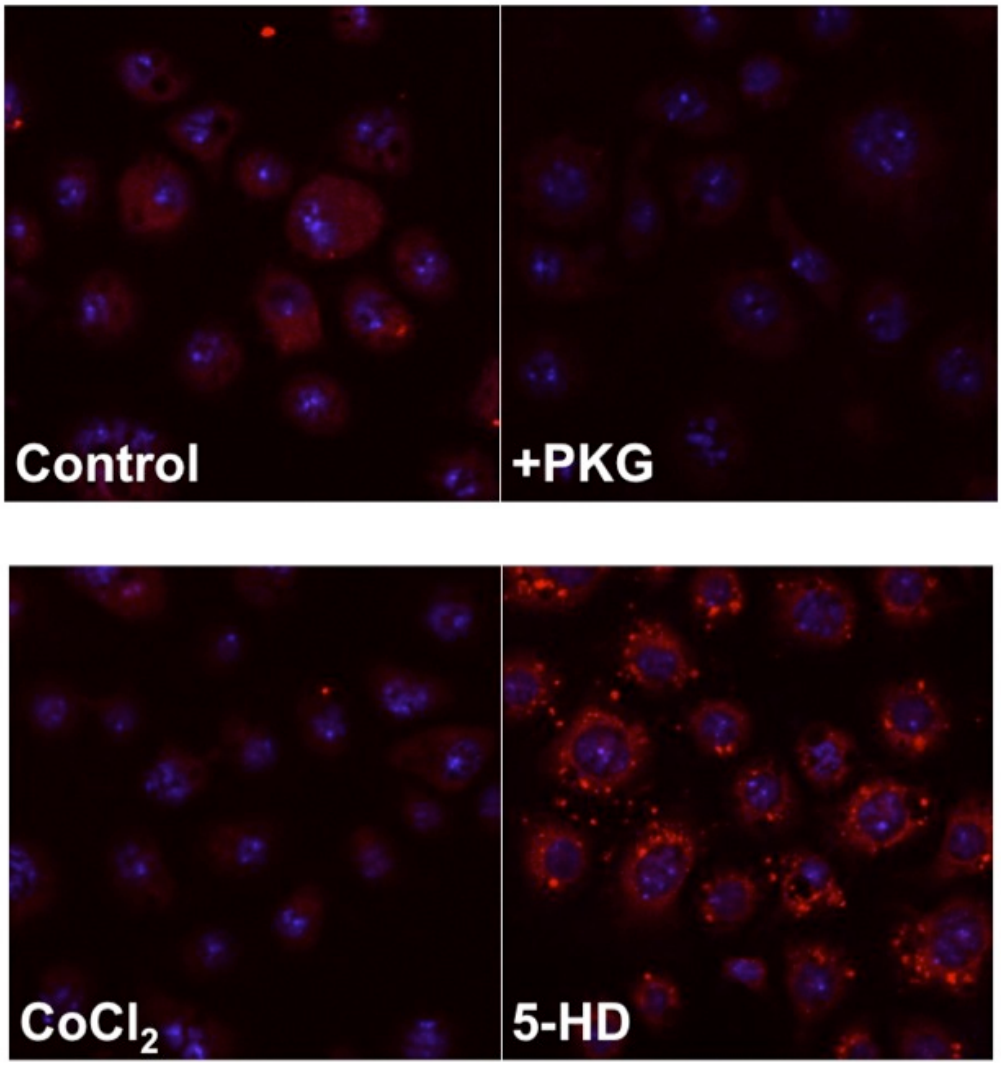

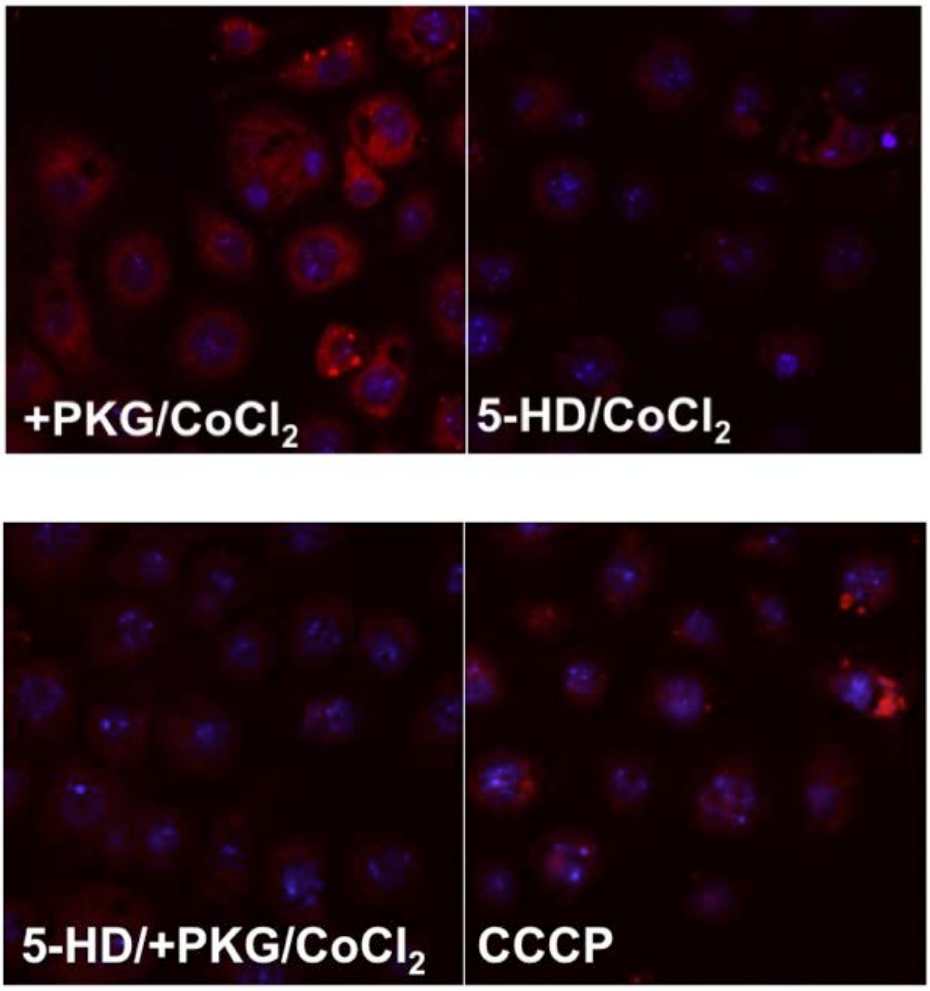

Figure 46. Effect of CoCl2- induced stress, PKG activation and 5-HD treatment on *Drosophila* S2 mitochondrial potential. Representative confocal microscopy images of cells treated with various combinations of chemical compounds of interest from 3-4 independent experiments. The images were taken at 630 × magnification.

4.3.7. Assessment of ATP production in cells with activated cGMP/PKG pathway during $CoCl_2$-induced stress

Studies of mitochondrial potential during cGMP/PKG signaling showed that during $CoCl_2$-induced stress, activation of PKG enzyme led to maintenance of mitochondrial

inner membrane potential as shown by healthy-looking active mitochondria (Fig. 46). On the other hand, co-treatment with 5-HD led to abrogation of this protection leading to a complete loss of mitochondrial membrane potential. Changes in ion channel current across the inner membrane of mitochondria may be reflected in changes in mitochondrial function and thus ATP production (Leyssens et al. 1996). Thus, next, ATP production upon manipulation of the PKG pathway upon cobalt chloride-induced stress, was measured. From the ATP measurements, addition of 8-Br-cGMP resulted in a decrease in ATP production though not statistically significant Fig. 47. When 8-Br-cGMP was co-administered with $CoCl_2$, there was a significant increase in ATP production compared to 8-Br-cGMP by itself. Addition of 5-HD with a subsequent treatment with $CoCl_2$ led to significant drop in ATP production and this drop was not rescued by the addition of the 8-Br-cGMP. Results of ATP assays are difficult to interpret due to possibility of activation of cellular compensatory mechanisms such as upregulation of glycolysis during times of energy deficiency or biochemical stress such as oxidative stress. When these results were compared to the results of mitochondrial membrane assessment, it was possible to draw a parallel between energy production (ATP) trend and mitochondrial inner membrane potential. High membrane potential as observed in control and 8-Br-cGMP-treated cells translated into higher amounts of ATP being produced. It was expected that 8-Br-cGMP, if acting on mitochondrial potassium ion channels, would disrupt mitochondrial inner membrane potential due to increased potassium current into mitochondrial matrix thus making the matrix more positive (Debska et al. 2001). On the other hand, treatment with $CoCl_2$ decreased ATP production and this was reflected by a lower mitochondrial potential. On the other hand, 5-HD treatment led to formation of mitochondrial aggregates but around

the aggregates, mitochondrial membrane potential appeared to be similar to control *Drosophila* S2 cells. It was previously reported in the literature that high and low membrane potentials are not suitable for maximal ATP production (Dimroth et al. 2000; Bagkos et al. 2014). This as well as the fact that clustered or aggregated mitochondria are markers of pathology in a cell could be the possible explanations why ATP levels upon 5-HD treatment were lower than of control (Kawai et al. 2001; Haga et al. 2003; Solans et al. 2006). On the other hand, addition of the mitoK_{ATP} ion channel blockers, was hypothesized to increase membrane potential by blocking the potassium current into the mitochondrial matrix thus making the mitochondrial intermembrane space more positive as was shown in mammalian mitochondria (Debska et al. 2001; Debska et al. 2002). Addition of 5-HD, together with $CoCl_2$ resulted in decreased membrane potential and statistically significant ATP production drop. This could be due to a possibility that $CoCl_2$ co-administered with 5-HD leads to further pathology than treatment with $CoCl_2$ only. Even though there was no increase in cell death observed after 4 hours of co-incubation of the cell with these two chemicals, it is possible that apoptotic events had been initiated and they quickly depleted cellular ATP reserves without showing degradation of plasma membrane yet. Similar to the described treatment, co-treatment of cells with 8-Br-cGMP, 5-HD, and $CoCl_2$ resulted in decreased membrane potential as well as statistically significant drop in ATP production. ATP levels there were identical to the ATP levels after 5-HD and $CoCl_2$ simultaneous treatment of *Drosophila* S2 cells. From this, it is possible that 5-HD blocked the protective effect of 8-Br-cGMP treatment on the ATP maintenance. These results further confirm the hypothesis that 5-HD blocks the cellular protection offered by activation of the cGMP/PKG pathway in *Drosophila* S2 cells exposed to toxic

compound $CoCl_2$.

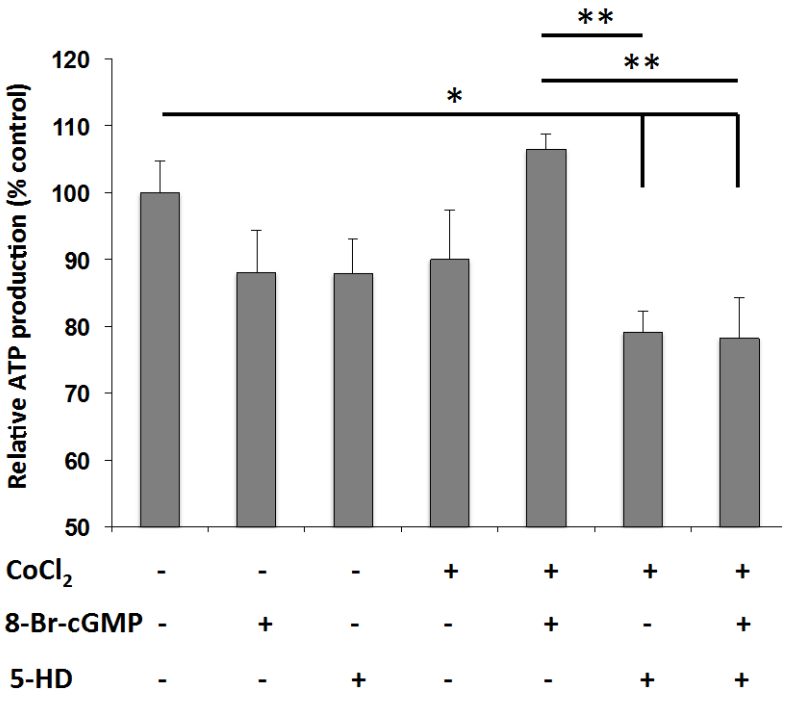

Figure 47. Effect of $CoCl_2$- induced stress, cGMP/PKG pathway activation, and mitoK$_{ATP}$ channel blockade on *Drosophila* S2 cellular ATP production. Stars "*" and "**" refer to significant differences between treatment and control, "*" - P<0.05, "**" – P<0.01, N=4-7.

4.4. Conclusions

In conclusion, in this set of studies, the protective potential of PKG pathway activation using activators of PKG enzyme (8-Br-cGMP and in some experiments sildenafil citrate) was investigated. It was shown that activation of this signaling pathway was protective in *Drosophila* S2 cell cultures exposed to cell death-inducing chemicals NaN_3, $CoCl_2$, and H_2O_2. To localize potential downstream targets of the PKG signaling pharmacological approach was used. Blockers and activators of potassium ion channels

such as TEA (a general and non-specific potassium ion channel blocker), 5-HD (a specific mitochondrial ATP-sensitive ion channel blocker that showed efficacy in mammalian models) and diazoxide (a specific mitochondrial ATP-sensitive ion channel activator that showed efficacy in mammalian models) were used (Chen et al., 2015; Wang et al., 2015; Martinez-Moreno et al., 2016). In cells treated with cobalt chloride, blockade of the mitochondrial potassium ion channels led to abrogation of the PKG-induced protection. On the other hand, blockade of mitochondrial potassium ion channels with 5-HD and concurrent treatment with 8-Br-cGMP and hydrogen peroxide still resulted in significant protection from the cell death. In addition, DZX only showed protection in $CoCl_2$-induced cell damage experimental setup. From this, it was hypothesized that 8-Br-cGMP-induced protection worked through different pathways affecting potassium ion channels localized to different subcellular compartments. My results indicated that during oxidative stress and simultaneous PKG activation possibly very few or no specific plasma membrane potassium ion channels were involved. On the other hand, it was shown that during $CoCl_2$-induced stress, mitochondrial potassium ion channels were involved. This result was unexpected but not fully surprising. It was previously shown in *Drosophila* neurons, that protection of synaptic function by PKG inhibition during acute oxidative stress possibly resulted from plasma membrane potassium ion channels being closed (Caplan et al., 2013). From this, it is likely that H_2O_2 and PKG interfere with each other in a specific manner not yet described. This function of PKG signaling may be protective not only to neurons but other cells such as hematocytes (likely precursors of the *Drosophila* S2 cells) that get directly exposed to H_2O_2. It will be important to further investigate if this specific protection is solely dependent on presence of H_2O_2 by addition of catalase or specific scavengers of

hydrogen peroxide. During $CoCl_2$-induced stress, which encompassed both oxidative and metabolic stresses, the PKG activation led to protection potentially through opening mitochondrial ion channels. Interestingly, no known electrophysiological experiments were done as of yet using isolated *Drosophila* mitochondria to measure potassium currents upon addition of 8-Br-cGMP, 5-HD, or DZX.

Next, to see if in case of $CoCl_2$, activation of PKG protected *Drosophila* S2 cells by means of decreased ROS production, it was demonstrated that $CoCl_2$ at 1mM led to significant production of intracellular ROS. Interestingly, 8-Br-cGMP treatment did not reduce ROS so it was next hypothesized that may be PKG activation was protective due to a different mechanism other than reduction of the overall amount of ROS. From the metabolic experiments investigating mitochondrial membrane potential and intracellular ATP production, it was found that 8-Br-cGMP led to a significant drop in mitochondrial inner membrane potential leading to a slight drop in ATP production, even though not statistically significant. During these studies, it was also found that $CoCl_2$ at 1mM did not change ATP production significantly as expected from Chapter 3 results. This was potentially due to a slight disturbance in pH (increased acidity) or potentially due to an upregulation of glycolysis. Interestingly, even though after addition of 5-HD, ATP levels dropped but not significantly, mitochondrial potential was extremely sensitive to the addition of this drug demonstrating clumping or aggregation of mitochondria and increased fluorescence of MitoTracker Red dye. Combinations of drug treatments, which included 5-HD resulted in a significant drop in ATP production as well as ATP potential. From this, 5-HD had a significant effect on cellular bioenergetics as reflected by both ATP production and mitochondrial membrane potential. It is possible, that there was a protective

mechanism or positive feedback mechanism that led to only small drops in energy production even though the mitochondrial inner membrane potential was disrupted. Moreover, in *Drosophila*, 5-HD and DZX could have a similar mechanism of action as in mammals but this needs to be further investigated using isolated fruit fly mitochondria and possibly genetic tools to knockout or overexpress those mitochondrial potassium ion channels.

It was previously hypothesized that PKG signaling may be targeting animals' metabolism by downregulating it and driving the whole animal into the state of hypometabolism much quicker than without additional activation of the PKG pathway. This might also depend on the saturation of the PKG enzyme with cGMP or its analogs. It is possible that *Drosophila* S2 cells already were protected from hypoxia/reoxygenation-like stresses by activating their intrinsic PKG pathway by synthesizing more of cGMP due to increased nitric oxide signaling. This could be indeed a natural mechanism of protection used by *Drosophila*. Inhibition of nitric oxide production or induction of nitric oxide scavenging in the case of intrinsic PKG-induced protection theoretically should result in cell death upon $CoCl_2$ treatment and addition of the PKG activator should rescue the protection. From this, more studies should be conducted using pharmacology and genetics to further elucidate the downstream effect of the cGMP/PKG signaling as well as of protective mechanisms activated by increased PKG enzyme activity.

CHAPTER 5

PKG-induced protection in mammalian in vitro models of hypoxia and oxidative stress

5.1. Introduction

Since cGMP/PKG molecular signaling pathway plays one of the key roles in protecting *D. melanogaster* from anoxia and reoxygenation insult, I next investigated whether activation of this pathway would also lead to neuronal protection in mammalian neurons, which are extremely susceptible to the aforementioned stresses (Graham 1977; Hinds 1985; Oliver et al. 1990). If such protection indeed exists, then molecules participating in the cGMP/PKG pathway as well as their pharmacological activators or inhibitors can be evaluated for their therapeutic potential upon pathological conditions such as stroke and neurodegenerative diseases caused by oxidative stress. I hypothesized that cGMP/PKG pathway activation would be protective in mammalian cell culture models of hypoxia/reoxygenation and oxidative stress. While cGMP/PKG-regulated signaling is known to function in a variety of vital processes, PKG's role in mammalian neuroprotection is not clear. In order to test whether the cGMP/PKG-mediated protection can be utilized in mammalian brain cells, rat primary cortical neurons (E17-E18) and human cortical neurons (HCN-2 cell line) were employed. The neurons were subjected to anoxia/reoxygenation and oxidative stress at 37°C and 5% CO_2 for different time periods,

and protective effects of compounds activating the GMP/PKG pathway on neuronal survival were determined through cytotoxicity studies.

5.1. Materials and methods

5.5.1. Rat primary cortical neuronal cell cultures

As previously mentioned, mammalian neurons are highly susceptible to anoxia, nutrient-deprivation, and oxidative damage. Since the brain cortex is a major site of stroke-caused damage, cortical neurons were used in this research study. Cell cultures were generated from fetal cortices extracted from pregnant Sprague Dawley rats bearing 17- to 18-day-old embryos. The primary neurons were grown for 11-15 days *in vitro* as previously described (Pan et al. 2010). To assess the quality of the neuronal cell cultures, immunocytochemistry experiments were performed using the following fluorescent stains: DAPI (stains nuclei of every cell, Millipore, Billerica, MS), NeuN (stains nuclei of neurons only), GFAP (stains nuclei of glial cells, Dako Agilent, Santa Clara, CA). Then, 20 × images were taken using a photo camera connected to an inverted fluorescent Zeiss Axiovert 200 microscope (Oberkochen, Germany). An image was taken using one of the three appropriate fluorescent filters and all three images were merged into one for co-localization analysis using ImageJ software (Schneider et al. 2012).

5.1.1. OGD and oxidative stress induction in rat cortical neurons

Rat neurons were subjected to a variety of treatment conditions in order to establish an appropriate *in vitro* ischemia/ reperfusion injury protocol. The general schematic of these treatments is shown in Fig. 48. On the day of the experiment, cells were treated with a maintenance medium (neurobasal medium) or saline, and then were subjected to normoxia, anoxia, and reoxygenation. At the end of each appropriate treatment, cellular

death was assessed. Different saline compositions were tested in order to determine the most effective protocol. Buffered saline solution (BSS), artificial cerebrospinal fluid (ACSF), and ischemic solution (IS) were tested for their effectiveness to induce oxygen-glucose-deprivation (OGD) as described by Yao et al. (2007). The ACSF solution contained 129mM NaCl, 3mM KCl, 1.3mM CaCl2, 1.5mM MagCl2, 21mM NaHCO3, 10mM glucose, and pH was adjusted to 7.4; the IS solution was composed of 30.24mM KCl, 47mM NaCl, 0.13mM CaCl2, 4mM NaHCO3, 33.76mM KOH, 0.1mM glutamate, 3mM glucose and the pH was adjusted to 6.4 (Yao et al. 2007). BSS solution contained 140mM NaCl, 5mM KCl, 2mM CaCl2, 20mM HEPES, 0.03mM glycine, and pH was adjusted to 7.4 (Yao et al. 2007). For normoxic pre-incubation and reoxygenation, BSS solution contained 3mM of glucose, whereas anoxic BSS had 0mM glucose concentration.

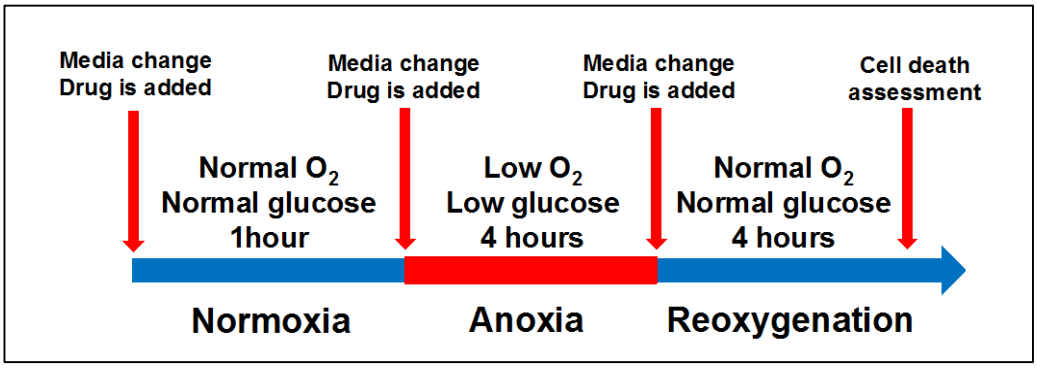

Figure 48. Graphical representation of the normoxia/anoxia/reoxygenation treatment.

5.1.2.HCN-2 cell cultures

The advantage of using human cortical neurons (HCN-2 cell line) is that they are specifically derived from human cortical tissues extracted from a patient with unilateral megalencephaly (Ronnett et al. 1990). This is relevant since the molecular studies in other animal species such as rodents may not be readily translated to human physiology. Furthermore, the human cortical neurons were received pre-purified from cellular contaminants such as glia, which could interfere with the experimental results if not removed. The cells were purchased from ATCC (Manassas, VA) and cultured as described in Ronnett et al. (1990). Briefly, cells were grown in Dulbecco's modified Eagle's medium supplied with 4mM L-glutamine and 1.5g/L sodium and 10% FBS. The cells were grown at 37°C and 5% CO_2 cell culture incubator in a T75 tissue culture flasks for 10-12 days until reaching about 90% confluence and then were detached from plastic of the tissue culture flasks using 0.25% (w/v) Trypsin-0.53mM EDTA solution, diluted in fresh medium, centrifuged at 125 × g for 10 minutes and split into 1:2 into fresh medium. Approximately 24 hours before the oxidative stress experiment, the HCN-2 cells were induced to differentiate by addition of 25ng/ml nerve growth factor (NGF), 0.5mM dibutyryl cyclic adenosine monophosphate (cAMP), and 0.5mM 1-isobutyl-3-methylxanthine (IBMX) (Ronnet et al., 1993). After differentiation incubation, the cells were pre-treated with 8-Br-cGMP to activate and then oxidative stress was induced.

5.1.3. Oxidative stress induction in HCN-2 cells

Oxidative stress was induced in HCN-2 cells only after differentiation incubation for at least 24 hours. The cells were either pre-treated with 100µM of 8-Br-cGMP for 24 hours or treated with 100µM 8-Br-cGMP 1 hour prior to the addition of 1.5mM or 100µM hydrogen peroxide, which was made fresh minutes prior to its addition. Then, the cells

were incubated for 4 hours at 37°C and 5% CO_2 incubator until cell death assessment.

5.1.4. Cell death assessment in cytotoxicity studies

Cell death assessment was carried out by propidium iodide (PI, stains dead cells) and acridine orange (AO, brightly stains live cells, upon death cells lose some of the green fluorescence) fluorescent staining (rat cortical neurons) as well as trypan blue exclusion method (HCN-2 cells) and PI/AnnexinV staining (HCN-2 cells). In these experiments, to determine cell mortality rates, the number of dead cells as well as total number of cells were counted using Zeiss Axiovert inverted fluorescent microscope and laboratory hand tally counter from Thermo Fisher Scientific (Waltham, MA).

5.1.5. Statistics

The results were expressed as the means ± S.E.M. The statistical analysis was done using Student t-tests and one-way ANOVA followed by the Student-Newman-Keuls *post-hoc* test to determine significant difference between the group means. The quantitative results with the $P<0.05$ were considered statistically different.

5.1.6. Results and discussion

5.1.7. Immunocytochemical identification of embryonic rat cell culture components

Merging of the DAPI-, NeuN-, GFAP-stained images revealed that the neuronal culture did not contain glia, since every DAPI-stained nuclei were also stained with the NeuN antibody and there was only one nucleus stained with GFAP marker (Fig. 49). This study was essential for the subsequent studies using rat cortical neurons as it was previously shown that glial cells can induce protection to cortical neurons during serum deprivation, excitotoxic, and ischemia-induced damage (Sweda et al. 2016). For example, it was shown

that glial-restricted precursors (progenitors of oligodendrocytes and some types of glia) induce protection in neonatal brain slices subjected to oxygen-glucose deprivation (Sweda et al. 2016).

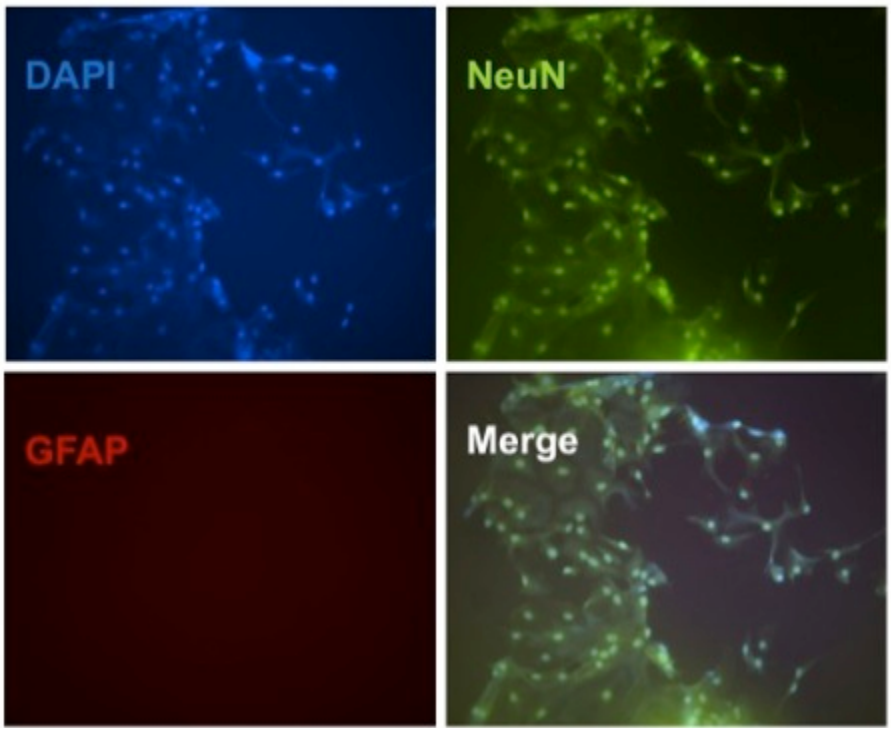

Figure 49. Immunostaining showing pure rat cortical neuronal culture without glia. DAPI: all cells; NeuN: neurons; GFAP: glia.

5.1.8. Development of in vitro model of ischemia and reperfusion in rat primary cortical neurons

An initial low oxygen study was adapted from the literature with O_2 levels between 0.1% and 0.5% (Fig. 50A) (Pan et al. 2011). Results of this study are shown in the Fig. 50B. Due to the observed low cell death (about 10%) during 20 hours of anoxia and 20

hours of reoxygenation in neurobasal maintenance medium (NBM), this oxygen deprivation setup did not appropriately mimic stroke-like situation since cells were resistant to this stress. These results could be due to the NBM playing a protective role due to its rich glucose (25mM), growth factor, and amino acid content as well as to the fact that embryonic neurons are much more resistant to lack of oxygen than adult neurons. Since glucose was available to the neurons, it is probable that during low oxygen condition, they used glucose as a substrate for glycolysis. Even though glycolysis is not a very efficient mechanism of energy production, it can still support the survival of the embryonic neurons. It was previously found that after induction of hypoxia, rat cortical neurons reduce and stabilize their ATP production for at least 3 hours of anoxia (Munns et al. 2003). Even though the idea of neonatal anoxia-tolerance has been shown many times before *in vivo* and *in vitro* in different mammalian species, the underlying mechanisms are still not clear (Alexander 1941; Singer 1999). Some of the known underlying mechanisms of fetal and neonatal neuronal protection include decreased density of ion channels in plasma membrane leading to a later anoxic depolarization, decreased but steady production of ATP, dramatic increase (up to 5-fold) of glycolysis, as well as decreased need for energy by the ATP-dependent ion pumps (Else and Hulbert 1987; Pérez-Pinzón et al. 1993; Singer 1999; Munns et al., 2003).

As hypoxic cell death was low in the high glucose maintenance medium, a modified oxygen-glucose deprivation (OGD) study was conducted as described in Fig. 50C. The anoxia treatment was performed inside an anoxic chamber with near 0% O_2 levels (Bactron Anaerobic Chamber, Sheldon Manufacturing, Cornelius, OR). First, a buffered saline solution (BSS) OGD set up was tested. There, neurons were first pre-incubated in the BSS

containing 3.0mM glucose for 1 hour in a normoxic incubator, then, were subjected to 4 hours of anoxia in BSS without glucose, and reoxygenated for additional 4 hours in BSS containing 3.0mM glucose. The results of this study are shown in Fig. 41D. This OGD setup demonstrated higher neuronal death during anoxia and reoxygenation compared to the previous study (about 50% of cell death vs. ~10%). In this experiment, the NBM was used as a "sham control" to demonstrate the effects of media/saline replacement on the neuronal cell death rates. Second, an artificial cerebrospinal fluid/ischemic solution (ACSF/IS) OGD set up was tested (Yao et al. 2007). There, neurons were first preincubated in the ACSF containing 10.0 mM glucose and physiological levels of ions for 1 hour; then, the cells were subjected to 4 hours of anoxia in IS containing 3.0mM glucose, 0.1mM glutamate, elevated concentrations of potassium ion, low concentrations of calcium, sodium, carbonate ions, and acidic pH 6.4. Subsequently, the cultures were reoxygenated for additional 4 hours in ACSF. The results of this study are shown in Fig. 50E. This OGD set up, as expected, resulted in higher neuronal death (more than 40%) during anoxia and reoxygenation compared to the results from the NBM-only oxygen-deprivation setup.

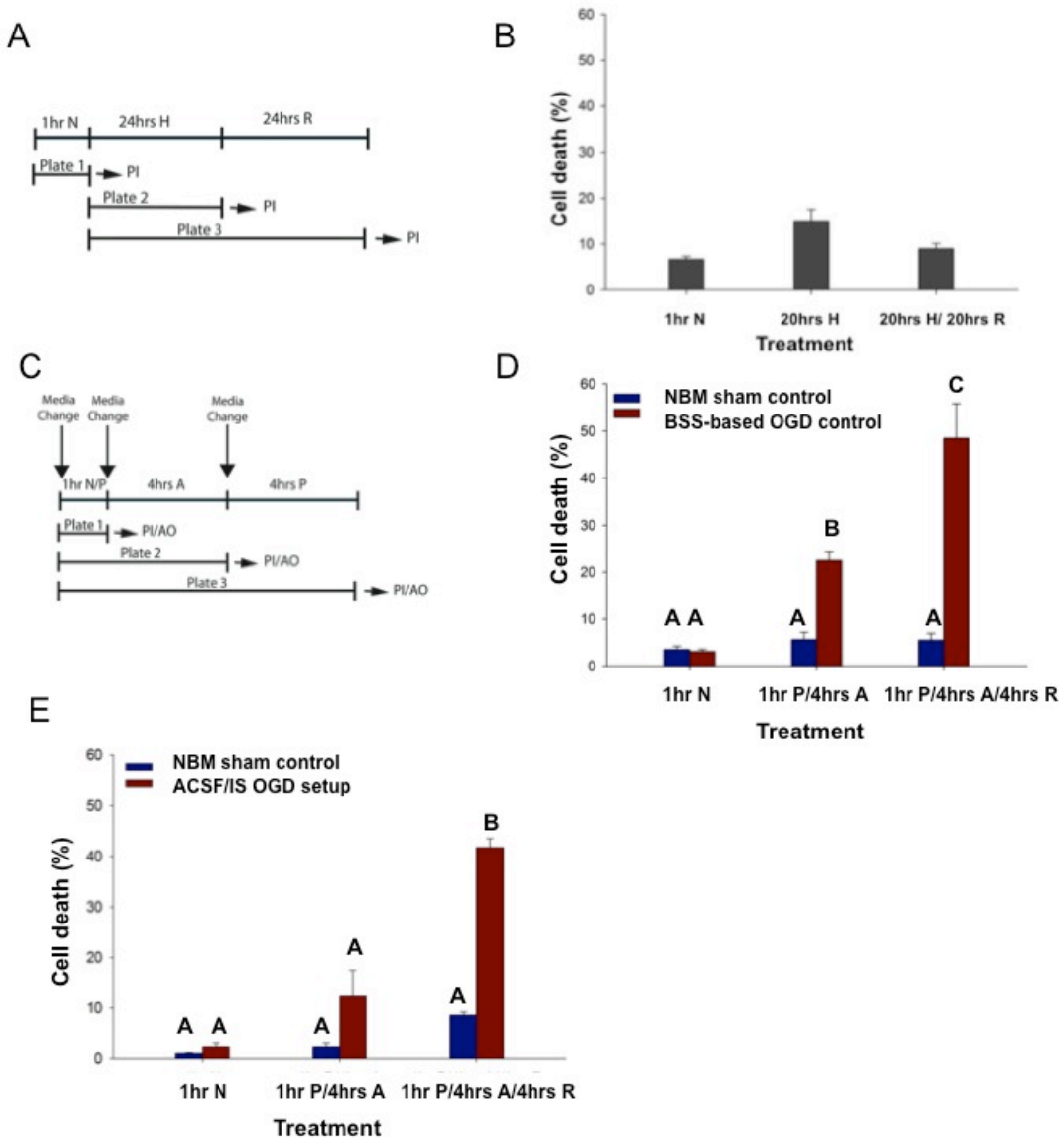

Figure 50. Development of in vitro ischemia and reperfusion injury model using OGD. A) Hypoxia/reoxygenation in NBM set up: N=normoxia, H=hypoxia, R=reoxygenation, PI=propidium iodide

staining. B) Death rates of neurons subjected to hypoxia/reoxygenation in NBM. C) Anoxia/reoxygenation generalized OGD set up: N=normoxia, P=preincubation. AO=acridine orange staining. D) Death rates of neurons subjected to anoxia/reoxygenation using BSS OGD setup. E) Death rates of neurons subjected to anoxia/reoxygenation using ACSF/IS. Different letters refer to a significant difference between treatment groups, $P<0.05$, N=3.

Even though both OGD setups demonstrated similar neuronal death patterns during anoxia and reoxygenation, it is possible that they may be utilized for different purposes in the future studies since they may mimic stroke during different time frames. In this manner, the BSS OGD set up provided stroke-like condition at the beginning of ischemia, when the cells attempt to activate their own protection mechanisms to try to overcome the anoxic insult. On the other hand, the ACSF/IS OGD set up already provides the neurons with the "made up" environment of a stroke that started some time ago as reflected by the IS composition and lower pH. Importantly, in ACSF/IS OGD setup, there was glucose present albeit at very low concentrations. This low glucose may have provided the cells a minor but still important source of energy. Moreover, ACSF had acidic pH which also could have been protective to the cells as was previously shown in *Drosophila* S2 cells (Chapter 3). This is seen in the marked differences in cell death when neurons were subjected to anoxia in BSS versus ACSF solutions. ACSF induced much lower cell death rates compared to the BSS solution after 4 hours of anoxia treatment. Interestingly, the reoxygenation in both models resulted in equivalent death rates of about 50%. It is possible, that presence of low concentrations of glucose as well as acidosis are protective during anoxia but not during oxidative stress as it was previously shown in astrocyte-neuron co-cultures (Ying et al. 1999). Importantly, the ACSF setup represents a more physiological

response of neurons to stroke-like conditions (including ischemia), thus it was used for subsequent experiments.

5.1.9. Pharmacological PKG pathway activation in rat primary cortical neurons subjected to anoxia, reoxygenation, or acute oxidative stress

ACSF/IS OGD-based *in vitro* stroke model to perform pharmacological treatments of primary rat neurons with 8-Br-cGMP, 8-pCPT-cGMP, and sildenafil citrate was used. The results of the studies are shown in Fig. 51. It was found that the reoxygenation caused significantly more cell death compared to the 4 hours of OGD alone (45% versus 9%). Interestingly, activation of the PKG pathway by 8-Br-cGMP caused significant protection when supplied at 50 µM, and 100 µM. Lower concentrations of 8-Br-cGMP were not significantly protective. Treatment with 100 µM of 8-Br-cGMP demonstrated the greatest protective effect on OGD-treated rat cortical neuronal survival. Conversely, the cells subjected to the OGD and subsequent reoxygenation were not protected by a direct activation of the PKG pathway. Furthermore, 50 µM 8-Br-cGMP resulted in unexpected toxicity, which may not be biologically significant.

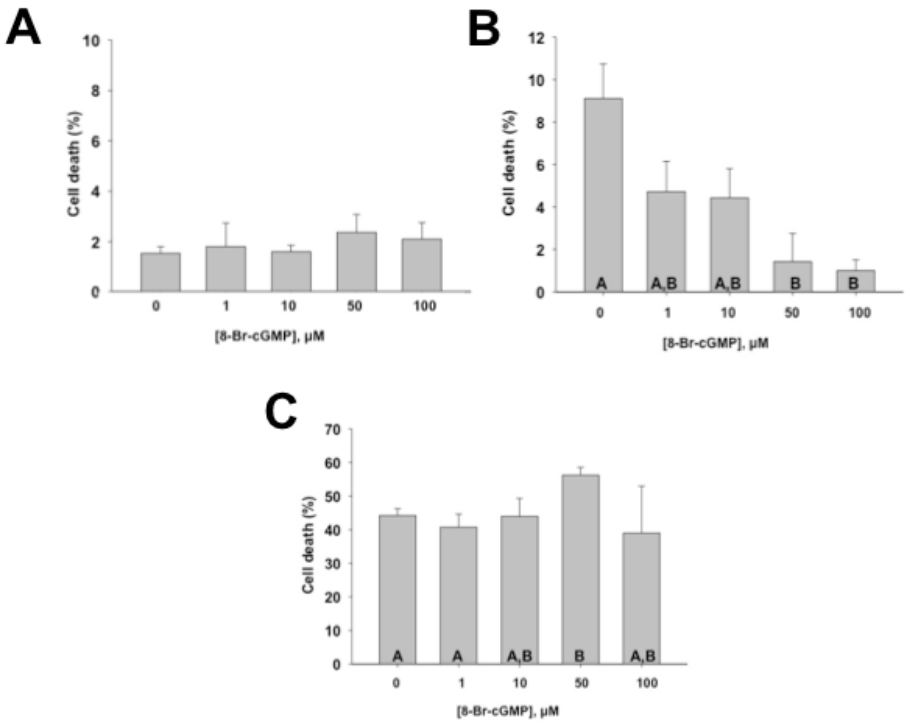

Figure 51. Effect of activating cGMP/PKG pathway in rat cortical neurons subjected to anoxia/reoxygenation stress upon 8-Br-cGMP treatment. A) Mortality of neurons subjected to normoxia in ICSF medium and 8-Br-cGMP at different concentrations. B) Mortality of neurons subjected to anoxia in IS medium and 8-Br-cGMP at different concentrations. C) Mortality of neurons subjected to anoxia in IS medium and reoxygenation in ACSF medium and simultaneous treatment with 8-Br-cGMP at different concentrations. Different letters refer to a significant difference between treatment groups, an absence of letters designates that there was no statistical significance between all experimental groups, $P<0.05$, N=3-4.

Next, I tested the protective efficacy of another synthetic cGMP analog, 8-pCPT-cGMP. The results of these experiments are shown in Fig. 52. After 4 hours of anoxia, 8-pCPT-cGMP induced similar cell toxicity pattern compared to the control normoxic 8-pCPT-cGMP treatments (Fig. 52A). From this pattern, 10µM 8-pCPT-cGMP appears to be

the least toxic concentration and slightly protective (no statistical significance found). On the other hand, 100µM 8-pCPT-cGMP was the most toxic concentration causing more than 100% increase in cell death in both normoxic and post-anoxic cell cultures. Interestingly, upon reoxygenation (Fig. 52A), 8-pCPT-cGMP did not show any significant protection as well as did not follow the same cell toxicity pattern as found in normoxic and post-anoxic cell neuronal cultures (Fig. 52B, C).

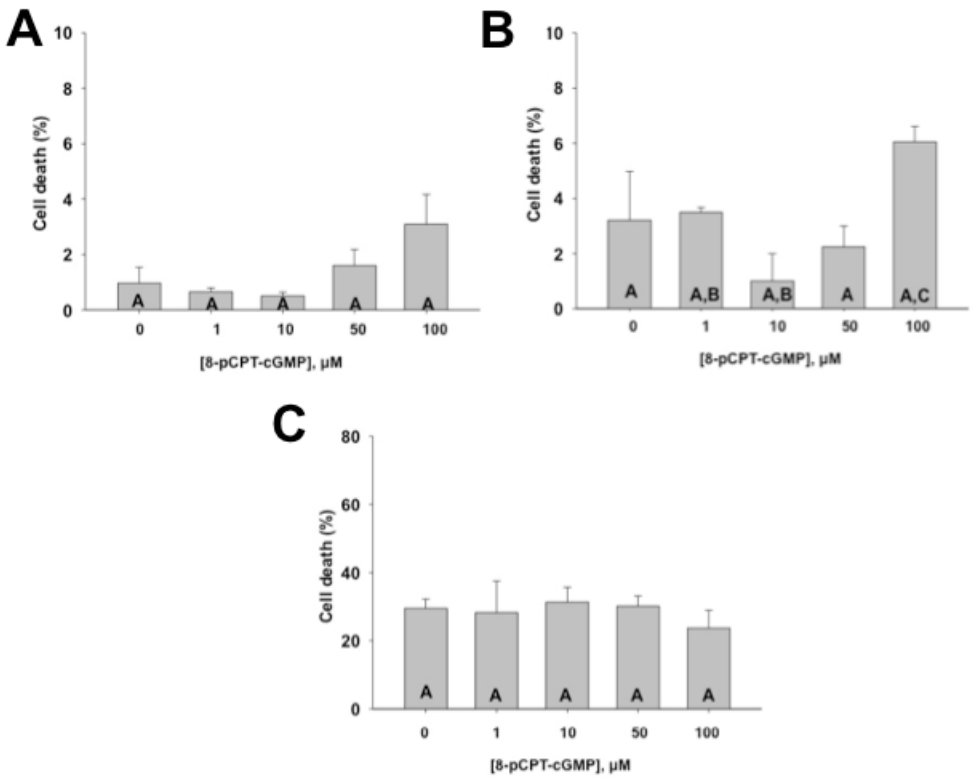

Figure 52. Effect of activating cGMP/PKG pathway in rat cortical neurons subjected to anoxia/reoxygenation stress upon 8-pCPT-cGMP treatment. A) Death rates of neurons subjected to normoxia in ICSF medium and 8-Br-cGMP at different concentrations. B) Death rates of neurons subjected to anoxia in IS medium and 8-pCPT-cGMP at different concentrations. C) Death rates of neurons subjected to anoxia in IS medium and reoxygenation in ACSF medium and simultaneous treatment with 8-pCPT-cGMP

at different concentrations. Different letters refer to a significant difference between the treatment groups; an absence of letters on the graph designates the fact that no statistical difference was found between the groups. $P<0.05$, N=2-3.

Next, I tested the effects of an indirect activator of the PKG enzyme, the specific inhibitor of the PDE5, sildenafil citrate, administered to rat cortical neuronal cell cultures at various final concentrations. The results of this set of experiments are shown in Fig. 53. There, cell death of neurons subjected to normoxia as well as at 4 hours of reoxygenation after 4 hours of anoxia was assessed. From this, it is possible that sildenafil citrate may be protective from anoxic stress itself but not from reoxygenation or reperfusion injury (Fig. 53B). It is possible that increased number of experimental trials would lead to a better resolution of protective trends if any. Moreover, it will be essential to test if sildenafil citrate offers any neuroprotection *in vitro* right after 4-hour exposure to anoxia and compare the results obtained with the specific PKG enzyme activators such as 8-Br-cGMP and 8-pCPT-cGMP.

From this, in all of the experiments involving a PKG pathway activator (direct or indirect), the normoxic preincubation led to increased cell toxicity with increasing concentration of a PKG activator (Fig. 51, 52, 53). This could be due to the fact that the pharmacological compounds used target another molecular signaling pathway. For instance, they could also activate cGMP-gated ion channels or lead to a low-grade ROS production as previously observed in published studies in heart-derived cells treated with oxytocin (Gonzalez-Reyes et al. 2015). The researchers in this study found that inhibition of the PKG pathway with KT5823 resulted in abrogation of oxytocin-induced protection

after cells were exposed to ischemia and reperfusion-type injury. Moreover, they showed that oxytocin leads to a transient production of ROS when the cells are not subjected to ischemia and reperfusion stresses. In addition, in cardiac K_{ATP} channel-transfected HEK-293 (human embryonic kidney cell line), PKG activation leads to opening of those channels but the PKG effect vanishes upon treatment with ROS scavenger N-2-mercaptopropionylglycine (MPG) (Chai et al. 2011). From this, some of the physiological responses to PKG activation include the intracellular formation of ROS or possibly only their presence, such as the presence of hydrogen peroxide but not of other reactive oxygen species.

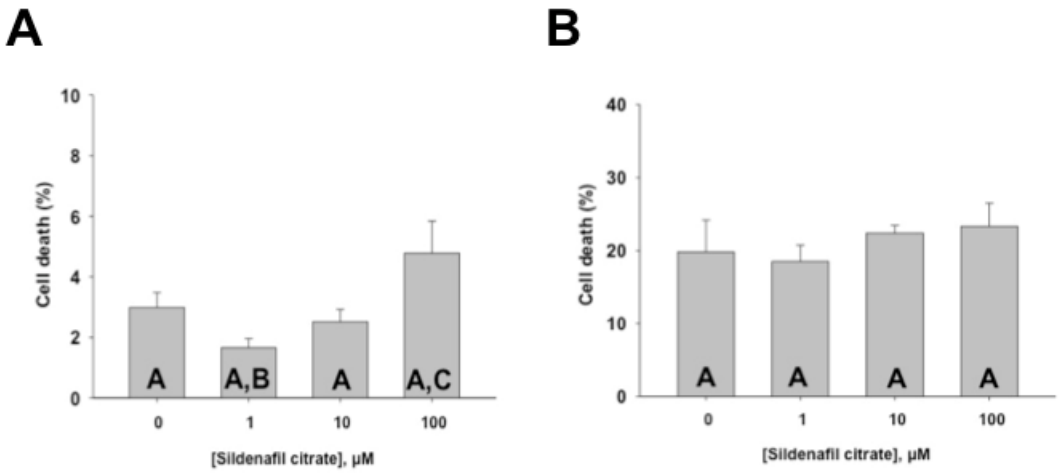

Figure 53. Effect of activating cGMP/PKG pathway in rat cortical neurons subjected to anoxia/reoxygenation stress under sildenafil citrate treatment. A) Death rates of neurons subjected to normoxia in ICSF medium and sildenafil citrate at different concentrations. B) Death rates of neurons subjected to anoxia in IS medium followed by reoxygenation in ICSF medium and sildenafil citrate at different concentrations. Different letters refer to a significant difference between treatment groups; an absence of letters on the graph designates the fact that no statistical difference was found between the groups, $P<0.05$, $N=4$.

It is possible, that reoxygenation is a complex process, which does not require neuronal hyperpolarization (functional downregulation) and induction of hypometabolism since oxygen is already available at this stage. Another possible reason for the results could be intrinsic biochemical properties of the cortical neuronal cultures employed in these studies, since they also did not respond (showed near 0% cell death) to the prolonged 100μM glutamate treatments (data not shown). The glutamate-induced cell death may be considered to be a marker of differentiated, mature cortical neurons (Zhang and Bhavnani 2005; Ray et al. 2006; Pan et al., 2010). Moreover, when the BSS-based OGD setup was used concurrently with the 8-Br-cGMP treatment, I did not find a significant protection from the PKG activation. This could be due to the nature of the BSS-based OGD setup. It is possible that for the PKG activation to be protective, cells need to be incubated in a low concentration of glucose as well as be more acidic than in BSS OGD protocol (0mM glucose, neutral pH in a high buffering capacity saline solution). It is possible, that the protective effect of PKG during anoxia is dependent or is regulated by intracellular pH levels as well as glucose availability. In the future, it will be necessary to further investigate the protective role of the cGMP/PKG signaling during anoxia by using specific blockers and activators of different targets of the pathway. Moreover, it will be interesting to assess the cGMP/PKG pathway activation effects, if any, on cellular metabolism by measuring ATP production, assessing mitochondrial membrane potential, as well as ROS damage upon drug treatments and during anoxia/reoxygenation stress.

Next, I examined effects of the PKG activation on rat cortical neurons exposed to H_2O_2-induced oxidative stress (Fig. 54). It was found that the rat cortical neurons were

sensitive to 1mM hydrogen peroxide treatment resulting in about 99% cell death. Interestingly 1μM of sildenafil citrate offered significant protection upon hydrogen peroxide-induced oxidative stress. Notwithstanding this, this level of protection may not be biologically relevant especially during acute physiological stress. Interestingly, the same concentration of sildenafil citrate was effective in *Drosophila* S2 cell culture studies described in Chapter 4 where S2 cells were exposed to 10mM hydrogen peroxide treatment. This data comparison demonstrates the drastic differences between susceptibilities to acute hydrogen peroxide stress between rat primary cortical neurons and *Drosophila* S2 cell line (1mM versus 10mM, respectively), which could be a result of unique protective molecular features expressing in the fruit fly cells but not in the rat primary neurons. It is important to note that two of the cell culture types discussed here are of different specialization: neuronal versus epithelial-macrophage-like. Furthermore, the culture media components and or incubation temperature also may play roles in such discrepancy. For instance, pH of the mammalian neuronal medium was 7.4, whereas pH of the *Drosophila* medium was at 7.0±0.2. In Chapter 3, it was found that acidosis was protective to *Drosophila* cells during cobalt chloride treatment and that acidosis decreased the amount of intracellular ROS. From this, pH of the treatment medium may play a role in the high susceptibility of rat cortical neurons to hydrogen peroxide stress. In addition, mammalian neurons were exposed to 37ºC, whereas *Drosophila* cells were incubated at room temperature. It is well known that higher temperatures exacerbate cellular and tissue injury and increase cell death (Heise 2006; Paital 2016). Moreover, the rat primary neuronal data demonstrated that higher concentrations of sildenafil citrate during the acute oxidative stress resulted in abrogation of significant protection in a concentration-

dependent manner potentially due to sildenafil citrate-induced cytotoxicity shown in control treatments in Fig. 53A. Surprisingly in *Drosophila* cell cultures 10µM of sildenafil citrate was protective, whereas 1µM was protective in rat neurons. A possible explanation for this could be differences in gene expression of the cGMP/PKG pathway targets and functional differences of PKG enzymes between the two species and cell types. This has to be further investigated. Furthermore, it will be interesting to test the susceptibility of primary *Drosophila* neurons (Sicaeros et al. 2007) to anoxia/reoxygenation as well as hydrogen peroxide-induced cellular stress.

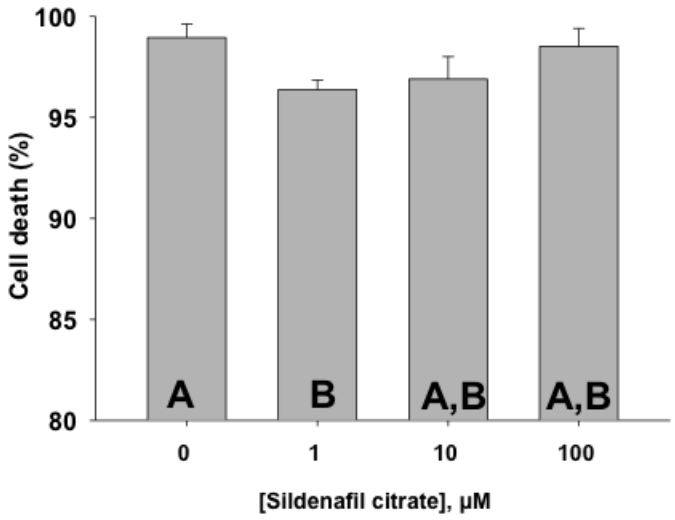

Figure 54. Activation of cGMP/PKG pathway in rat cortical neurons subjected to acute oxidative stress under 1µM sildenafil citrate treatment. Death rates of neurons subjected to acute oxidative stress induced by hydrogen peroxide and treated with sildenafil citrate at different concentrations. Different letters refer to a significant difference between treatment groups, $P<0.05$, $N=4$.

From the data, hydrogen peroxide stress and oxidative stress induced by reoxygenation may have different signaling mechanisms and effects on rat neurons; as a

result, this difference must be further investigated. It is also possible, that H_2O_2 acts as a second messenger in addition to oxidizing cellular components (Bombicino et al. 2017; Roy et al. 2017). Moreover, in mammalian smooth muscles, it was shown that activation of the PKG pathway follows ROS formation (Negash et al. 2007). If rat cortical neurons are only protected during anoxia and not reoxygenation, in future experiments, it will be possible to add antioxidant pharmacological compounds during reoxygenation phase of ischemia and reperfusion *in vitro* and *in vivo* and see if there is a full protection from anoxia/reoxygenation stress.

5.1.10. Pharmacological PKG pathway activation in human cortical neurons subjected to acute oxidative stress

After assessing the cGMP/PKG pathway neuroprotection ability in primary rat cortical neurons subjected to acute oxidative stress, a different type of adult mammalian neurons - human cortical neurons (HCN-2 cell line) was employed. This was done to investigate an extent of the cGMP/PKG pathway-mediated neuroprotection, if any, in human *in vitro* model. It is known that numerous neuroprotective molecules effective in a rodent model did not show a significant efficacy in human clinical trials (Xu and Pan 2013). These cells were used on the second day of differentiation using NGF and the differentiated neuron images are shown in Fig. 55. For this set of experiments, neurons were subjected to different concentrations of H_2O_2-induced oxidative stress and then, the cell death assessment was carried out using either propidium iodide or trypan blue exclusion method (Fig. 56, 57).

First, human neurons were pre-treated with 100µM 8-Br-cGMP for one hour and then were exposed to 1.5mM hydrogen peroxide for 4 hours. At the end of incubation, the

neurons were stained with propidium iodide/annexin V fluorescent stains to assess the level of necrosis and apoptosis in the treated cells (Fig. 56). Almost every cell treated only with hydrogen peroxide was stained with propidium iodide dye indicating that the concentration of the stressor in this experimental setup was too high resulting in almost a complete necrosis of neurons. On the other hand, neuronal cells pre-treated with 100µM 8-Br-cGMP resulted in significant protection. Another interesting finding was that 8-Br-cGMP induced apoptosis in some human neurons not subjected to H_2O_2-generated oxidative stress (Fig. 56). This could be due to 8-Br-cGMP's ability to induce mild disruption of mitochondria and formation of ROS as shown in preconditioning phenomenon and microglia potassium calcium-dependent ion channel activation (Xu et al. 2004; Ferreira et al. 2015).

Next, it was necessary to assess cell damage of neurons subjected to a lower concentration of hydrogen peroxide to be able to quantify the cell death since 1mM concentration showed to be very toxic to the human neurons. The neurons were incubated with 100µM hydrogen peroxide for 4 hours after they were pretreated with 8-Br-cGMP either for 1 or 24 hours. Different pre-treatment times were chosen to investigate if the 8-Br-cGMP-induced protection is due to a short-term or long-term activation of the PKG pathway. The results of this study are shown in Fig. 57. There, hydrogen peroxide-induced cell death whereas hydrogen peroxide insult after the PKG activation showed significant cell protection. To add, it was interesting to observe a similar level of protection in cultures pretreated with the 8-Br-cGMP for different periods of time. Notwithstanding this difference, it was difficult to conclude whether the long- or the short-term 8-Br-cGMP exposures played a protective role in this experimental setup. It is possible that the PKG activation by cGMP analogs in human cortical neurons could have a protective effect

during stress only through decreasing cellular metabolism and the pathway requires hydrogen peroxide for the protection to be offered.

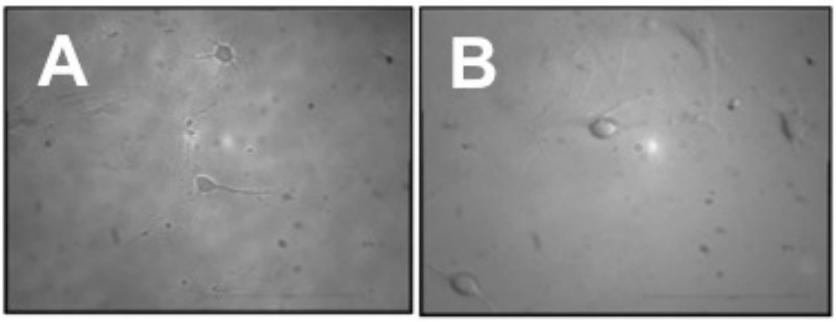

Figure 55. HCN-2 neuronal specialization. A) Day 1 incubation with NGF; B) Day 2 incubation with NGF.

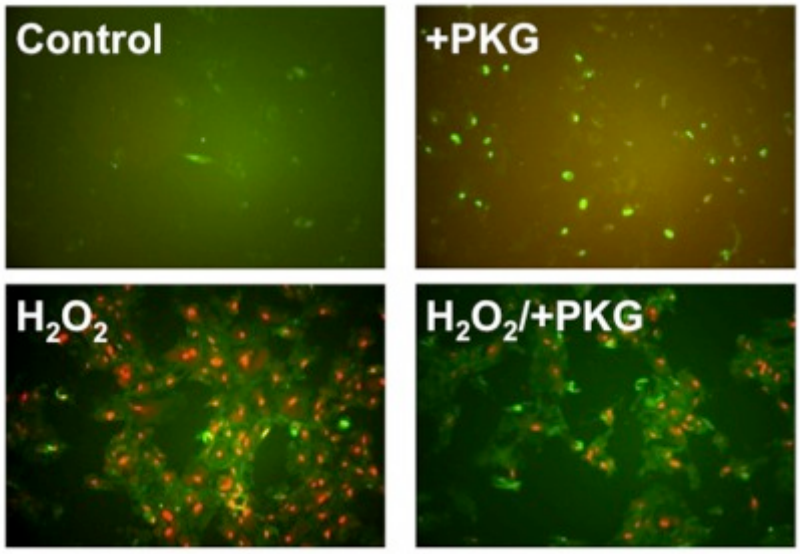

Figure 56. Image of HCN-2 cells exposed to 1.5mM of hydrogen peroxide for 4 hours with or without 100µM of 8-Br-cGMP treatments. The representative images demonstrate composites of propidium iodide (red-orange, necrosis) and annexin V (green, apoptosis) stains.

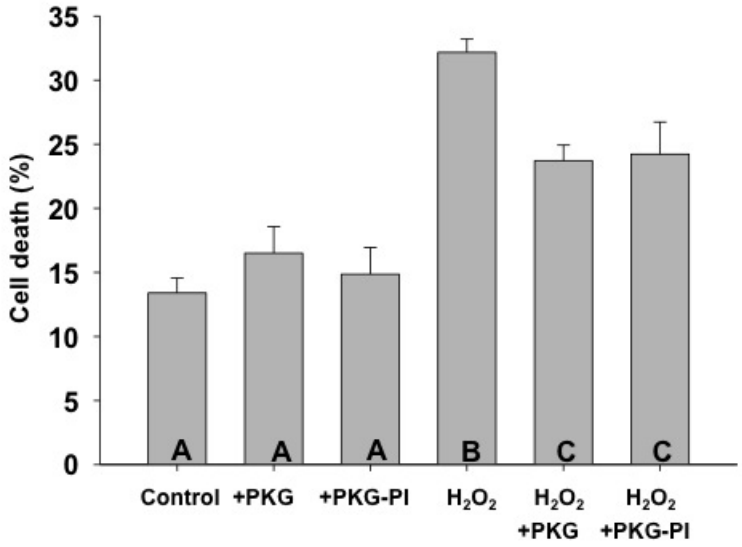

Figure 57. Death rates of HCN-2 cells exposed to 100µM of hydrogen peroxide as assessed by trypan blue exclusion method. "+PKG" represents treatments with 100µM of 8-Br-cGMP just prior to the treatment with the oxidative stress-inducing chemical. "+PKG-PI" represents 24-hour pre-incubation with 100µM of 8-Br-cGMP. Different letters represent statistical significance between groups, $P<0.05$, $N=3$.

5.2. Conclusions

To summarize, in this set of experiments, rat primary cortical neurons and human neuronal cell line were used to determine a neuroprotective potential of the PKG activation in mammalian brain cells during anoxia, reoxygenation, as well as upon acute oxidative stress. From the results, activation of the PKG pathway in rat primary neurons was significantly protective upon treatment with 50µM and 100µM of 8-Br-cGMP for 4 hours of anoxia. The same concentration of 8-Br-cGMP surprisingly did not protect reoxygenated rat neuronal cells. Similarly, the PKG pathway activation with another synthetic cGMP analog 8-pCPT-cGMP as well as PDE5 inhibitor sildenafil citrate did not result in significant protection after anoxia/reoxygenation. When rat neurons were subjected to acute oxidative stress induced by hydrogen peroxide, there was a significant protection at

1μM sildenafil citrate. Similar to rat neurons, human HCN-2A cells exhibited neuroprotection upon hydrogen peroxide-induced stress and the cGMP/PKG activation. Furthermore, it was observed that the 8-Br-cGMP treatment in the absence of a stress, drove some but not all human neurons into apoptosis. This mechanism of PKG-induced apoptosis in human neurons needs to be further investigated. It will also be important to study the underlying mechanisms behind the cGMP/PKG pathway's protection selectivity in different types of oxidative stress: reoxygenation versus acute oxidative stress by hydrogen-peroxide treatment. In addition, it will be necessary to develop experimental protocols in which mammalian neurons subjected to stroke-like conditions will be treated with PKG-activating pharmacological compounds as well as various types of antioxidants to potentially increase the extent of neuroprotection offered by the cGMP/PKG pathway. One of the main goals of such study would be to identify molecular compounds that induce biologically relevant levels of neuroprotection in mammalian brain in pre-clinical models for ischemic stroke.

GRAND CONCLUSIONS

In conclusion, the present research showed different effects of the cGMP/PKG molecular pathway modulation *in vivo* and *in vitro* in an invertebrate *Drosophila* as well as in mammalian neuronal cell cultures. The goal of the studies was to determine if the pharmacological cGMP/PKG pathway activation increased survival of *Drosophila* as well as neurons subjected to stroke-like conditions. Furthermore, specific effects of the cGMP/PKG activation on fruit fly metabolism were investigated. The overall purpose of this research was to uncover novel protective strategies that can be employed in cells subjected to low oxygen and oxidative stress conditions.

Since in previous studies from our lab it was shown that an increased PKG protein expression and enzyme activity leads to neuronal protection from anoxia and reoxygenation stresses in *Drosophila in vivo*, one of the study here further investigated differences between flies with different levels of PKG protein. Here it was demonstrated for the first time that fruit flies with high and low PKG enzymatic activity responded to lack of oxygen by modulating their mitochondrial dynamics as well as oxidative metabolism. From citrate synthase activity assays and Western bots, it was found that sitter fruit flies, the low PKG animals, showed an increase in mitochondrial density at 8 hours post short-term anoxia (1 hour) whereas rover flies' mitochondrial density stayed at the same levels as in control normoxic flies. Moreover, increase in mitochondrial density in sitters was reflected in higher metabolic levels compared to rover fruit flies.

Furthermore, rover fruit flies demonstrated a significantly deeper state of hypometabolism during exposure to anoxia compared to sitter fruit flies.

Next, the effect of the pharmacological cGMP/PKG pathway activation was investigated. The wild type fruit flies were either grown on a solid fly food containing sildenafil citrate or were provided sildenafil citrate dissolved in a liquid food only 24 hours prior to the anoxic stress followed by reoxygenation in normal oxygen conditions. These studies showed that fruit flies did not have a taste aversion to sildenafil citrate at tested concentrations and that sildenafil citrate was neuroprotective in both pharmacological treatment setups upon anoxia/reoxygenation stress. This confirmed the hypothesis that to demonstrate neuroprotection upon anoxia/reoxygenation, *Drosophila* can be provided with a pharmacological cGMP/PKG pathway activator such as sildenafil citrate, a potent inhibitor of PDE5, either throughout the lifespan of an animal or at least 24 hours prior to an anoxic insult. Decreasing the time of drug exposure prior to a stroke-like stress allows for further deciphering of mechanisms of PKG-induced protection in *Drosophila.*

Next, to translate PKG *in vivo* studies to *in vitro* model to further dissect the cGMP/PKG pathway molecular participants, *Drosophila* S2 cells were used. It was hypothesized that activation of the cGMP/PKG pathway in *Drosophila* cells would result in increased survival upon stroke-like conditions. In order, to test this hypothesis, it was necessary to develop an *in vitro* model of stroke-like stress. To induce this type of stress, sodium azide, cobalt chloride, and hydrogen peroxide were employed. Sodium azide and cobalt chloride were used to mimic low oxygen/low ATP cellular production, whereas hydrogen peroxide was employed to induce acute oxidative stress. It was shown, for the first time here, that sodium azide, being a toxic compound, decreased ATP production to

critically low levels; this energy decrease may be equivalent to a complete gas anoxia. Hydrogen peroxide was shown to induce intracellular calcium influx before a cell death by ruptured plasma membrane, as was expected from mammalian studies. Next, it was found that cobalt chloride, being a hypoxia mimetic, decreased ATP production but in a concentration-dependent pattern; it also induced a significant amount of oxidative stress. During these experiments, an interesting mechanism of protection from low oxygen and oxidative stress was uncovered. It was found that an induction of acidosis by lowering pH of a *Drosophila* cell culture medium was protective. This protection was offered through an increased production of ATP by *Drosophila* cells as well as decreased production of reactive oxygen species. It will be essential to further investigate molecular signaling and biochemical mechanisms that underlie this protection. Potentially, this mechanism, when induced in insect cells naturally, protects an organism from low oxygen and oxidative stress-induced injury. From this, pharmacological changes in pH before, during, and after the stress should be manipulated. Moreover, since a similar phenomenon has been previously observed in human cells such as the ones composing tumors, *Drosophila* S2 cells could share some of their gene expression patterns. If this is true, then *Drosophila* cells could also be used as a model for cancer research.

Since mechanisms of action of the stress-inducing compounds were determined, cobalt chloride and hydrogen peroxide were chosen to carry out cGMP/PKG pathway-targeting pharmacological treatments upon a stress. It was found that *Drosophila* S2 cells were protected from both, cobalt chloride- and hydrogen peroxide-induced stress when the cGMP/PKG pathway was activated. Next, the specific downstream targets of the signaling were studied. From this research, it was found that mitochondrial ATP-sensitive potassium

ion channels were potentially involved only in protection from cobalt chloride stress but not during hydrogen peroxide-induced stress. Moreover, it was determined that the cGMP/PKG activation protected *Drosophila* S2 cells from the cobalt chloride-induced injury by a mechanism other than a reduction of ROS production. Because of this fact, I tested the effects of cGMP/PKG signaling during the hypoxia-like stress on the mitochondrial function. To do this, mitochondrial inner membrane potential and ATP production were assessed upon PKG activation. In this set of experiments, it was determined that PKG activation by itself led to a decreased membrane potential and a slight decrease in ATP production. Cobalt chloride disrupted mitochondrial potential and led to a slight decrease in ATP production. On the other hand, when *Drosophila* cells were exposed to the hypoxia mimetic, cGMP/PKG pathway activation led to an increase in mitochondrial membrane potential as well as ATP. From this, this effect potentially was the one that induced cellular protection from the cobalt chloride-induced cell death. This means that the cGMP/PKG pathway potentially modulates cellular metabolism in *Drosophila in vitro.*

After showing that a pharmacological activation of the cGMP/PKG protected *Drosophila in vivo* and *in vitro*, the cytoprotective potential of the cGMP/PKG pathway activation in mammalian cells was tested. It was found, that activation of PKG enzyme was protective in rat primary cortical neurons right after onset of low oxygen stress. On the other hand, sildenafil citrate was protective in the rat neurons exposed to acute hydrogen peroxide treatment. Similar to rat cortical neurons, activation of the cGMP/PKG pathway led to cytoprotection in human cortical neurons subjected to hydrogen peroxide stress. From the *Drosophila* cell culture studies as well as from using mammalian *in vitro* models

of low oxygen and oxidative stress, it was hypothesized that oxidative stress generated upon the reoxygenation from anoxia or upon treatment with hypoxia mimetics might be indeed different in cellular signaling from the acute oxidative stress incurred by hydrogen peroxide.

As a result of the above studies, it was possible to investigate different biological and biochemical effects of the cGMP/PKG pathway activation. These experiments were performed *in vivo* and *in vitro* using *Drosophila* as the animal model as well as *in vitro* using mammalian cells such as rat primary cortical neurons and human cortical neurons. The knowledge of the demonstrated experimental models as well as of the cGMP/PKG pathway will allow discovering new targets of cellular and whole body protection upon stroke-like stress. Furthermore, knowing the potential targets of a cytoprotection will help to develop new pharmacological compounds with increased specificity as well as novel methods for their delivery to oxygen-deprived regions of the brain.

REFERENCES

Abdul HM, Butterfield DA (2007) Involvement of PI3K/PKG/ERK1/2 signaling pathways in cortical neurons to trigger protection by cotreatment of acetyl-L-carnitine and alpha-lipoic acid against HNE-mediated oxidative stress and neurotoxicity: implications for Alzheimer's disease. Free Radic Biol Med 42:371–84. doi: 10.1016/j.freeradbiomed.2006.11.006

Abernethy WB, Butterworth JF, Prielipp RC, et al (1995) Calcium entry attenuates adenylyl cyclase activity. Chest 107:1420–1425. doi: 10.1378/chest.107.5.1420

Aksoy Y, Balk M, Ogus H (2004) The Mechanism of inhibition of human erythrocytes catalase by azide. Turk J Biol 28:65–70.

Allen AM, Anreiter I, Neville MC, Sokolowski MB (2017) Feeding-related traits are affected by dosage of the foraging gene in *Drosophila melanogaster*. Genetics 205:761–773. doi: 10.1534/genetics.116.197939

Andoh T, Chiueh CC, Chock PB (2003) Cyclic GMP-dependent protein kinase regulates the expression of thioredoxin and thioredoxin peroxidase-1 during hormesis in response to oxidative stress-induced apoptosis. J Biol Chem 278:885–90. doi: 10.1074/jbc.M209914200

Assad AR, Delou JM, Fonseca LM, et al (2009) The role of K_{ATP} channels on propofol preconditioning in a cellular model of renal ischemia-reperfusion. Anesth Analg 109:1486–1492. doi: 10.1213/ANE.0b013e3181b7639

Bae S, Jeong HJ, Cha HJ, et al (2012) The hypoxia-mimetic agent cobalt chloride induces cell cycle arrest and alters gene expression in U266 multiple myeloma cells. Int J Mol Med 30:1180–1186. doi: 10.3892/ijmm.2012.1115Bagkos G, Koufopoulos K, Piperi C (2014) A new model for mitochondrial membrane potential production and storage. Med Hypotheses 83:175–181. doi: 10.1016/j.mehy.2014.05.001

Beere HM (2005) Death versus survival: functional interaction between the apoptotic and stress-inducible heat shock protein pathways. J Clin Investig 10:2633–2639. doi: 10.1172/JCI26471

Behmenburg F, Dorsch M, Huhn R, et al (2015) Impact of mitochondrial Ca^{2+}-sensitive potassium (mbkca) channels in sildenafil-induced cardioprotection in rats. PLoS One 10:1–12. doi: 10.1371/journal.pone.0144737

Benasayag-Meszaros R, Risley MG, Hernandez P, et al (2015) Pushing the limit: Examining factors that affect anoxia tolerance in a single genotype of adult *D. melanogaster*. Sci Rep 5:1–5. doi: 10.1038/srep09204

Bing OH, Brooks WW, Messer JV (1973) Heart muscle viability following hypoxia: protective effect of acidosis. Science 180:1297–1298. doi: 10.1126/science.180.4092.1297

Bombicino SS, Iglesias DE, Rukavina-Mikusic IA, et al (2017) Hydrogen peroxide, nitric oxide and ATP are molecules involved in cardiac mitochondrial biogenesis in diabetes. Free Radic Biol Med 112:267–276. doi: 10.1016/j.freeradbiomed.2017.07.027

Bonuccelli G, Tsirigos A, Whitaker-Menezes D, et al (2010) Ketones and lactate “fuel” tumor growth and metastasis: Evidence that epithelial cancer cells use oxidative mitochondrial metabolism. Cell Cycle 9:3506–3514. doi: 10.4161/cc.9.17.12731

Bruce JIE, Elliott AC (2007) Oxidant-impaired intracellular Ca^{2+} signaling in pancreatic acinar cells: role of the plasma membrane Ca^{2+}-ATPase. 938–950. doi: 10.1152/ajpcell.00582.2006.

Buster DW, Nye J, Klebba JE, Rogers GC (2010) Preparation of *Drosophila* S2 cells for Light Microscopy. J Vis Exp 1–5. doi: 10.3791/1982

Caplan SL, Milton SL, Dawson-Scully K (2012) A cGMP-dependent protein kinase (PKG) controls synaptic transmission tolerance to acute oxidative stress at the *Drosophila* larval neuromuscular junction. J Neurophysiol. doi: 10.1152/jn.00784.2011

Caretti A, Bianciardi P, Ronchi R, et al (2008) Phosphodiesterase-5 inhibition abolishes neuron apoptosis induced by chronic hypoxia independently of hypoxia-inducible factor-1alpha signaling. Exp Biol Med (Maywood) 233:1222–30. doi: 10.3181/0802-RM-73

Chachami G, Simos G, Hatziefthimiou A, et al (2004) Cobalt induces hypoxia-inducible factor-1α expression in airway smooth muscle cells by a reactive oxygen species- and PI3K-dependent mechanism. Am J Respir Cell Mol Biol 31:544–551. doi: 10.1165/rcmb.2003-0426OC

Chai Y, Zhang DM, Lin YF (2011) Activation of cGMP-dependent protein kinase stimulates cardiac ATP-sensitive potassium channels via a

ROS/calmodulin/CaMKII signaling cascade. PLoS One. doi: 10.1371/journal.pone.0018191

Chandel NS, Maltepe E, Goldwasser E, et al (1998) Mitochondrial reactive oxygen species trigger hypoxia-induced transcription. Proc Natl Acad Sci U S A 95:11715–20. doi: 10.1073/pnas.95.20.11715

Charette M, Darveau CA, Perry SF, Rundle HD (2011) Evolutionary consequences of altered atmospheric oxygen in *Drosophila melanogaster*. PLoS One 6:e26876. doi: 10.1371/journal.pone.0026876

Costa ADT, Pierre SV, Cohen MV, et al (2008) cGMP signalling in pre- and post-conditioning: The role of mitochondria. Cardiovasc Res 77:344–352. doi: 10.1093/cvr/cvm050

Currin RT, Gores GJ, Thurman RG (1991) Protection by acidotic pH against anoxic cell killing in perfused rat liver: evidence for a pH paradox. FASEB J 5:207–10.

Zhang DX, Borbouse L, Gebremedhin D, Mendoza SA, Zinkevich NS, Li R (2008) H_2O_2-induced dilation in human coronary arterioles: Role of protein kinase G dimerization and large-conductance Ca^{2+}- activated K^+ channel activation. Circ Res 29:1883–1889. doi: 10.3174/ajnr.A1256.Functional

Dawson LA, Routledge C (1995) Differential effects of potassium channel blockers on extracellular concentrations of dopamine and 5-HT in the striatum of conscious rats. Br J Pharmacol 116:3260–3264. doi: 10.1111/j.1476-5381.1995.tb15133.x

Dawson TL, Gores GJ, Nieminen AL, et al (1993) Mitochondria as a source of reactive oxygen species during reductive stress in rat hepatocytes. Am J Physiol 264:C961–7.

Debska G, Kicinska A, Skalska J, et al (2002) Opening of potassium channels modulates mitochondrial function in rat skeletal muscle. Biochim Biophys Acta 1556:97–105.

Debska G, May R, Kicińska A, et al (2001) Potassium channel openers depolarize hippocampal mitochondria. Brain Res 892:42–50.

Dekanty A (2005) The insulin-PI3K/TOR pathway induces a HIF-dependent transcriptional response in *Drosophila* by promoting nuclear localization of HIF- /Sima. J Cell Sci 118:5431–5441. doi: 10.1242/jcs.02648

Denk A, Wirth T, Baumann B (2000) NF-κB transcription factors: Critical regulators of hematopoiesis and neuronal survival. Cytokine Growth Factor Rev 11:303–320. doi: 10.1016/S1359-6101(00)00009-5

Deshpande SA, Yamada R, Mak CM, et al (2015) Acidic food pH increases palatability and consumption and extends *Drosophila* lifespan. J Nutr 145:2789–2796. doi: 10.3945/jn.115.222380

Dey R, Moraes CT (2000) Metabolism and bioenergetics: lack of oxidative phosphorylation and low mitochondrial membrane potential decrease susceptibility to apoptosis and do not modulate the protective effect of Bcl-xL in osteosarcoma cells lack of oxidative phosphorylation. J of Biol Chem 275:7087–7094. doi: 10.1074/jbc.275.10.7087

Dijkers PF, Farrell PHO (2009) Dissection of a hypoxia-induced, nitric oxide – mediated signaling cascade. 20:4083–4090. doi: 10.1091/mbc.E09

Dimroth P, Kaim G, Matthey U (2000) Crucial role of the membrane potential for ATP synthesis by $F_{(1)}F_{(o)}$ ATP synthases. J Exp Biol 203:51–9.

Doggrell SA, Bishop BE (1996) Effects of potassium channel blockers on the action potentials and contractility of the rat right ventricle. Gen Pharmacol 27:379–85. doi: 10.1016/0306-3623(95)00111-5

Domoki F, Perciaccante JV, Veltkamp R, et al (1999) Mitochondrial potassium channel opener diazoxide preserves neuronal-vascular function after cerebral ischemia in newborn pigs. Editorial Comment. Stroke 30:2713–2719. doi: 10.1161/01.STR.30.12.2713

Eigentler A, Draxl A, Wiethüchter A (2012) Laboratory Protocol : Citrate synthase a mitochondrial marker enzyme. 11:1–11.

Else PL, Hulbert AJ (1987) Evolution of mammalian endothermic metabolism: "leaky" membranes as a source of heat. Am J Physiol - Regul Integr Comp Physiol 253:R1–R7.

Fazekas JF, Alexander FAD, and Himwich HE (1941) Tolerance of the newborn to anoxia. Am J of Phys 134:2, 281-287

Fernández-Tomé P, Lizasoain I, Leza JC, et al (1999) Neuroprotective effects of DETA-NONOate, a nitric oxide donor, on hydrogen peroxide-induced neurotoxicity in cortical neurones. Neuropharmacology 38:1307–15.

Ferreira R, Wong R, Schlichter LC (2015) KCa3.1/IK1 channel regulation by cGMP-dependent protein kinase (PKG) via reactive oxygen species and CaMKII in microglia: An immune modulating feedback system? Front Immunol 6:1–14. doi: 10.3389/fimmu.2015.00153

Frankenreiter S, Bednarczyk P, Kniess A, et al (2017) cGMP-elevating compounds and ischemic conditioning provide cardioprotection against ischemia and reperfusion

injury via cardiomyocyte-specific BK channels. Circulation 136:2337–2355. doi: 10.1161/CIRCULATIONAHA.117.028723

Gonzalez-Reyes A, Menaouar A, Yip D, et al (2015) Molecular mechanisms underlying oxytocin-induced cardiomyocyte protection from simulated ischemia-reperfusion. Mol Cell Endocrinol 412:170–181. doi: 10.1016/j.mce.2015.04.028

Gores GJ, Nieminen AL, Fleishman KE, et al (1988) Extracellular acidosis delays onset of cell death in ATP-depleted hepatocytes. Am J Physiol 255:C315–22.

Graham DI (1977) Pathology of hypoxic brain damage in man. J Clin Pathol 170–180. doi: 10.1136/jcp.s3-11.1.170

Gutiérrez-venegas G, Guadarrama-solís A, Muñoz-seca C, Arreguín-cano JA (2015) Hydrogen peroxide-induced apoptosis in human gingival fibroblasts. 8:15563–15572.

Haga N, Fujita N, Tsuruo T (2003) Mitochondrial aggregation precedes cytochrome c release from mitochondria during apoptosis. Oncogene 22:5579–5585. doi: 10.1038/sj.onc.1206576

Heise K (2006) Oxidative stress during stressful heat exposure and recovery in the North Sea eelpout *Zoarces viviparus* L. J Exp Biol 209:353–363. doi: 10.1242/jeb.01977

Herson PS, Lee K, Pinnock RD, et al (1999) Hydrogen peroxide induces intracellular calcium overload by activation of a non-selective cation channel in an insulin-secreting cell line. J Biol Chem 274:833–841. doi: 10.1074/jbc.274.2.833

Hetts SW (1998) To die or not to die: an overview of apoptosis and its role in disease. J Am Med Assoc 279:300–307.

Higgins LH, Withers HG, Garbens A, et al (2009) Hypoxia and the metabolic phenotype of prostate cancer cells. Biochim Biophys Acta - Bioenerg 1787:1433–1443. doi: 10.1016/j.bbabio.2009.06.003

Hinds CJ (1985) Prevention and treatment of brain ischaemia. Br Med J (Clin Res Ed) 291:758–760. doi: 10.1136/bmj.291.6498.758

Houten SM, Auwerx J (2004) PGC-1 alpha: Turbocharging mitochondria. Cell 119:5–7.

Ibrahim-Hashim A, Abrahams D, Enriquez-Navas PM, et al (2017) Tris–base buffer: a promising new inhibitor for cancer progression and metastasis. Cancer Med 6:1720–1729. doi: 10.1002/cam4.1032

Inoue I, Nagase H, Kishi K, Higuti T (1991) ATP-sensitive K^+ channel in the mitochondrial inner membrane. Nature 352:244–247.

Ja WW, Carvalho GB, Mak EM, et al (2007) Prandiology of *Drosophila* and the CAFE assay. Proc Natl Acad Sci 104:8253–8256. doi: 10.1073/pnas.0702726104

Josephson RA, Silverman HS, Lakatta EG, et al (1991) Study of the mechanisms of hydrogen peroxide and hydroxyl free radical-induced cellular injury and calcium overload in cardiac myocytes. J Biol Chem 266:2354–2361.

Kaun KR, Riedl CL, Chakaborty-Chatterjee M, et al (2007) Natural variation in food acquisition mediated via a *Drosophila* cGMP-dependent protein kinase. J Exp Biol 210:3547–3558. doi: 10.1242/jeb.006924

Kawai A, Nishikawa S, Hirata A, Endo T (2001) Loss of the mitochondrial Hsp70 functions causes aggregation of mitochondria in yeast cells. J Cell Sci 114:3565–74.

Khacho M, Tarabay M, Patten D, et al (2014) Acidosis overrides oxygen deprivation to maintain mitochondrial function and cell survival. Nat Commun 5:1–15. doi: 10.1038/ncomms4550

Khavandi K, Baylie RL, Sugden SA, et al (2016) Pressure-induced oxidative activation of PKG enables vasoregulation by Ca^{2+}sparks and BK channels. Sci Signal. doi: 10.1126/scisignal.aaf6625

Kulikova OI, Fedorova TN (2016) Effects of antioxidants on the viability of the human neuroblastoma SH-SY5Y cell culture under the conditions of heavy-metal toxicity. Biol Med 08:4–8. doi: 10.4172/0974-8369.1000305

Lahiri S, Roy A, Baby SM, et al (2006) Oxygen sensing in the body. Prog Biophys Mol Biol 91:249–286. doi: 10.1016/j.pbiomolbio.2005.07.001

LeBel CP, Ischiropoulos H, Bondy SC (1992) Evaluation of the probe 2′,7′-Dichlorofluorescin as an indicator of reactive oxygen species formation and oxidative stress. Chem Res Toxicol 5:227–231. doi: 10.1021/tx00026a012

Lehman JJ, Barger PM, Kovacs A, et al (2000) Peroxisome proliferator-activated receptor gamma coactivator-1 promotes cardiac mitochondrial biogenesis. J Clin Invest 106:847–56. doi: 10.1172/JCI10268

Levin I (1913) Distribution of vital stains in animals with inoculable tumors. J Med Res XXIX:1–8.

Leyssens A, Nowicky AV, Patterson L, et al (1996) The relationship between mitochondrial state, ATP hydrolysis, $[Mg^{2+}]_{(i)}$ and $[Ca^{2+}]_{(i)}$ studied in isolated rat cardiomyocytes. J Physiol 496:111–128. doi: 10.1113/jphysiol.1996.sp021669

Li D, Tong W, Liu D, et al (2017a) Astaxanthin mitigates cobalt cytotoxicity in the MG-63 cells by modulating the oxidative stress. BMC Pharmacol Toxicol 18:1–7. doi: 10.1186/s40360-017-0166-1

Li L, Xiao L, Hou Y, et al (2016) Sestrin2 silencing exacerbates cerebral ischemia/reperfusion injury by decreasing mitochondrial biogenesis through the AMPK/PGC-1α pathway in rats. Sci Rep 6:1–11. doi: 10.1038/srep30272

Li PA, Hou X, Hao S (2017b) Mitochondrial biogenesis in neurodegeneration. J Neurosci Res 95:2025–2029. doi: 10.1002/jnr.24042

Liang H, Ward WF (2006) PGC-1alpha: a key regulator of energy metabolism. Adv Physiol Educ 30:145–51. doi: 10.1152/advan.00052.2006

Liu Q, Xu Z, Mao S, et al (2015) Effect of hypoxia on hypoxia inducible factor-1α, insulin-like growth factor I and vascular endothelial growth factor expression in hepatocellular carcinoma HepG2 cells. Oncol Lett 9:1142–1148. doi: 10.3892/ol.2015.2879

Liu Y, Ren G, Rourke B, et al (2001) Pharmacological comparison of native mitochondrial K_{ATP} channels with molecularly defined surface K_{ATP} channels. Mol Pharmacol 59:225–230. doi: 10.1124/mol.59.2.225

Liu Z, Sun Y, Qiao Q, et al (2017) Sesamol ameliorates high-fat and high-fructose induced cognitive defects via improving insulin signaling disruption in the central nervous system. Food Funct 8:710–719. doi: 10.1039/C6FO01562J

Lu WC, Chen CJ, Hsu HC, et al (2010) The adaptor protein SH2B1β reduces hydrogen peroxide-induced cell death in PC12 cells and hippocampal neurons. J Mol Signal 5:33–41. doi: 10.1186/1750-2187-5-17

Luzhkov VB, Åqvist J (2001) Mechanisms of tetraethylammonium ion block in the KcsA potassium channel. FEBS Lett 495:191–196. doi: 10.1016/S0014-5793(01)02381-X

Maeda Yasuhiro Yoshioka S, Kitao T, Kishino T, et al (2006) Inducing the formation of catalase hydrogen peroxide-induced apoptosis by nitric oxide protects macrophages from nitric oxide protects macrophages from hydrogen peroxide-induced apoptosis by inducing the formation of catalase. J Immunol Ref 176:4675–4681. doi: 10.4049/jimmunol.176.8.4675

Manresa MC, Taylor CT (2017) Hypoxia Inducible Factor (HIF) hydroxylases as regulators of intestinal epithelial barrier function. Cell Mol Gastroenterol Hepatol 3:303–315. doi: 10.1016/j.jcmgh.2017.02.004

Marin-Garcia J, Goldenthal MJ (2000) Mitochondrial biogenesis defects and neuromuscular disorders. Pediatr Neurol 22:122–129. doi: 10.1016/S0887-8994(99)00117-4

Marino ML, Pellegrini P, Di Lernia G, et al (2012) Autophagy is a protective mechanism for human melanoma cells under acidic stress. J Biol Chem 287:30664–30676. doi: 10.1074/jbc.M112.339127

Massie MR, Lapoczka EM, Boggs KD, et al (2003) Exposure to the metabolic inhibitor sodium azide induces stress protein expression and thermotolerance in the nematode Caenorhabditis elegans. Cell Stress Chaperones 8:1–7. doi: 10.1379/1466-1268(2003)8<1:ETTMIS>2.0.CO;2

McLeod CJ, Pagel I, Sack MN (2005) The mitochondrial biogenesis regulatory program in cardiac adaptation to ischemia - A putative target for therapeutic intervention. Trends Cardiovasc Med 15:118–123. doi: 10.1016/j.tcm.2005.05.001

Miyashita K, Itoh H, Tsujimoto H, et al (2009) Biogenesis and prevention of obesity. Diab. 58:2880-2892. doi: 10.2337/db09-0393.

Moger WH (1983) Effects of the calcium channel blockers cobalt, verapamil, and D600 on Leydig cell steroidogenesis. Biol Reprod 28:528–535.

Moreland RB, Goldstein I, Kim NN (1999) Sildenafil citrate, a selective phosphodiesterase type 5 inhibitor : research and clinical implications in erectile dysfunction. TEM 10:97–104.

Morimoto Y, Morimoto Y, Kemmotsu O, Alojado ES (1997) Extracellular acidosis delays cell death against glucose-oxygen deprivation in neuroblastoma x glioma hybrid cells. Crit. Care Med. 25:841–847.

Mukherjee S, Basar MA, Davis C, Duttaroy A (2014) Emerging functional similarities and divergences between *Drosophila Spargel/dPGC-1* and mammalian PGC-1 protein. Front Genet 5:216. doi: 10.3389/fgene.2014.00216

Mulier B, Rahman I, Watchorn T, et al (1998) Hydrogen peroxide-induced epithelial injury: The protective role of intracellular nonprotein thiols (NPSH). Eur Respir J 11:384–391. doi: 10.1183/09031936.98.11020384

Munns SE, Meloni BP, Knuckey NW, Arthur PG (2003) Primary cortical neuronal cultures reduce cellular energy utilization during anoxic energy deprivation. J Neurochem 87:764–772. doi: 10.1046/j.1471-4159.2003.02049.x

Nag S, Resnick A (2017) Stabilization of hypoxia inducible factor by cobalt chloride can alter renal epithelial transport. Physiol Rep 5:1–15. doi: 10.14814/phy2.13531

Nakamura K, Kamouchi M, Kitazono T, et al (2009) Amiloride inhibits hydrogen peroxide-induced Ca^{2+} responses in human CNS pericytes. Microvasc Res 77:327–334. doi: 10.1016/j.mvr.2008.12.001

Negash S, Gao Y, Zhou W, et al (2007) Regulation of cGMP-dependent protein kinase-mediated vasodilation by hypoxia-induced reactive species in ovine fetal pulmonary veins. Am J Physiol Lung Cell Mol Physiol 293:L1012–L1020. doi: 10.1152/ajplung.00061.2007

Nisoli E, Clementi E, Moncada S, Carruba MO (2004a) Mitochondrial biogenesis as a cellular signaling framework. Biochem Pharmacol 67:1–15. doi: 10.1016/j.bcp.2003.10.015

Nisoli E, Clementi E, Paolucci C, et al (2003) Mitochondrial biogenesis in mammals: The role of endogenous nitric oxide. 299:896–900.

Nisoli E, Falcone S, Tonello C, et al (2004b) Mitochondrial biogenesis by NO yields functionally active mitochondria in mammals. Proc Natl Acad Sci U S A 101:16507–12. doi: 10.1073/pnas.0405432101

Nilsson B, Norberg K, Siesjô BK (1975) Biochemical events in cerebral ischaemia. Br. J. Anaesth. 47:751–760.

Okahashi N, Nakata M, Sumitomo T, et al (2013) Hydrogen peroxide produced by oral streptococci snduces macrophage cell death. PLoS One 8:1–6. doi: 10.1371/journal.pone.0062563

Oldenburg O, Qin Q, Krieg T, et al (2004) Bradykinin induces mitochondrial ROS generation via NO, cGMP, PKG, and mitoK_{ATP} channel opening and leads to

cardioprotection. Am J Physiol Heart Circ Physiol 286:H468–76. doi: 10.1152/ajpheart.00360.2003

Oliver CN, Starke-Reed PE, Stadtman ER, et al (1990) Oxidative damage to brain proteins, loss of glutamine synthetase activity, and production of free radicals during ischemia/reperfusion-induced injury to gerbil brain. Proc Natl Acad Sci U S A 87:5144–5147. doi: 10.1073/pnas.87.13.5144

Osborne KA. (1997) Natural behavior polymorphism due to a cGMP-dependent protein kinase of *Drosophila*. Science (80-) 277:834–836. doi: 10.1126/science.277.5327.834

Paital B (2016) Longevity of animals under reactive oxygen species stress and disease susceptibility due to global warming. World J Biol Chem 7:110. doi: 10.4331/wjbc.v7.i1.110

Palumbo DR, Occhiuto F, Spadaro F, Circosta C (2012) *Rhodiola rosea* extract protects human cortical neurons against glutamate and hydrogen peroxide-induced cell death through reduction in the accumulation of intracellular calcium. Phyther Res 26:878–883. doi: 10.1002/ptr.3662

Pan C, Gupta A, Prentice H, Wu J-Y (2010) Protection of taurine and granulocyte colony-stimulating factor against excitotoxicity induced by glutamate in primary cortical neurons. J Biomed Sci 17 Suppl 1:S18. doi: 10.1186/1423-0127-17-S1-S18

Pérez-Pinzón MA, Nilsson GE, Lutz PL (1993) Relationship between ion gradients and neurotransmitter release in the newborn rat striatum during anoxia. Brain Res 602:228–233. doi: 10.1016/0006-8993(93)90687-I

Petit PX, Susin S-A, Zamzami N, et al (1996) Mitochondria and programmed cell death. FEBS Lett 396:7–13.

Pfeiffenberger C, Lear BC, Keegan KP, Allada R (2010) Locomotor activity level monitoring using the *Drosophila* activity monitoring (DAM) system. Cold Spring Harb Protoc 5:1238–1242. doi: 10.1101/pdb.prot5518

Prakasam G, Singh RK, Iqbal MA, et al (2017) Pyruvate kinase M knockdown induced signaling via AMP-activated protein kinase promotes mitochondrial biogenesis, autophagy, and cancer cell survival. J Biol Chem 292:jbc.M117.791343. doi: 10.1074/jbc.M117.791343

Raefsky SM, Mattson MP (2017) Roles in neuroplasticity and disease resistance. Free Radic Biol Med 102:203–216. doi: 10.1016/j.freeradbiomed.2016.11.045

Ray SK, Karmakar S, Nowak MW, Banik NL (2006) Inhibition of calpain and caspase-3 prevented apoptosis and preserved electrophysiological properties of voltage-gated and ligand-gated ion channels in rat primary cortical neurons exposed to glutamate. Neuroscience 139:577–95. doi: 10.1016/j.neuroscience.2005.12.057

Rera M, Bahadorani S, Cho J, et al (2012) Modulation of longevity and homeostasis by the *Drosophila* PGC-1 homolog. Cell Met. 14:623–634. doi: 10.1016/j.cmet.2011.09.013.

Robertson HE, Boyer PD (1955) The effect of azide on phosphorylation accompanying electron transport and glycolysis. J Biol Chem 214:295–305.

Rofstad EK, Mathiesen B, Kindem K, Galappathi K (2006) Acidic extracellular pH promotes experimental metastasis of human melanoma cells in athymic nude mice. Cancer Res 66:6699–6707. doi: 10.1158/0008-5472.CAN-06-0983

Rogers RP, Rogina B (2014) Increased mitochondrial biogenesis preserves intestinal stem cell homeostasis and contributes to longevity in Indy mutant flies. Aging (Albany NY) 6:335–350. doi: 10.18632/aging.100658

Ronnett GV, Hester LD, Nye JS, et al (1990) Human cortical neuronal cell line: establishment from a patient with unilateral megalencephaly. Science 248:603–5.

Roy J, Galano J-M, Durand T, et al (2017) Physiological role of reactive oxygen species as promoters of natural defenses. FASEB J 31:fj.201700170R. doi: 10.1096/fj.201700170R

Russell LK, Mansfield CM, Lehman JJ, et al (2004) Cardiac-specific induction of the transcriptional coactivator peroxisome proliferator-activated receptor γ coactivator-1α promotes mitochondrial biogenesis and reversible cardiomyopathy in a developmental stage-dependent manner. Circ Res 94:525–533. doi: 10.1161/01.RES.0000117088.36577.EB

Santos RX, Correia SC, Wang X, et al (2010) Alzheimer's disease: Diverse aspects of mitochondrial malfunctioning. Int J Clin Exp Pathol 3:570–581. doi: 3(5):570-581

Scheiner R, Sokolowski MB, Erber J (2004) Activity of cGMP-dependent protein kinase (PKG) affects sucrose responsiveness and habituation in *Drosophila melanogaster.* Learn Mem 11:303–11. doi: 10.1101/lm.71604

Schneider CA, Rasband WS, Eliceiri KW (2012) NIH Image to ImageJ: 25 years of image analysis. Nat Methods 9:671–675. doi: 10.1038/nmeth.2089

Schneider I (1972) Cell lines derived from late embryonic stages of *Drosophila melanogaster*. J Embryol Exp Morphol 27:353–65.

Shen W, Hao J, Feng Z, et al (2011) Lipoamide or lipoic acid stimulates mitochondrial biogenesis in 3T3-L1 adipocytes via the endothelial NO synthase-cGMP-protein kinase G signalling pathway. Br J Pharmacol 162:1213–1224. doi: 10.1111/j.1476-5381.2010.01134.x

Sicaeros B, Campusano JM, O'Dowd DK (2007) Primary neuronal cultures from the brains of late stage *Drosophila* pupae. J Vis Exp 5–7. doi: 10.3791/200

Singer D (1999) Neonatal tolerance to hypoxia: A comparative-physiological approach. Comp Biochem Physiol - A Mol Integr Physiol 123:221–234. doi: 10.1016/S1095-6433(99)00057-4

Smith MA, Herson PS, Lee K, et al (2003) Hydrogen-peroxide-induced toxicity of rat striatal neurones involves activation of a non-selective cation channel. J Physiol 547:417–425. doi: 10.1113/jphysiol.2002.034561

Solans A, Zambrano A, Rodríguez M, Barrientos A (2006) Cytotoxicity of a mutant huntingtin fragment in yeast involves early alterations in mitochondrial OXPHOS complexes II and III. Hum Mol Genet 15:3063–3081. doi: 10.1093/hmg/ddl248

Speakman JR, Selman C (2003) Physical activity and resting metabolic rate. Proc Nutr Soc 62:621–634. doi: 10.1079/PNS2003282

Steliou K, Perrine SP, Faller DV (2009) Lactic acid in cancer and mitochondrial disease. Drug Dev Res 70:499–511. doi: 10.1002/ddr.20342

Stetler RA, Leak RK, Yin W, et al (2012) Mitochondrial biogenesis contributes to ischemic neuroprotection afforded by LPS pre-conditioning. J Neurochem 123 Suppl :125–37. doi: 10.1111/j.1471-4159.2012.07951.x

Stewart BA, Atwood HL, Renger JJ, et al (1994) Improved stability of *Drosophila* larval neuromuscular preparations in haemolymph-like physiological solutions. J Comp Physiol A 175:179–191. doi: 10.1007/BF00215114

Stridh H, Kimland M, Jones DP, et al (1998) Cytochrome c release and caspase activation in hydrogen peroxide- and tributyltin-induced apoptosis. FEBS Lett. 429:351–355.

Tedesco I, Luigi Russo G, Nazzaro F, et al (2001) Antioxidant effect of red wine anthocyanins in normal and catalase-inactive human erythrocytes. J Nutr Biochem 12:505–511. doi: 10.1016/S0955-2863(01)00164-4

Thomas GP, Sims SM, Cook MA, Karmazyn M (1998) Hydrogen peroxide-induced stimulation of L-type calcium current in guinea pig ventricular myocytes and its inhibition by adenosine A1 receptor activation. J Pharmacol Exp Ther 286:1208–1214.

Thornton C, Jones A, Nair S, et al (2017) Mitochondrial dynamics, mitophagy and biogenesis in neonatal hypoxic-ischaemic brain injury. FEBS Lett 1–19. doi: 10.1002/1873-3468.12943

Tian X, He W, Yang R, Liu Y (2017) Dl-3-n-butylphthalide protects the heart against ischemic injury and H9c2 cardiomyoblasts against oxidative stress: Involvement of mitochondrial function and biogenesis. J Biomed Sci 24:1–10. doi: 10.1186/s12929-017-0345-9

Trafton J, Tombaugh G, Yang S, Sapolsky R (1996) Salutary and deleterious effects of acidity on an indirect measure of metabolic rate and ATP concentrations in CNS cultures. Brain Res. 731:122–131.

Tsujimoto Y (1997) Apoptosis and necrosis: Intracellular ATP level as a determinant for cell death modes. Cell Death Differ 4:429–434. doi: 10.1038/sj.cdd.4400262

Tulsawani R, Kelly LS, Fatma N, et al (2010) Neuroprotective effect of peroxiredoxin 6 against hypoxia-induced retinal ganglion cell damage. BMC Neurosci 11:125. doi: 10.1186/1471-2202-11-125

Utani A (2010) Laminin-3 chain-derived peptide promotes keratinocyte migration and wound closure: Clustering of syndecan-4 and integrin-1. Seikagaku 82:327–331. doi: 10.1091/mbc.E08

Valerio A, Bertolotti P, Delbarba A, et al (2011) Glycogen synthase kinase-3 inhibition reduces ischemic cerebral damage, restores impaired mitochondrial biogenesis and prevents ROS production. J Neurochem 116:1148–1159. doi: 10.1111/j.1471-4159.2011.07171.x

Vijayasarathy C, Damle S, Lenka N, Avadhani NG (1999) Tissue variant effects of heme inhibitors on the mouse cytochrome c oxidase gene expression and catalytic activity of the enzyme complex. Eur J Biochem 266:191–200.

Visch HJ, Koopman WJH, Leusink A, et al (2006) Decreased agonist-stimulated mitochondrial ATP production caused by a pathological reduction in endoplasmic reticulum calcium content in human complex I deficiency. Biochim Biophys Acta - Mol Basis Dis 1762:115–123. doi: 10.1016/j.bbadis.2005.09.001

Wang P, Li L, Zhang Z, et al (2016) Time-dependent homeostasis between glucose uptake and consumption in astrocytes exposed to $CoCl_2$ treatment. Mol Med Rep 13:2909–2917. doi: 10.3892/mmr.2016.4873

Wegener G, Moratzky T (1995) Hypoxia and anoxia in insects: microcalorimetric studies on two species (*Locusta* m*igratoria* and *Manduca sexta*) showing different degrees of anoxia tolerance. Thermochim Acta 251:209–218. doi: 10.1016/0040-6031(94)02009-D

Weinberg JM (2011) Mitochondrial biogenesis in kidney disease. J Am Soc Nephrol 22:431–436. doi: 10.1681/ASN.2010060643

Whitaker RM, Wills LP, Stallons LJ, Schnellmann RG (2013) cGMP-selective phosphodiesterase inhibitors stimulate mitochondrial biogenesis and promote recovery from acute kidney injury. J Pharmacol Exp Ther 347:626–34. doi: 10.1124/jpet.113.208017

Whittemore ER, Loo DT, Watt JA, Cotmans CW (1995) A detailed analysis of hydrogen peroxide-induced cell death in primary neuronal culture. Neuroscience 67:921–932. doi: 10.1016/0306-4522(95)00108-U

Wu Y, Gao B, Xiong QJ, et al (2017) Acid-sensing ion channels contribute to the effect of extracellular acidosis on proliferation and migration of A549 cells. Tumor Biol 39:1–8. doi: 10.1177/1010428317705750

Wyatt GR, Meyer WL (1959) The chemistry of insect hemolymph. III. Glycerol. J Gen Physiol 42:1005–1011. doi: 10.1085/jgp.42.5.1005

Wyatt TA, Lincoln TM, Pryzwansky KB (1991) Vimentin is transiently co-localized with and phosphorylated by cyclic GMP-dependent protein kinase in formyl-peptide-stimulated neutrophils. J Biol Chem 266:21274–21280.

Xie Y, Li J, Fan G, et al (2014) Reperfusion promotes mitochondrial biogenesis following focal cerebral ischemia in rats. PLoS One 9:e92443. doi: 10.1371/journal.pone.0092443

Xu S-Y, Pan S-Y (2013) The failure of animal models of neuroprotection in acute ischemic stroke to translate to clinical efficacy. Med Sci Monit Basic Res 19:37–45. doi: 10.12659/MSMBR.883750

Xu Z, Ji X, Boysen PG (2004) Exogenous nitric oxide generates ROS and induces cardioprotection: involvement of PKG, mitochondrial K_{ATP} channels, and ERK. Am J Physiol Heart Circ Physiol 286:H1433–40. doi: 10.1152/ajpheart.00882.2003

Xylander WER (2009) Physico-chemical properties of haemolymph of *Chilopoda* and *Diplopoda* (*Myriapoda, Arthropoda*): protein content, pH, osmolarity. SOIL Org 81:431–439.

Yao H, Sun X, Gu X, et al (2007) Cell death in an ischemic infarct rim model. J Neurochem 103:1644–53. doi: 10.1111/j.1471-4159.2007.04879.x

Ying W, Han SK, Miller JW, Swanson RA. (1999) Acidosis potentiates oxidative neuronal death by multiple mechanisms. J Neurochem 73:1549–1556. doi: 10.1046/j.1471-4159.1999.0731549.x

Yokomizo A, Moriwaki M (2006) Effects of uptake of flavonoids on oxidative stress induced by hydrogen peroxide in human intestinal Caco-2 cells. Biosci Biotechnol Biochem 70:1317–1324. doi: 10.1271/bbb.50604

Zeeshan M, Murugadas A, Ghaskadbi S, et al (2017) Ecotoxicological assessment of cobalt using Hydra model: ROS, oxidative stress, DNA damage, cell cycle arrest,

and apoptosis as mechanisms of toxicity. Environ Pollut 224:54–69. doi: 10.1016/j.envpol.2016.12.042

Zhang B, Ma JX (2008) SERPINA3K prevents oxidative stress induced necrotic cell death by inhibiting calcium overload. PLoS One. doi: 10.1371/journal.pone.0004077

Zhang L, Han J (2017) Branched-chain amino acid transaminase 1 (BCAT1) promotes the growth of breast cancer cells through improving mTOR-mediated mitochondrial biogenesis and function. Biochem Biophys Res Commun 486:224–231. doi: 10.1016/j.bbrc.2017.02.101

Zhang Y, Bhavnani BR (2005) Glutamate-induced apoptosis in primary cortical neurons is inhibited by equine estrogens via down-regulation of caspase-3 and prevention of mitochondrial cytochrome c release. BMC Neurosci 6:13. doi: 10.1186/1471-2202-6-13

Zhu J, Wang KZQ, Chu CT (2013) After the banquet. Autophagy 9:1663–1676. doi: 10.4161/auto.24135

Zmijewski JW, Banerjee S, Bae H, et al (2010) Exposure to hydrogen peroxide induces oxidation and activation of AMP-activated protein kinase. J Biol Chem 285:33154–33164. doi: 10.1074/jbc.M110.143685

Zou W, Yan M, Xu W, et al (2001) Cobalt chloride induces PC12 cells apoptosis through reactive oxygen species and accompanied by AP-1 activation. J Neurosci Res 64:646–53.